CAPITAL UNIVERSITY OF SCIENCE AND TECHNOLOGY, ISLAMABAD

A Study on Fractionation of *Azadirachta indica* Leaf Extract and its Antioxidant and Antidiabetic Attributes

by

Asad Ullah Nasir

A thesis submitted in partial fulfillment for the degree of Master of Science

in the

Faculty of Health and Life Sciences
Department of Bioinformatics and Biosciences

2026

CERTIFICATE OF APPROVAL

A Study on Fractionation of *Azadirachta indica* Leaf Extract and its Antioxidant and Antidiabetic Attributes

by

Asad Ullah Nasir

(MBS243020)

THESIS EXAMINING COMMITTEE

S. No.	Examiner	Name	Organization
(a)	External Examiner	Dr. Zaheer Ahmad	AIOU, Islamabad
(b)	Internal Examiner	Dr. Arshia Amin Butt	CUST, Islamabad

Dr. Rizwan ur Rehman
Thesis Supervisor
April, 2026

Dr. Syeda Marriam Bakhtiar
Head
Dept. of Bioinfo. & Biosciences
April, 2026

Dr. Sahar Fazal
Dean
Faculty of Health & Life Sciences
April, 2026

Author's Declaration

I, **Asad Ullah Nasir** hereby state that my MS thesis titled "**A Study on Fractionation of *Azadirachta indica* Leaf Extract and its Antioxidant and Antidiabetic Attributes**" is my own work and has not been submitted previously by me for taking any degree from Capital University of Science and Technology, Islamabad or anywhere else in the country/abroad.

At any time if my statement is found to be incorrect even after my graduation, the University has the right to withdraw my MS Degree.

(Asad Ullah Nasir)

Registration No: MBS243020

Plagiarism Undertaking

I solemnly declare that research work presented in this thesis titled "**A Study on Fractionation of *Azadirachta indica* Leaf Extract and its Antioxidant and Antidiabetic Attributes**" is solely my research work with no significant contribution from any other person. Small contribution/help wherever taken has been duly acknowledged and that complete thesis has been written by me.

I understand the zero tolerance policy of the HEC and Capital University of Science and Technology towards plagiarism. Therefore, I as an author of the above titled thesis declare that no portion of my thesis has been plagiarized and any material used as reference is properly referred/cited.

I undertake that if I am found guilty of any formal plagiarism in the above titled thesis even after award of MS Degree, the University reserves the right to withdraw/revoke my MS degree and that HEC and the University have the right to publish my name on the HEC/University website on which names of students are placed who submitted plagiarized work.

(Asad Ullah Nasir)

Registration No: MBS243020

Acknowledgement

I am grateful to ALLAH almighty, the Most Merciful and Beneficent, for this piece of work. I send my humble salutations to the Holy Prophet Muhammad (PBUH), the epitome of guidance and knowledge. I would like to extend my deepest gratitude to my supervisor, Dr. Rizwan Ur Rehman, for his invaluable guidance, support and insightful feedback throughout this journey. His encouragement and expertise have been instrumental in the successful completion of this work. Besides this, I am not only thankful to all supportive staff for their valuable assistance and cooperation, but also my colleagues for their support and guidance. I also indebted to all faculty members of the Bioinformatics and Bioscience department at Capital University of Science and Technology for their great expertise, constructive suggestions and motivation that shaped me to understand the complex scenarios in a systematic way which helped me in the completion of this work. I extend my heartfelt thanks to CUST, Islamabad for providing me with the necessary resources and support.

My deepest gratitude goes to my family: my grandparents, especially my beloved mother, and my dear father, Hashmat Javeed, whose unwavering support and sacrifices have brought me here. My siblings, have been a constant source of motivation. The care of my uncles and aunts means me a lot after the death of my father, without their support It wouldn't possible for me to reach the winning line of this race. Moreover, I am thankful to my wife for being my motivation, giving me respect and having belief in me, she was my constant source of strength throughout this journey.

Meanwhile, I am highly thankful to Higher Education Commission of Pakistan, who provided the research funding under the project **#NRPU 16186 Title "Isolation and Identification of therapeutic agents involved in the activation of PPAR-γ to ameliorate Type 2 Diabetes**" for the accomplishment of the thesis.

(Asad Ullah Nasir)

Abstract

Type 2 diabetes mellitus (T2DM) is a common metabolic disorder that is accompanied by insulin resistance and an abnormality in glucose metabolism, leading to persistent hyperglycemia and serious health issues worldwide. The rising prevalence of T2DM requires the search for efficient, safe, and affordable therapeutic strategies, thus underscoring the importance of using traditional medicinal plants such as *Azadirachta indica*, also known as neem. This plant has been used for centuries in Ayurvedic medicine and other traditional practices because of its high phytochemical content, including phenols, flavonoids and alkaloids, which are recognized for their antioxidant activity. This research aims to explore the fractionation of the methanolic leaf extract of *Azadirachta indica* through column chromatography. These fractions were analyzed through thin-layer chromatography and combined to form three super-fractions i.e., NF1, NF2 and NF3. These were further evaluated for their antioxidant and antidiabetic potential through different bioactivity assays. The findings revealed the presence of strong antioxidant properties and potent inhibitory action of α-glucosidase and α-amylase enzymes in NF1. The phytochemical screening of super-fractions through ESI-MS indicated the presence of GABA, purpurin, cyclopropanecarbonyl chloride, honokiol, spermidine and aspartic acid in positive and negative modes. These compounds were docked against T2DM target proteins i.e., Akt2, PI3K-α, PPAR-γ, IRS-2 and PDX-1. Purpurin from super-fraction NF1 was selected as lead compound because of high docking score i.e., -9.5 against Akt2 and good ADMET and interaction profile. To test the additional efficiency of purpurin, it was evaluated against the commercial anti-diabetic drug metformin. Comparing purpurin with metformin with respect to ADMET analysis, which was comparable, though the docking score and interaction profile of purpurin are better than those of metformin. Thus, it is concluded at this stage that NF1 proved to be a good fraction in the context to anti-oxidative and anti-diabetic activities. Moreover, the lead compound purpurin from NF1 possesses the ability to be a potential anti-diabetic drug of the future.

Keywords: Type 2 diabetes mellitus, purpurin, ADMET profile, anti-diabetic, super-fractions, anti-oxidative

Contents

List of Figures

List of Tables

Abbreviations

AMPK	AMP-activated protein kinase
BCAAs	Branched-chain amino acids
CGM	Continuous glucose monitor
DAG	Diacylglycerol
DM	Diabetes mellitus
DPP-4	Dipeptidyl peptidase-4
ER	Endoplasmic reticulum
FDA	Food and Drug Administration
FOXO1	Forkhead box protein O1
G6Pase	Glucose-6-phosphatase
GLP-1	Glucagon-like peptide-1
GLUT4	Glucose transporter type 4
GSK3	Glycogen synthase kinase 3
HFrEF	Heart failure with reduced ejection fraction
HSL	Hormone-sensitive lipase
HbA1c	Hemoglobin A1c
IDF	International Diabetes Federation
IKK	Inhibitor of kappa B kinase
IL-6	Interleukin-6
INSR	Insulin receptor
iPSCs	Induced pluripotent stem cells
IRS	Insulin receptor substrate
JNK	c-Jun N-terminal kinase
LC-MS/MS	Liquid chromatography–mass spectrometry/mass spectrometry

NCCIH	National Center for Complementary and Integrative Health
mTORC1	Mechanistic target of rapamycin complex 1
mTOR	Mechanistic target of rapamycin
PDK1	Phosphoinositide-dependent kinase 1
PEPCK	Phosphoenolpyruvate carboxykinase
PI3K	Phosphoinositide 3-kinase
PKB	Protein kinase B (Akt)
PKC	Protein kinase C
PPAR-γ	Peroxisome proliferator-activated receptor gamma
PTEN	Phosphatase and tensin homolog
PTP1B	Protein tyrosine phosphatase 1B
RNAi	RNA interference
ROS	Reactive oxygen species
S6K	Ribosomal protein S6 kinase
SGLT2	Sodium-glucose cotransporter 2
SH2	Src homology 2 domain
SOCS	Suppressor of cytokine signaling
T1DM	Type 1 diabetes mellitus
TNF-α	Tumor necrosis factor-alpha
TNFR	Tumor necrosis factor receptor
TZDs	Thiazolidinediones
UTI	Urinary tract infection

Chapter 1

Introduction

Diabetes mellitus (DM) is a widespread chronic metabolic condition marked by sustained hyperglycemia due to impairments in insulin production, insulin action, or both. It is primarily categorized into two sorts [1]. In type 1 diabetes, an autoimmune reaction culminates in the obliteration of insulin-secreting beta cells in the pancreas, culminating in the body's incapacity to synthesize insulin. In type 2 diabetes, the body develops resistance to insulin, resulting in a progressive decrease in insulin sensitivity and an inability to sustain normal blood glucose levels. Type 2 diabetes mellitus (T2DM) constitutes 90% of diabetes cases and is mostly associated with lifestyle variables, including obesity, sedentary behavior, and inadequate dietary practices, resulting in an increase in global prevalence [1–3].

The World Health Organization reported that 830 million people globally had diabetes in 2022. The International Diabetes Federation projects that 589 million people are living with diabetes among them 34.5 million Pakistanis population had diabetes in 2025 and will reach 70.2 million in 2050 and Africa will be the highest in percentage increase 142%. Diabetes-related medical costs now exceed $1 trillion annually worldwide, and more than 81% of individuals with the disease reside in low- and middle-income nations where access to care and the cost of medications are limited [4].

Diabetes results from a complex interplay of physiological systems that impair the body's capacity to manage blood glucose levels [5]. The insulin signaling pathway is an essential mechanism that governs glucose homeostasis in pancreatic β-cells. It entails reducing glucose release from the liver [6], enhancing glucose uptake in muscle and adipose tissue [7], promoting lipid accumulation, and suppressing the release of free fatty acids from adipocytes. To maintain glucose homeostasis, insulin binds to the extracellular α subunit of the insulin receptor, initiating phosphatidylinositol 3-kinase/kinase B (PI3K/Akt) signaling [8].

Akt facilitates glycogen synthesis by phosphorylating Forkhead Box Protein O1 (FOXO1) [9], inactivating Glycogen Synthase Kinase 3 (GSK3), and promoting the translocation of glucose transporter type 4 (GLUT4) [10]. Furthermore, it promotes protein synthesis and alleviates the inhibition of mTOR signaling pathways [11].

This method enhances glycogen synthesis, suppresses gluconeogenesis, and elevates glucose absorption. The Peroxisome Proliferator-Activated Receptors (PPAR) pathway is involved in regulating gene expression, hence controlling fat and glucose balance through its nuclear receptor PPAR-γ [12]. Interfering with these glucose regulation mechanisms may result in metabolic diseases such as diabetes.

Typ1e 2 diabetes mellitus (T2DM) is characterized by gut dysbiosis, oxidative damage, mitochondrial dysfunction, inflammation, hyperglycemia, and hyperlipidemia [13]. This leads to β-cell destruction and insulin resistance, characterized by compromised insulin-mediated glucose uptake in muscle and adipose tissue due to the malfunction of the GLUT4 glucose transport system and inadequate insulin suppression of hepatic glucose synthesis stemming from sustained gluconeogenesis [14]. This altered glucose metabolism can precipitate macrovascular illnesses, including peripheral artery disease [15], arrhythmia, cerebrovascular disease, atherosclerosis, cardiomyopathy, coronary heart disease, and stroke [16]. Diabetic people may also experience microvascular complications, including dementia, diabetic retinopathy [17], peripheral neuropathy [18, 19], renal failure [20], foot injuries, and hearing loss. These complications diminish quality of life and elevate morbidity and mortality rates [21]. Effective management of T2DM is essential to

avert these consequences and enhance patient health [18]. Current oral drugs for Type 2 Diabetes Mellitus (T2DM) include metformin , sulfonylureas [22], thiazolidinediones (TZDs) [23], sodium-glucose cotransporter 2 (SGLT2) inhibitors [24], and dipeptidyl peptidase-4 (DPP-4) inhibitors [25].

However, these treatments frequently have restricted long-term effectiveness and may be linked to detrimental side effects. Metformin, a primary treatment for type 2 diabetes mellitus, may induce gastrointestinal complications [26] and lactic acidosis [27]. Sulfonylureas, which promote insulin secretion, may result in hypoglycemia [28] and weight gain [29].

The adverse effects of thiazolidinedione that activate PPAR-γ encompass weight gain, fluid retention, and an elevated risk of heart failure and bone fractures [23]. SGLT2 inhibitors lead to genitourinary disorders, [30] acute renal injury, elevated urine output, and volume depletion, while the side effects of DPP-4 inhibitors encompass upper respiratory and urinary tract infections [31].

Injectable therapy is advised for the effective management of diabetes mellitu, as oral drugs sometimes prove inadequate in controlling hyperglycemia. Synthetic insulin is the most often utilized injectable therapy. Insulin is effective for diabetes mellitus; however, it may induce severe hypoglycemia, headaches, visual disturbances, diaphoresis, palpitations, and abdominal pain. Amylin analogs are commonly utilized alongside other diabetic drugs to manage postprandial glycemia, although they may induce hypoglycemia [28], nausea, and weight gain. Glucagon-Like Peptide-1 (GLP-1) agonists stimulate β-cell GLP receptors to enhance insulin synthesis, although may lead to severe bodily deformity due to significant weight loss, as well as nausea and vomiting. Alongside medication therapies, lifestyle modifications such as dietary changes, physical activity, and weight management are essential for diabetes management, as they improve insulin sensitivity, promote healthy weight, and enhance metabolic control.

Nonetheless, implementing and sustaining lifestyle modifications might prove difficult for several persons with diabetes, highlighting the necessity for more tailored and efficacious adjunctive therapy strategies for T2DM management. The

drawbacks of traditional antidiabetic therapies, including unwanted effects, expenses, and mere symptomatic alleviation, have necessitated the exploration of new approaches. In this context, plants have garnered significant interest due to their cost-effectiveness, accessibility, and minimal or absent adverse effects compared to synthetic pharmaceuticals [32–34]. Numerous epidemiological studies have highlighted the importance of consuming foods rich in phytocompounds for the management and prevention of illnesses, including diabetes mellitus. Bioactive compounds found in various plant parts, such as tannins, polyphenols, carotenoids, anthocyanins, flavonoids, and saponins, exhibit diverse therapeutic properties, including the modulation of glucose metabolism, enhancement of insulin sensitivity, and reduction of oxidative stress and inflammation [35, 36]. Understanding how these plant-derived components influence the pathophysiology of T2DM will enhance preventative strategies and their implications [37].

Experiments have revealed the potential of over 410 medicinal herbs to prevent diabetes [38]. The capacity of plants to improve pancreatic tissue function often yields anti-hyperglycemic actions, resulting in increased insulin secretion and thereby lowering blood glucose levels [39]. The *Gymnema sylvestre* plant contains pentacyclic triterpenoid saponins that impede glucose absorption, promote insulin production, and improve insulin sensitivity [40]. *Cinnamomum verum* has polyphenolic chemicals that impede carbohydrate-hydrolyzing enzymes [41, 42], enhance glycemic regulation, and adjust insulin sensitivity [43]. *Trigonella foenum-graecum* contains flavonoids, alkaloids, and saponins that prolong stomach emptying, block carbohydrate-hydrolyzing enzymes, and enhance insulin sensitivity [44]. Berberine, a plant-derived isoquinoline alkaloid, exhibits various modes of action, such as decreasing α-glucosidase activity, activating signaling through Adenosine Monophosphate-Activated Protein Kinase (AMPK), modulating insulin pathways, and enhancing mitochondrial function [7, 45].

Neem, frequently called "the village pharmacy," also known as *Azadirachta indica*, is a plant staple of traditional medicine that has been used for thousands of years [46]. Native to the Indian subcontinent, this fast-growing evergreen tree is well-known for its exceptional durability and a rich phytochemical profile that supports

its numerous medicinal uses. Strong limonoids like azadirachtin and nimbolide, as well as flavonoids and terpenoids, are among the many bioactive substances that give it its effectiveness and broad-spectrum pharmacological characteristics [47]. These include strong antibacterial and anti-inflammatory properties as well as antidiabetic, antioxidant, and even antitumor properties [48–50]. *Azadirachta indica* has emerged as a leading example of nature's complex response to contemporary health issues, bridging traditional knowledge with modern scientific research [51]. This trend is fueled by a desire for holistic wellness, worries about the negative effects of synthetic drugs, and increasing scientific validation [52].

Recent research has demonstrated its promise for managing diabetes because of its phytoconstituents, which have the ability to affect several metabolic pathways. These investigations have typically shown that it has positive effects on glycemic indices, such as the enzymes α-amylase and α-glucosidase that hydrolyze carbs in diabetics, inflammation, stress from oxidation, and reduction of glucose tolerance [53]. There is, however, a dearth of study on *Azadirachta indica* that focuses on certain markers implicated in the insulin signaling cascade and pathways leading to increased insulin release triggered by glucose.

This study examines the antidiabetic potential of *Azadirachta indica* in the rat insulin-secreting β cell line INS-1 to increase insulin secretion by using its phytocompounds as a method of ameliorating type 2 diabetes [54], taking into account the therapeutic properties of various plants in the activation of PPAR-γ and insulin signaling pathways [55]. Additionally, the activities and mechanisms of action that promote insulin production in response to glucose will be identified [56]. This research will illustrate how *Azadirachta indica* medicinal compounds can improve insulin sensitivity to ameliorate T2DM.

1.1 Problem Statement

T2DM is a major global health issue with increasing prevalence and serious complications. Current treatments are synthetic, costly, and most often provide symptomatic relief with undesirable pathological side effects, necessitating a need to

explore some natural therapeutic compounds with profound antidiabetic effect and less side effects.

1.2 Aim and Objectives

This research aims to screen and assess the therapeutic effectiveness of phytochemical agents from *Azadirachta indica* with potential antidiabetic profile, that could be used to ameliorate T2DM.

The study entails the following objectives.

i. To perform the phytochemical screening of *Azadirachta indica* extract through different chromatography techniques.

ii. To elucidate the antioxidant, total polyphenol and invitro antidiabetic attributes of the therapeutic fractions

iii. To characterize different fractions through LC-MS technique

iv. To evaluate the molecular docking of these compounds with INS and PPAR-γ pathway proteins through computational analysis.

Chapter 2

Literature Review

2.1 Diabetes

Diabetes mellitus is a chronic metabolic illness marked by high blood glucose levels due to the body's inability to make or properly use insulin, a hormone essential for managing glucose homeostasis. This intricate and multifaceted illness has become a global health issue, with its incidence consistently rising globally [1].

2.2 Prevalence of Diabetes

The International Diabetes Federation reported that in 2025, 589 million persons aged 20 to 79 were living with diabetes globally, with projections indicating an increase to 783 million by 2045. Significant geographical disparities exist in the prevalence of diabetes. Forecasts suggest that the incidence of the illness will escalate by 134% in Africa, 68% in South-East Asia, and 13% in Europe. Approximately 37 million Americans, including roughly 11.3% of the population, are afflicted with diabetes. In Australia, the statistic is one in twenty persons, equating to around 1.3 million people. China astonishingly has the greatest incidence of diabetes, with a total of 141 million persons affected. Alarmingly, over 283,000

Americans under the age of 20 are afflicted with the disease, with the United States reporting around 1.4 million new cases each year [57].

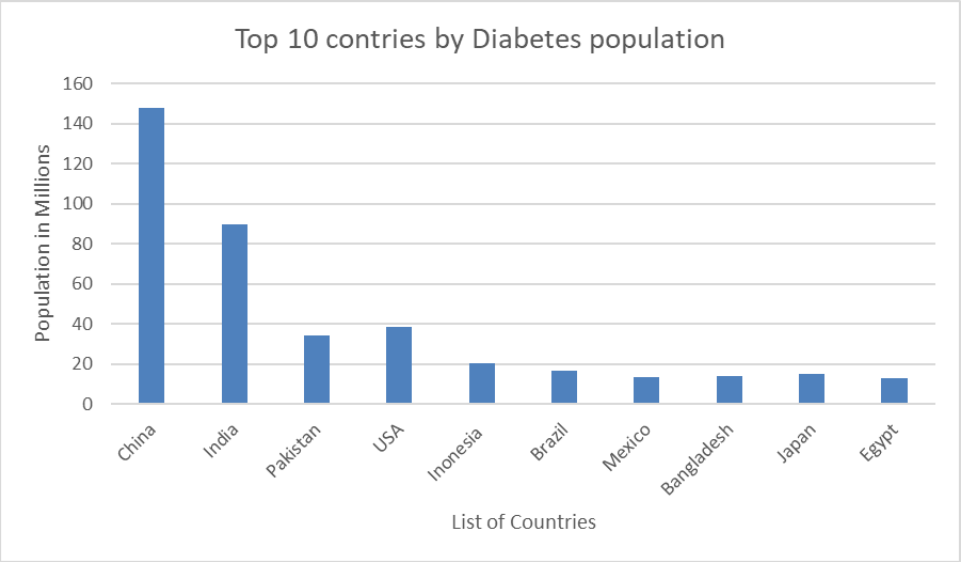

FIGURE 2.1: Prevalence of Diabetes's in the world according to International Diabetics Federation Diabetes Atlas, 11 edition. this graph shows the total number of diabetes individuals in the different countries.

Furthermore, around 240 million persons globally have undiagnosed diabetes, suggesting that almost half of adults with the ailment are oblivious to their status. According to that report Pakistan is at 4^{th} rank globally, behind China, India and USA. According to the World Health Organization, a 2011 study indicated that 12.9 million individuals globally had diabetes, including 9.4 million diagnosed cases. According to the International Diabetes Federation, about 26.7% of the Pakistani population had diabetes in 2022, equating to around 33 million individuals affected by the condition which rise to 34.5 in 2024. This concerning figure is significant and rising annually. The substantial increase in diabetes incidence underscores the urgent necessity for improved management strategies, preventative initiatives, and innovative treatment modalities to curtail the diabetes epidemic in Pakistan and beyond.

Though the South Asian populations in India, Bangladesh, and Sri Lanka share a common genetic predisposition to insulin resistance, Pakistan has a higher prevalence of diabetes in a disproportionate way because of the more adverse dietary and metabolic interactions. In Pakistan, the diets are a combination of a high glycemic

load and saturated/trans fat, which result in postprandial hyperglycemia, lipotoxicity, and insulin signaling through inflammatory pathways. Other South Asians, on the contrary, are more likely to consume more fiber-rich food, legumes, and unsaturated fats, which enhance glycemic regulation and insulin sensitivity. In addition, central adiposity is more prevalent in Pakistan to stimulate the release of pro-inflammatory adipokines and aggravate insulin resistance. Such metabolic disruptions, paired with reduced physical activity and less effective preventive health care systems, help to explain the substantially high rates of diabetes in Pakistan, in spite of relatively similar regional risk factors.

2.3 Classification of Diabetes

The development of diabetes mellitus entails intricate interactions among genetic, environmental, and behavioral variables. The fundamental issue of this intricate illness is the dysregulation of glucose metabolism, mostly caused by deficiencies in insulin synthesis and function. Frequent urination, polydipsia, polyphagia, tiredness, and ketoacidosis are the predominant symptoms of diabetes mellitus. Historically, diabetes was classified by age of onset or treatment modality; however, contemporary categorization emphasizes the pathogenic mechanisms that result in hyperglycemia. The phrases insulin-dependent and noninsulin-dependent are often employed to delineate the pathophysiological states of diabetes. Accurate classification of diabetes is crucial for clinical treatment and epidemiological studies. The three principal forms of this disease are type 1, type 2, and gestational diabetes mellitus (GDM), in addition to maturity-onset diabetes of the young (MODY), neonatal diabetes mellitus (NDM), type 3c, and latent autoimmune diabetes in adults (LADA) [5]. Following some of them explained briefly.

2.3.1 Diabetes Mellitus Type 1

Type 1 diabetes is an autoimmune disorder that results in the death of insulin-secreting beta cells. It is rather rare, comprising around 5-10% of all diabetes

cases, and usually manifests during childhood or adolescence. Type 1 diabetes is commonly termed insulin-dependent diabetes due to inadequate insulin synthesis. Individuals with type 1 diabetes require daily insulin injections, a specific diet, and regular blood glucose monitoring for survival [3].

2.3.2 Diabetes Mellitus Type 2

T2DM, commonly referred to as adult-onset diabetes, predominantly impacts middle-aged and older adults, arising from both inadequate insulin production and insulin resistance. It is more common and constitutes the bulk of diabetes cases globally. Approximately 90% of the 800 million individuals globally diagnosed with diabetes have Type 2 Diabetes Mellitus (T2DM). Risk factors for Type 2 Diabetes Mellitus including obesity, sedentary lifestyle, genetic susceptibility, and increasing age. It is a metabolic disorder that predisposes individuals to several other diseases and is mostly responsible for lower limb amputations, myocardial infarctions, cerebrovascular accidents, visual impairment, and renal failure. Management of type 2 diabetes often involves implementing lifestyle modifications such as dietary adjustments and enhanced physical activity, alongside the use of drugs to regulate blood glucose levels [13, 58]

2.3.3 Gestational Diabetes Mellitus

Diabetes that was previously undetected before to pregnancy but identified during the second or third trimester is termed gestational diabetes mellitus. About 13% of all newborns are impacted by it. Gestational diabetes mellitus (GDM) generally resolves postpartum; however, around 50% of afflicted women may subsequently acquire type 2 diabetes mellitus. The placenta secretes substances throughout pregnancy that might diminish insulin efficacy, resulting in the onset of gestational diabetes mellitus (GDM). Although several symptoms of T2DM manifest in GDM, diagnosis typically depends on prenatal screening methods, such as fasting glucose assessments, rather than patient-reported symptoms. The management of

gestational diabetes entails techniques like the adoption of a nutritious diet, participation in physical activity, monitoring of blood glucose levels, and occasionally the use of oral drugs [59].

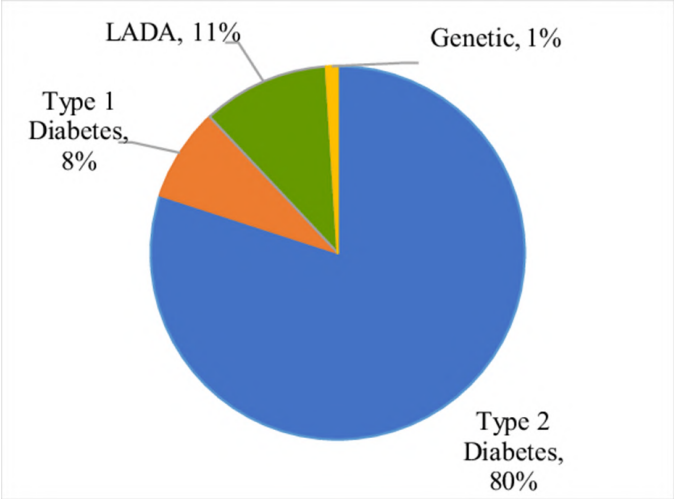

FIGURE 2.2: This pie chart shows the prevalence of different types of diabetes. Among these most common is T2DM, followed by LADA, T1DM and Genetic.

2.4 Glucose Metabolism in the Body

Glucose metabolism is a multifaceted process crucial for the body's balance and energy production. It encompasses several routes and organs that collaborate to guarantee the effective utilization or storage of glucose in accordance with the body's requirements. The ratio of glucose entering to glucose exiting the circulation affects blood glucose concentration [60]. Upon consumption of food, carbohydrates are assimilated and transformed into monosaccharides by amylases. This results in elevated blood glucose concentrations in the circulation. The pancreas regulates blood sugar levels by secreting two crucial chemicals, glucagon and insulin. The incretion action activates β-cells in the pancreas, promoting insulin synthesis and secretion. Insulin facilitates the absorption of glucose by cells, particularly muscle and adipose cells, hence reducing blood glucose levels. It further facilitates the conversion of glucose into glycogen for storage in the liver and muscle tissues. Moreover, blood glucose concentrations stimulate insulin production, which is regulated by the hormones GLP-1 and glucose-dependent insulinotropic polypeptide (GIP) [61]. GLUT molecules facilitate the transport of

glucose from the bloodstream into cells across cell membranes via diffusion, hence reducing excess glucose in circulation. Conversely, glucagon released when glucose level of blood decline, such as during fasting. It prompts the liver to transform glycogen that is stored into glucose and release it to the circulation, hence elevating blood sugar levels. The liver is crucial for glucose metabolism. It reserves glucose as glycogen and participates in gluconeogenesis, producing glucose from non-carbohydrate substrates like as amino acids and glycerol during extended fasting. The capacity to alternate between glucose storage and production is crucial for sustaining stable blood sugar levels. The kidneys are essential for glucose control. They extract glucose from the bloodstream and reabsorb it, preventing its loss in urine. They also engage in gluconeogenesis and facilitate the clearance of insulin from the circulation, which is essential for preserving insulin sensitivity and overall glucose homeostasis. The body utilizes intricate homeostatic systems to maintain blood glucose levels.

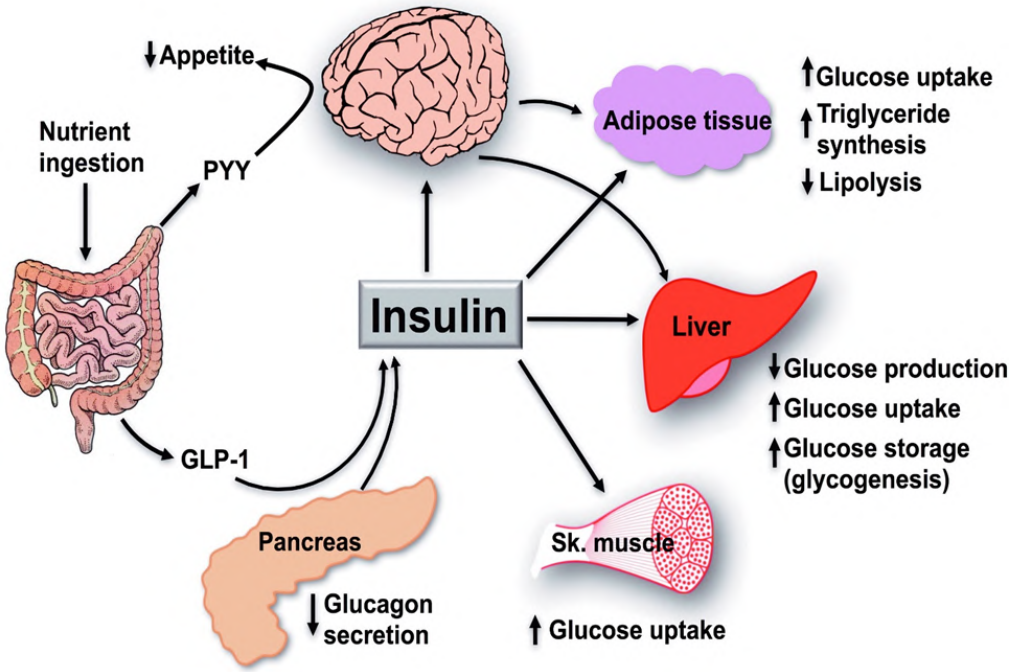

FIGURE 2.3: Equilibrium of glucose. The pancreas is notified when blood glucose levels rise as a result of a meal (Path 1). Insulin, a peptide hormone, is released in reaction. Insulin allows glucose from the bloodstream to be absorbed into the cell through interactions with downstream target cells in the body, such as the liver and muscle tissue. Glycogen is a carbohydrate that is stored as extra glucose. As a result, blood glucose levels stabilize. Several hours after consuming a meal, blood glucose levels will start to decrease (Path 2). This instructs the liver cells to convert glycogen to glucose monomers. After that, the bloodstream may receive the glucose again [62].

Negative feedback loops are essential in this process; they identify fluctuations in blood glucose levels and initiate reactions to re-establish equilibrium. Negative feedback loops are essential in this process; they identify fluctuations in blood glucose levels and initiate reactions to re-establish equilibrium. Insulin production increases while glucagon secretion decreases in response to elevated blood sugar levels, and conversely, glucagon secretion increases while insulin production decreases as blood glucose levels decline, as seen in figure 2.3.

This dynamic interaction guarantees that glucose levels stay within a normal range, often between 70 and 110 mg/dL. Disruption of the glucose regulating system can result in metabolic diseases, including diabetes mellitus [63].

2.5 Insulin Signaling Pathway

Postprandial tissue insulin sensitivity stimulates insulin secretion from β-cells in the pancreas to maintain stable glucose levels in the body. This homeostatic system involves various mechanisms across different organs, including the attenuation of heightened glucose absorption by muscle and adipose tissue due to hepatic glucose release, the augmentation of lipid accumulation in the liver and adipocytes, and the suppression of free fatty acid release from adipocytes.

A complex insulin-dependent signal transduction cascade regulates these metabolic processes. An intricate signal transduction cascade reliant on insulin regulates these metabolic processes [64]. The insulin signalling network has proximal and distal portions. The insulin receptor, insulin receptor substrate proteins (IRS), phosphoinositide 3-kinase (PI3K), and Akt are all located in the proximal area. These pieces are part of a larger network that is dynamically regulated by inputs from combinatorial signaling.

The distal section encompasses Akt substrates that are intricately associated with various physiological functions of insulin and are often unique to particular cell types. Figure 2.4 illustrates that distal elements interact with proteins and are often phosphorylated at many locations located inside unstructured domains [65].

2.5.1 Proximal Insulin Signaling

The tetrameric configuration of the insulin receptor has two transmembrane β-subunits and two extracellular α-subunits. The extracellular α-subunit binds insulin, resulting in autophosphorylation of the β-subunit at tyrosine residues (Y972, Y1158, Y1162, and Y1163). This phosphorylation enhances the receptor's inherent tyrosine kinase activity. The insulin receptor (INSR) gene encodes the receptor, which exists in two isoforms, IR-A and IR-B, that vary in their affinity for insulin binding [66].

The activated INSR attracts IRS proteins (IRS1–IRS4), which undergo phosphorylation at certain tyrosine residues, therefore generating docking sites for proteins containing SH2 domains. IRS1 plays a significant role in skeletal muscle and adipose tissue glucose uptake, whereas IRS2 is crucial for pancreatic β-cell activity and hepatic glucose control. Conversely, IRS3 and IRS4 exhibit tissue-specific activities [67].

Phosphoinositide 3-kinase is attracted to IRS proteins through its SH2 domains. The activation of PI3K leads to the transformation of phosphatidylinositol 4,5-bisphosphate (PIP2) into phosphatidylinositol 3,4,5-trisphosphate (PIP3) at the plasma membrane. PIP3 functions as a docking site for phosphoinositide-dependent kinase-1 (PDK1) and Akt, sometimes referred to as protein kinase B (PKB).

PDK1 phosphorylates Akt at threonine 308, while mTORC2 phosphorylates Akt at serine 473, resulting in complete activation. Akt possesses many isoforms: Akt1 governs cell survival and proliferation, Akt2 is essential for glucose homeostasis, and Akt3 plays a role in brain development [11].

2.5.2 Distal Insulin Signaling

In muscle and adipose tissue, active AKT phosphorylates AS160 (TBC1D4), which inhibits Rab proteins that facilitate GLUT4 vesicle trafficking.

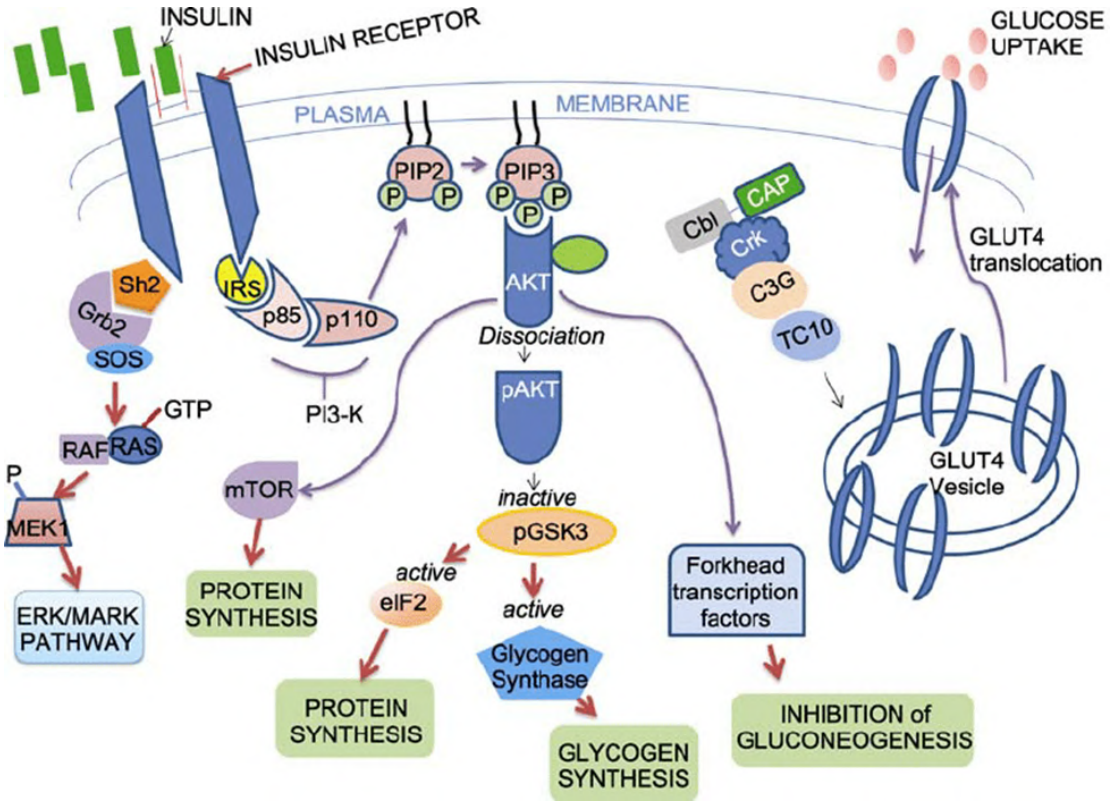

FIGURE 2.4: The binding of insulin stimulates its receptor, triggering two main processes. The initial pathway, the ERK branch, encompasses Grb2 and a kinase cascade (Ras, Raf, MEK) to activate ERK1/2 and facilitate cell proliferation. The principal metabolic pathway is insulin receptor substrates (IRS) activating PI 3-kinase to generate PIP3, subsequently resulting in Akt activation. Akt subsequently enhances glucose absorption by facilitating the translocation of GLUT4 transporters to the cell membrane, therefore permitting cellular glucose entry [68].

The phosphorylation of AS160 renders it inactive, facilitating the transfer of GLUT4 vesicles to the plasma membrane for glucose uptake. Akt phosphorylates and inactivates glycogen synthase kinase-3 (GSK3) to maintain glycogen synthase activity and facilitate glycogen storage in muscle and liver tissues. It further inhibits lipolysis in adipose tissue by phosphorylating PDE3B, hence decreasing cAMP levels and obstructing hormone-sensitive lipase (HSL). Concurrently, it stimulates lipogenesis through the mTORC1-SREBP1 pathway. mTORC1, stimulated by Akt, facilitates anabolic activities such as protein synthesis and cell proliferation via the activation of S6 kinase (S6K) and 4E-BP1. In hepatocytes, Akt phosphorylates FOXO1, hence preventing its nuclear localisation. This inhibits the transcriptional activity of gluconeogenic genes such as PEPCK and

G6Pase [68].

2.5.3 Skeletal Muscle Insulin Signaling

Skeletal muscle eliminates 80% of postprandial glucose, preserving glucose homeostasis. 75% of glucose is eliminated in the muscle because it promotes glycolysis, or glycogen production. The pancreas produces insulin, which binds to INSR to absorb glucose and store glycogen as blood glucose rises. INSR activation causes phosphorylation and dephosphorylating via S6K, AKT, PKC, and PDK1. These proteins govern glucose-metabolizing muscle pathways [69].

Akt2-controlled storage vesicles (GSVs) transport GLUT4 to the plasma membrane. Other downstream effects dephosphorylate glycogen metabolic proteins and increase glycogen synthesis, raising G6P. IRS1/PI3K/AKT pathway maintenance is needed for muscle glucose absorption after insulin stimulation.

Tyrosine IRS phosphorylation stimulates PI3K recruitment and insulin-stimulated glucose uptake, while serine and threonine do the reverse. Studies on mice show that Akt2 knockouts are severely glucose insensitive, but Akt1 knockoffs grow and tolerate glucose properly. Akt2 matters more for insulin-stimulated glucose absorption [7, 70].

2.5.4 Liver Insulin Signaling

INSR trans-auto phosphorylation, activation, and recruitment of scaffold signaling proteins including IRS1 and IRS2 start hepatic insulin signaling. IRS1 may have had a larger role in proper glucose homeostasis, because deleting both isoforms lowered insulin-activated PI3K-Akt activity. Insulin's hepatocellular action depends on Akt signaling, which targets FOXO1, mTORC1, and GSK3 [6].

FOXO-regulated transcriptional gluconeogenic genes are suppressed by insulin in fed states. FOXO1 targets Akt with Thr24, Ser256, and Ser319 phosphorylation sites. In addition, insulin affects genes that convert sugar to fat through

de novo lipogenesis (DNL). Sterol regulatory element-binding transcription factor protein-1c controls this pathway. This protein is controlled by insulin but can be suppressed by PI3K-Akt-mTORC1 axis suppression. By modulating hepatocyte protein synthesis, insulin aids fat and carbohydrate metabolism [9].

2.5.5 Adipose Tissue Insulin Signaling

Pro-inflammatory cytokines, adipokines, and free fatty acids from adipose tissue impact fat and carbohydrate metabolism. It reacts to insulin, which promotes pre-adipocyte growth into adipocytes, prevents lipolysis, and improves glucose and fatty acid absorption, causing triglyceride buildup. IRS1 and IRS2 mediate insulin signaling in adipocytes, showing how IRS-PI3K-AKT2-GLUT4 has physiologic implications. Rab-GAP-TBC1D helps adipocytes communicate insulin by trafficking vesicles and translocating GLUT4 to the cell membrane [71, 72].

Adipose tissue uses insulin to suppress lipolysis, which breaks down lipid triglycerides into fatty acids and glycerol for energy during activity or fasting. Controlling lipolysis requires protein kinase A signaling. In fed states, insulin promotes AKT2, which activates PDE3 and inhibits PKA, limiting lipolysis.

Conversely, adipose tissue insulin resistance decreases Akt2 phosphorylation, prolonging lipolysis. This increases circulating and non-esterified fatty acid production, which the liver and muscle absorb and produce ectopic lipid accumulation [8].

2.6 PPAR-γ Signaling Pathway

PPAR-γ is a ligand-activated transcription factor of the nuclear hormone receptor class, involved in several physiological processes, particularly the regulation of glucose metabolism, fatty acid storage, inflammation, adipogenesis, and insulin sensitivity [74]. Two isoforms of PPAR exist: PPARγ1 and PPARγ2. PPARγ2 is located in adipose tissues, whereas PPARγ1 is found in several organs, including

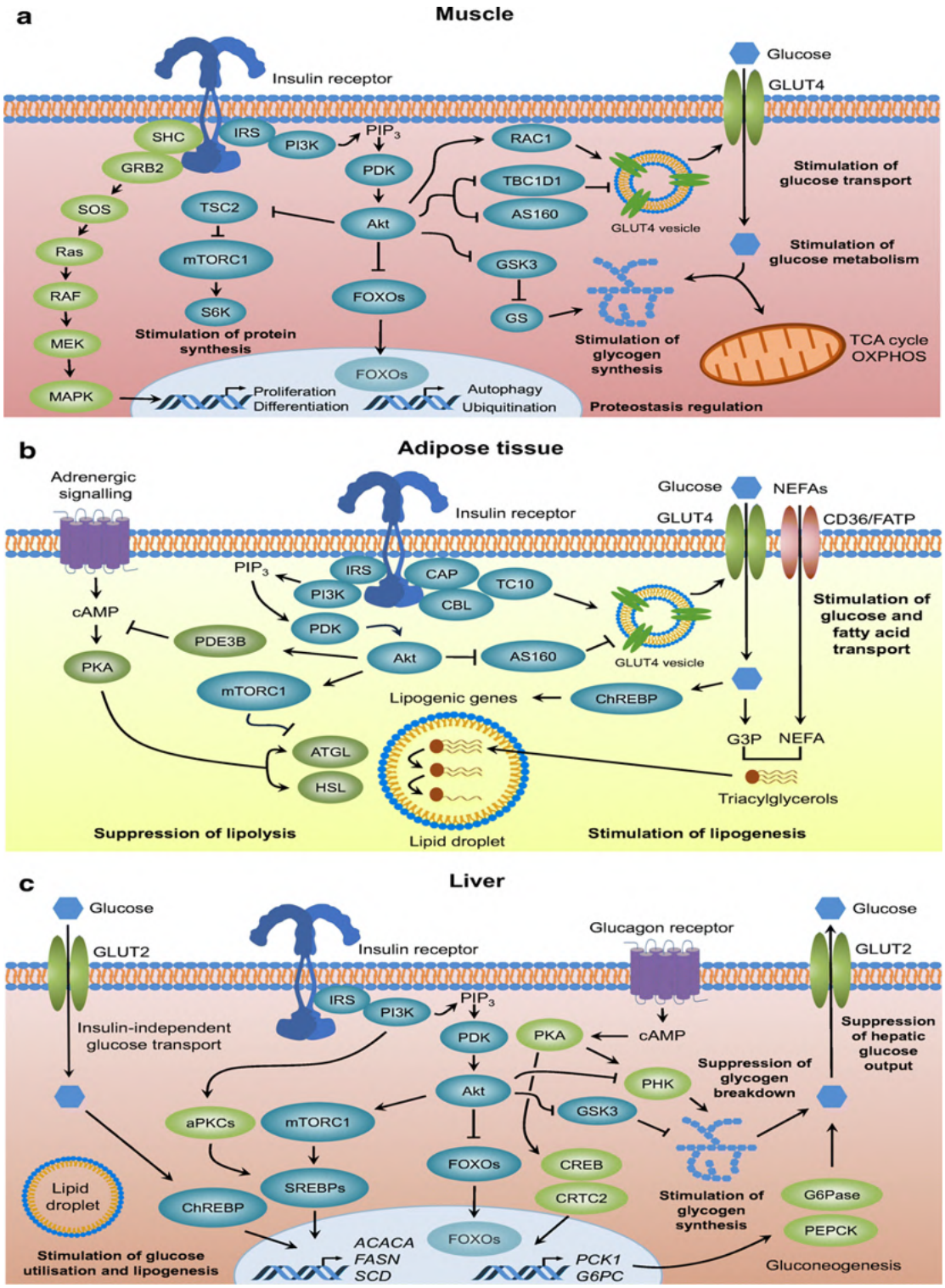

FIGURE 2.5: Classical tissue insulin signaling. Insulin binding activates intrinsic tyrosine kinase and phosphorylates multisite insulin receptor and IRS. Tyrosine-phosphorylated IRS docks PI3K, forming PIP3 and activating PDK-dependent Akt, which inhibits catabolic pathways in (a) skeletal muscle, (b) adipose tissue, and (c) the liver while promoting nutrient use, storage, and other anabolic processes. atypical PKC, ATGL, adipose triglyceride lipase, CAP, Cbl-associated protein, CBL, proto-oncogene, G3P, glyceraldehyde 3-phosphate, G6Pase, GRB2, growth factor receptor bound protein 2; GS, glycogen synthase, HSL, hormone-sensitive lipase, MAPK, mitogen-activated protein kinases, MEK, MAPK kinase, and OXPHOS, oxidative phosphorylation [73].

phagocytes, adipose tissue, and the small intestine. In mammals, in addition to PPAR-γ, there are PPARα and PPARβ/δ. PPARα is a key activator of oxidative fatty acid metabolism and serves as the designated target for hypolipidemic agents. It is located in the kidneys, liver, heart, skeletal muscles, and adipose tissue [12].

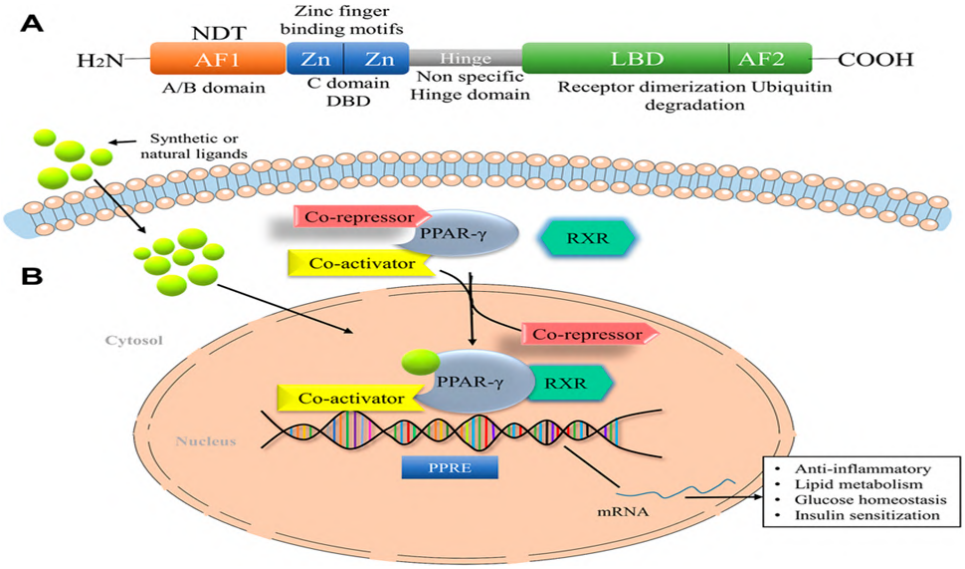

FIGURE 2.6: The mechanisms of action and structural domains of PPAR-γ. The domain structure of PPAR-γ enhances DNA binding at the DNA-binding domain (DBD). The ligand-binding pocket is how the ligand-binding domain (LBD) finds agonists. By interacting with the coactivator, PPAR-γ ligand binding to the heterodimer made up of RXR, PPAR-γ, and corepressor promotes PPAR-γ transcription activity. NF-κB, nuclear factor kappa-light-chain-enhancer of activated B cells; AF1, activation function 1; AF2, activation function 2; NTD, N-terminal domain; LBD, ligand binding domain; RXR, retinoid X receptor; STAT, signal transducer and activator of transcription[75].

Like PPARα, PPARβ/γ is extensively expressed and is crucial to fatty acid oxidation in liver, heart, and skeletal muscle. PPARs consist of three unique functional domains: The N-terminal transactivation domain, the highly conserved DNA-binding domain (DBD), and the C-terminal ligand-binding domain (LBD). Following the anchoring of PPARs to their DNA template binding sites via the DBD, they invariably form complexes with the RXR or retinoid X receptor, which binds to specific places of the target gene's DNA. PPAR response elements (PPREs) refer to specific sections of DNA [76, 77]. Figure 5 depicts the significant differences in target gene transactivation induced by coactivators attracted to diverse ligands in relation to the PPAR-receptor interaction.

Natural compounds such as amorfrutins, polyacetylenes, alkamides, sesquiterpene lactones, diterpenoids, triterpenoids, flavonoids, stilbenes, and neolignans function as PPAR agonists. Insulin resistance is promoted by pro-inflammatory cytokines released from persistently inflamed adipose tissue in type 2 diabetes. Agonists of PPAR have been shown to enhance fatty acid oxidation and inhibit hepatic glucose production, resulting in a reduction in pro-inflammatory cytokines and an increase in plasma levels of adiponectin, which is positively associated with insulin sensitivity [14]. It was shown that the administration of a PPAR-γ agonist enhanced the phosphorylation of tyrosine in IRS-1, the insulin receptor, and activated Akt. Skeletal muscles exhibited enhanced Akt phosphorylation and increased PI3K activity induced by insulin.

In Type 2 Diabetes Mellitus, thiazolidinediones, synthetic insulin - sensitizing agents, activate the PPAR-γ pathway by enhancing basal glucose uptake in muscle cells and adipocytes through the translocation of GLUT4 and GLUT1 to the cell membrane. However, they may induce significant adverse effects, including increased overall adiposity, fluid retention, heightened risk of heart failure, and bone fractures, resulting in their withdrawal from the market. Identifying ligands with an optimal pharmacological profile, which attract coactivators and confer antidiabetic advantages with little to no side effects, can be arduous [14]. The optimal profile of a PPAR agonist should facilitate coactivator insertion that enhances energy expenditure and glucose utilization while preventing fat storage. Plant extracts include common PPAR activators, such as polyunsaturated fatty acids, resulting in elevated response rates when assessed for PPAR activity.

2.7 Insulin Resistance and T2DM Pathophysiology

Several mechanisms contribute to T2DM pathophysiology, including decreased beta cell insulin secretion, increased α cell glucagon secretion, increased liver glucose production, neurotransmitter dysfunction, insulin resistance, lipolysis, kidney

reabsorption, small intestine incretin effect, and impaired glucose uptake by peripheral tissues. This leads to insulin resistance and β-cell loss [78].

Insulin resistance impairs muscle and adipocyte glucose uptake and hepatic glucose synthesis. This illness is characterized by hyperinsulinemia, where blood insulin levels are greater than glucose levels after fasting and eating. Hyperinsulinemia compensates for peripheral tissue insulin resistance (IR) to normalize blood glucose [79].

In insulin-resistant persons, the pancreas cannot make enough insulin, disrupting whole-body glucose homeostasis and causing hyperglycemia and glucose intolerance, the hallmarks of type 2 diabetes. Patients with type 2 diabetes generally have relative hyperinsulinemia until the disease is severe.

In insulin resistance, muscle and adipose cells' GLUT4 glucose transport pathway fails, preventing insulin from initiating glucose transfer [80]. IR is defined by the failure to limit hepatic glucose production, largely caused by gluconeogenesis. Insulin levels must now be evaluated to identify insulin resistance in humans, which is seldom done in clinical practice because many patients do not have high blood glucose.

Thus, IR is seldom diagnosed or treated in people. There is no means to detect this susceptible subset, and most IR patients develop type 2 diabetes, which may need additional vulnerability to β-cell failure.

2.7.1 Multiple Insulin Resistance Factors in T2DM

Several intrinsic and extrinsic causes cause insulin resistance in T2DM. The digestive tract or target cell absorbs cell-extrinsic factors, which are circulating or paracrine substances from cells or tissues. Metabolites include hormones, cytokines, lipids, and others. Cell-intrinsic variables often remain after extrinsic influences are eliminated or normalized owing to genetic or epigenetic effects. These variables can impair insulin receptor- or kinase-mediated signaling, leading type 2 diabetes insulin resistance [81].

2.7.1.1 External Factors

Extrinsic variables such gut microbiota, circulating metabolites, inflammatory signals, and adipose tissue cause type 2 diabetes insulin resistance. Over nutrition increases circulating fatty acid levels and ectopic lipid deposition in the liver and muscle, which releases intermediate metabolites such ceramides and DAG, which worsen insulin resistance. These intermediate metabolites activate the novel PKC family, decreasing tyrosine and increasing serine/threonine phosphorylation of insulin receptor proteins [82].

Even though IRS1 is the best studied substrate for insulin resistance, serine / threonine phosphorylation affects insulin receptor substrate 2 signaling. Fatty acid molecules increase IRS1 Ser/Thr phosphorylation and activate toll-like receptor 4, which enhances JNK and IKK activities. It reduces insulin's impact. Through PKC and protein phosphatase 2A activation, ceramide accumulation inhibits Akt2 [83].

Increasing adipose tissue inflammation and hypoxia also cause enlargement. The variables promote the recruitment of proinflammatory macrophages, which produce cytokines such as TNF-α and IL-6. Cytokine receptors, such as the TNF-α receptor (TNFR), worsen insulin resistance [84].

Cytokine signaling induces SOCS1 and SOCS3 protein synthesis. These proteins directly connect to the insulin receptor via SH2 domains, reducing IRS1/2 tyrosine phosphorylation and promoting ubiquitination and proteasomal degradation. In insulin-resistant tissues, endoplasmic reticulum stress and reactive oxygen species increase, inducing more serine/threonine kinases, IKK isoforms, and JNK.

Branched and aromatic amino acids in the circulation are associated to insulin resistance in rats; decreasing them can boost insulin sensitivity. The gut microbiota's regulation over short-chain fatty acid and BCAA production may impact systemic insulin sensitivity [84, 85].

Many environmental factors can change systemic tissue and insulin signaling. Obesity causes adipose tissue growth and insulin dysfunction. This can cause lipid

accumulation, mitochondrial dysfunction, reactive oxygen species, and endoplasmic reticulum stress in insulin-sensitive organs. Over nutrition affects exosomal miRNA release and systemic metabolism [86].

2.7.2 Intrinsic Factors

In vitro studies of type 2 diabetes insulin resistance have demonstrated that regulated cell culture can reduce cell-autonomous factors and external stimulation. Insulin resistance, metabolic abnormalities, and PI3K activity and AKT/GSK3 phosphorylation associated with IRS-1 are found in skeletal muscle biopsy procedures from type 2 diabetics and cultured myoblasts [73].

Primary cell models using RNA interference (RNAi), chemical genetics, or CRISPR are inadequate for finding insulin resistance molecular pathways due to their limited expandability and screening capabilities. Induced stem cells with pluripotency (iPSCs) may multiply and differentiate into many lineages, allowing patient cells to be used for gene-editing, mechanistic studies, and comprehensive omics [87, 88].

Recent iPSC research has examined signaling defects that cause type 2 diabetes-related insulin resistance in skeletal muscles. Similar to diabetic muscle, iPSC-derived myoblasts (iMyos) from patients have impaired insulin signaling, Akt/ GSK3/ FOXO1 phosphorylation, and glucose absorption due to insulin and mitochondrial respiration. Global phosphoproteomics using LC-MS/MS shows that these anomalies are part of a multi-dimensional signaling network of approximately 725 proteins with 1200 serine/threonine phosphorylation sites.

The discovery of molecular abnormalities that change signaling will be a major future priority. Kinase and phosphatase co-activators, ionic milieu, scaffolding proteins, redox balance, and other factors may contribute. Even if genetic reprogramming of iPSCs removes most epigenetic markers, understanding the root issue is challenging [89].

With profiling technology, long non-coding RNAs and miRNAs' capacity to affect cell metabolism has become clearer. In vitro models, tissues from rat models,

and humans with type 2 diabetes and obesity have identified a system of changed micro RNAs that target the IRS/PI3K/Akt cascade and insulin receptor, causing metabolism problems.

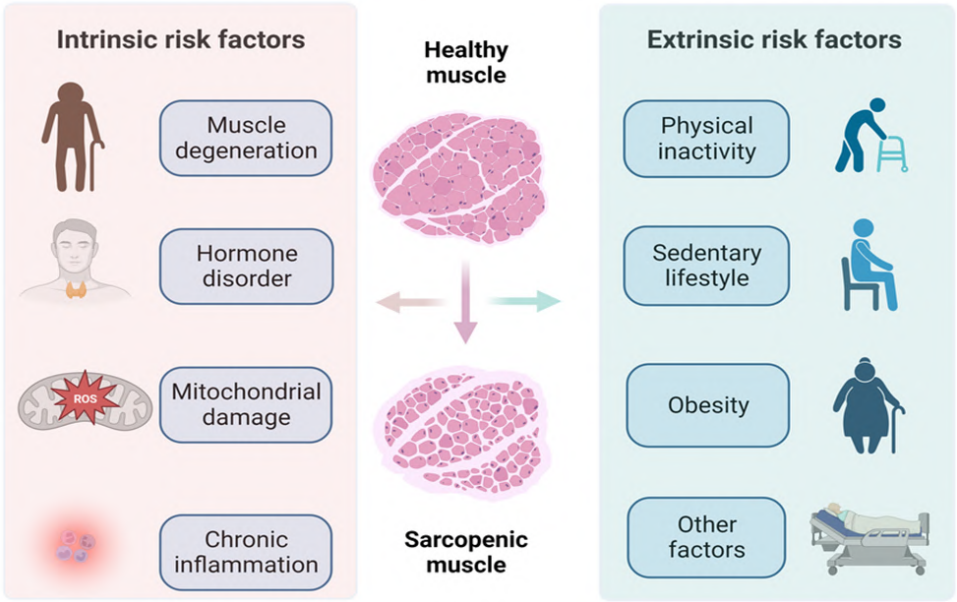

FIGURE 2.7: This diagram illustrates that sarcopenic muscle (muscle loss and dysfunction) is caused by a combination of Intrinsic (e.g., mitochondrial damage, inflammation) and Extrinsic (e.g., inactivity, obesity) risk factors. The progression from healthy muscle to sarcopenic muscle represents a major physiological pathway leading to insulin resistance. The overall message highlights the role of both biological aging and lifestyle in metabolic health decline.

2.8 Type 2 Diabetes Mellitus and Associated Health Complications

Diabetes can lead to significant problems, categorized into macrovascular and microvascular types. Neurological, renal, and ocular damage exemplify microvascular complications, whereas macrovascular complications encompass peripheral vascular disease, stroke, and cardiovascular disease. Paralysis, gangrene, and lesions are all outcomes of peripheral vascular disorders. The incidence of microvascular problems surpasses that of macrovascular consequences, including stroke, congestive heart failure, coronary artery disease, angina, and myocardial infarctions. Both gradual and episodic problems may lead to further organ damage and permanent

loss of function. Additional concerns encompass dental disease, diminished susceptibility to infections, and macrosomia in pregnant women with diabetes [90].

2.8.1 Cardiovascular Disorders

A primary cause of mortality in diabetics is cardiovascular disease, which accounts for up to 65% of all fatalities. Ischemic heart disease and stroke are the predominant morbidities linked to diabetes, with mortality rates among diabetic patients being two to four times higher than those of non-diabetic individuals. Moreover, those with diabetes possess a twofold increased risk of stroke.

More than 70 percent of individuals with diabetes either exhibit hypertension or are receiving pharmacological treatment for it. Risk factors for cardiovascular disease including hypertension, hypercholesterolemia, and tobacco use [16].

2.8.2 Periodontal Disorders

Diabetes can lead to oral health complications, such as periodontal disease. Diabetes can affect dental health by modifying the makeup of saliva, the vital fluid that preserves oral moisture. Saliva plays a crucial role in preventing dental decay by washing away food particles, inhibiting bacterial growth, and neutralizing the acids created by bacteria. Saliva includes minerals that safeguard oral tissues and aid in the prevention of tooth decay [91].

Diabetes and specific drugs for its management might diminish saliva production by the salivary glands in the oral cavity. A reduction in salivary flow increases the likelihood of dental caries, periodontal disease, and other oral health issues. Moreover, diabetes can increase glucose concentrations in saliva. In instances of diabetes, elevated blood glucose levels can lead to the accumulation of excess glucose in saliva. Glucose in saliva can act as a nutrition for detrimental bacteria, which, together with food particles, creates a soft, sticky layer called plaque. Neglecting to eliminate plaque can result in its calcification along the gum line, creating a deposit known as tartar, which may incite gum disease [91, 92].

2.8.3 Peripheral Arterial Disease

It is defined by the constriction of blood arteries that convey blood to the extremities, abdomen, and kidneys. The risk in diabetic individuals rises with age, duration of diabetes, and the presence of neuropathy.

The risk is further elevated by additional cardiovascular disease risk factors, including homocysteine and C-reactive protein levels. It is characterized by intermittent claudication and resting pain induced by perfusion in the affected limbs [15].

2.8.4 Retinopathy

This is a prevalent microvascular consequence in diabetic individuals, resulting in approximately 10,000 occurrences of blindness each year. It is associated with extended hyperglycemia and may manifest up to seven years prior to the diagnosis of type 2 diabetes.

The incidence increases with age; 27% of individuals aged seventy or older experienced visual degeneration, compared to 15% of those aged 18 to 44. Women with diabetes had a greater propensity for visual impairment compared to males. Timely identification and intervention can avert up to 90% of blindness associated with retinopathy. All diabetes patients should get a dilated eye examination annually [17].

2.8.5 Kidney Disease

Patients exhibiting persistent proteinuria in the absence of urinary tract infections or other medical conditions are diagnosed with diabetic nephropathy. Diabetic proteinuria may be apparent at diagnosis, however clinical nephropathy manifests rather late in type 1 diabetes. Diabetic nephropathy is rare during the initial 10 to 15 years of diabetes, thereafter escalating rapidly to a zenith at around 18 years, after which it begins to decline.

It accounted for 44% of newly diagnosed chronic renal failure in 2002. Diabetic nephropathy is associated with several risk factors, including metabolic control, blood pressure, hypertension, genetic predisposition, weight gain, hemorrhage, and tobacco consumption [20].

2.8.6 Peripheral Neuropathy

This condition commonly affects 30% to 50% of patients with diabetes, with hyperglycemia being the principal risk factor. Additional risk variables include age, duration of disease, tobacco use, hypertension, elevated triglycerides, increased body mass index, alcohol consumption, and greater height. The most widespread form of sensorimotor polyneuropathy is diabetic neuropathy, which can result in pain, muscle weakness, and sensory loss.

Years may elapse before indications of sensory impairment, such as burning and numbness in the feet, become apparent. Neuropathic pain can be intense; yet, only 11% to 32% of persons with polyneuropathy report experiencing it. It results in impairments and functional limits, including an elevated risk of lower-extremity amputation and ulcerated feet [18, 19].

2.9 Management and Treatment of T2DM Complications

Diabetes mellitus is a chronic condition without an accepted cure, necessitating ongoing care and therapy. Exercise, pharmacotherapy, and nutritional intervention constitute the treatment regimen. Maintaining optimal blood glucose levels is essential to prevent complications.

Regular aerobic activity is indicated to sustain a healthy body weight, regulate blood pressure, reduce blood cholesterol, and lower blood glucose levels. The specific kind of diabetes mellitus diagnosed dictates the pharmacotherapeutic intervention. Type 2 diabetes mellitus can be controlled with many oral medications,

and physicians employ clinical judgement to select the optimal therapy combination [18]. The therapies presently available for diabetes management are outlined below.

2.9.1 Glucose Monitoring

Monitoring blood glucose levels is crucial for assessing the efficacy of the present treatment regimen. It provides guidance on daily and, at times, hourly diabetes management. The FreeStyle Libre is a continuous glucose monitoring device that operates for a duration of 14 days. It retains glucose measurements for eight hours with a small, circular sensor containing a slender fiber inside [93].

Continuous glucose monitors (CGMs) provide real-time data and alerts without the need for physical sensor scanning, hence increasing their prevalence in the management of type 2 diabetes. Ever sense, the first implanted continuous glucose monitor (CGM), delivers glucose information for up to 180 days when utilized with a portable transmitter and smartphone application. Three trials including patients with Type 2 Diabetes Mellitus evaluated its safety and accuracy, demonstrating that it delivers precise readings and possesses a higher safety profile compared to conventional transcutaneous continuous glucose monitors. It is appropriate for individuals with comorbid conditions, extended sensor longevity, and on-body notifications [10].

2.9.2 Insulin

Individuals with type 1 diabetes must administer synthetic insulin to sustain life and regulate their condition. Certain individuals with type 2 diabetes require insulin therapy. Various forms of synthetic insulin are available. They begin at different speeds and persist in the body for varying durations [94]. The four primary modalities of insulin administration are rapid-acting inhaled insulin, insulin pens, insulin pumps, and syringe-based injectable insulin [87]. Insulin pens for Type 2 Diabetes patients have advanced to include memory capabilities, caps,

and attachments to enhance monitoring and adherence to dose. Insulin pumps are a practical and mobile solution for pediatric Type 1 Diabetes patients and have been utilized since the 1970s; nonetheless, their application is discouraged by NICE recommendations [95]. In type 2 diabetes, glucose-responsive insulin delivery systems, also known as artificial pancreas systems, utilize direct insulin pump administration informed by real-time glucose readings from a continuous glucose monitor (CGM) [96].

2.9.3 Salubrious Lifestyle

Although pharmaceutical interventions offer therapeutic alternatives, lifestyle adjustments are essential for the management of diabetes mellitus. Embracing a nutritious diet and participating in consistent physical exercise are crucial for attaining best results in conjunction with medical treatments. Diet significantly affects blood pressure, weight management, and blood glucose levels. Physical exercise has several benefits, such as enhanced tissue sensitivity to insulin, improved glycemic control, positive impacts on blood pressure and lipid profiles, promotion of weight loss, and cardiovascular advantages [21].

2.9.4 Insulin Sensitizers

The two classifications of medications categorized as insulin sensitizers are thiazolidinediones (rosiglitazone and pioglitazone) and biguanides (metformin).

2.9.4.1 Biguanides

Obese patients with type 2 diabetes are often administered biguanides, with metformin commonly utilized alongside insulin or other oral antidiabetic agents. The primary purpose of Metformin is to decrease hepatic glucose synthesis by inhibiting gluconeogenesis and glycogenolysis, enhancing peripheral insulin sensitivity, and alleviating hyperglycemia. This enhances hepatic insulin sensitivity, aiding in the

reduction of baseline plasma glucose levels. Furthermore, AMPK, which regulates the metabolism of lipids and glucose, is activated by metformin. Upon activation, AMPK inhibits the expression of two essential hepatic gluconeogenic genes, PEPCK and G6Pase, therefore enhancing fatty acid oxidation and lipolysis while concurrently reducing gluconeogenesis and lipogenesis. This leads to enhanced glucose metabolism in the splanchnic bed, accompanied by other metabolic advantages such as triglyceride reduction and inhibition of fatty acid oxidation [97].

2.9.4.2 Thiazolidinedione

The FDA has approved two thiazolidinedione medicines for the treatment of type 2 diabetes: pioglitazone and rosiglitazone. Thiazolidinediones operate by binding to the PPAR-γ receptor, predominantly located in adipocytes, hence facilitating gene transcription through interaction with the retinoic-X receptor. A nuclear response element binds to this heterodimer, influencing glucose and lipid metabolism. Thiazolidinediones (TZDs) additionally inhibit the production of TNF-α in adipocytes, underscoring their significance in cellular metabolism [23].

2.9.5 Insulin Secretagogues

Insulin secretagogues, namely sulfonylureas and meglitinides, lower blood glucose levels by stimulating insulin secretion.

2.9.5.1 Sulfonylureas

Sulfonylureas, including glibenclamide, gliclazide, glipizide, and glimepiride, augment the beta-cell's responsiveness to glucose by inhibiting potassium-sensitive ATP channels on the cell membrane. This diminishes potassium cellular efflux and facilitates calcium inflow via voltage-dependent Ca2+ channels, resulting in the release of pre-formed insulin granules. This enhances the responsiveness of beta cells to both glucose and non-glucose secretagogues, resulting in increased insulin secretion across all blood glucose levels [22].

2.9.5.2 Meglitinides

Type 2 diabetes can be remedied with meglitinide analogues nateglinide and repaglinide. These medicines modulate insulin secretion from beta cells by influencing potassium efflux via potassium channels. Meglitinides has overlapping molecular binding sites with sulfonylureas, including two shared sites and one unique site. In contrast to sulfonylureas, meglitinides do not directly influence insulin exocytosis [22].

2.9.6 Incretin-Based Therapeutics

Incretin-based treatments are a category of drugs employed to treat T2DM by using the physiological effects of incretin hormones, chiefly glucagon-like peptide-1 (GLP-1) and glucose-dependent insulinotropic polypeptide (GIP). This include GLP-1 mimetic and dipeptidyl peptidase 4 inhibitors.

2.9.7 α-Glucosidase Inhibitors

Individuals with type 2 diabetes may be managed with the α-glucosidase inhibitors acarbose, miglitol, and voglibose. Acarbose inhibits the glycosidase enzymes located in the brush border of enterocyte intestinal villi. A decrease in intestinal glucose absorption is accomplished by inhibiting the breakdown of disaccharides and oligosaccharides. By diminishing the increase in postprandial glucose levels, α-glycosidase inhibitors decrease postprandial insulin concentrations [25].

2.9.8 Sodium-Glucose Cotransporter-2 Inhibitors

A unique class of antidiabetic agents known as sodium-glucose transporter 2 (SGLT2) inhibitors lowers blood glucose levels by influencing the renal handling of glucose. Invokana, the inaugural SGLT2 inhibitor, has obtained FDA clearance for the treatment of Type 2 Diabetes Mellitus (T2DM). Dosage reduction

is advised for mild impairment, while administration is prohibited in instances of severe liver illness or renal impairment. Sergliflozin has demonstrated, via clinical investigations and animal research, a dose-dependent effect on urine glucose excretion. While it has been demonstrated to induce mild side effects such as headache, sore throat, and dyspepsia in diabetic persons, it significantly reduced weight in healthy obese individuals [24].

2.9.9 Amylin Analogues

Individuals with Type 1 Diabetes Mellitus (T1DM) and Type 2 Diabetes Mellitus (T2DM) already administered prandial insulin may gain advantages from the adjunctive use of pramlintide. Individuals diagnosed with both gastroparesis and hypoglycemia unawareness are advised against its use due to the increased risk of hypoglycemia. To mitigate the risk of hypoglycemia, dose titration is recommended, and prandial insulin doses should be reduced by 50% at the beginning of therapy [98].

2.10 Adverse Effects of Diabetes Treatments

Oral hypoglycemic medications and insulin are fundamental to diabetes management, efficiently controlling hyperglycemia. Nevertheless, these medications may exhibit adverse side effects and often fail to completely manage the condition.

2.10.1 Hypoglycemia

Hypoglycemia may arise from the use of insulin or insulin secretagogues such as sulfonylureas and meglitinides, particularly when meals are omitted or during heavy physical exertion. These medicines bind to sulfonylurea receptors and inhibit ATP-sensitive potassium channels, resulting in depolarization and calcium influx, which subsequently stimulates insulin secretion from the pancreas. The

symptoms encompass dizziness, sweating, palpitations, disorientation, and, in extreme instances, loss of consciousness [28].

2.10.2 Weight Gain and Loss

Thiazolidinediones and insulin treatment are linked to weight gain. They enhance insulin sensitivity and facilitate adipogenesis, resulting in fat gain. Insulin may also enhance hunger and promote fat accumulation. Weight gain can exacerbate diabetes control and elevate cardiovascular risks. Thiazolidinediones (TZDs) may influence bone metabolism by enhancing osteoclast activity and diminishing bone density. Weight reduction is frequently observed with GLP-1 receptor agonists and SGLT2 inhibitors. These pharmaceuticals inhibit hunger and enhance glucose excretion, resulting in weight reduction. It may be advantageous for overweight people but might be unfavorable for others [29].

2.10.3 Gastrointestinal Disorders

Gastrointestinal complications frequently occur with biguanides, such as metformin, and GLP-1 receptor agonists. They can modify gut flora and impede stomach emptying, leading to abdominal discomfort and diarrhea. GLP-1 agonists activate the central nervous system, resulting in nausea and emesis. GLP-1 agonists and DPP-4 inhibitors can cause pancreatitis by eliciting an inflammatory response in the pancreas due to heightened insulin secretion or changes in pancreatic enzyme function [26].

2.10.4 Lactic Acidosis

Lactic acidosis is a medical emergency, particularly affecting those with renal impairment. Metformin suppresses gluconeogenesis and may result in lactate buildup, particularly when renal function is impaired. The symptoms encompass myalgia, respiratory distress, stomach discomfort, and general malaise [27].

2.10.5 Cardiovascular Disorders

SGLT2 inhibitors facilitate glucose excretion in urine, fostering an environment favorable to bacterial proliferation, leading to frequent urination, dysuria, fever, and lumbar discomfort. These drugs may result in dehydration and diminished renal perfusion, potentially leading to acute kidney damage [31].

2.10.6 Hepatotoxicity

Alterations in vision are linked to fast fluctuations in blood glucose levels, especially concerning insulin. Variations in glucose levels can result in oedema of the ocular lens, causing visual distortion. Allergic reactions may arise with any medicine, although they are particularly prevalent with DPP-4 inhibitors and SGLT2 inhibitors. Hypersensitivity and dermatological responses arise when the immune system responds to medication constituents, leading to rashes, blisters, and pruritus. Certain diabetic medicines may enhance photosensitivity, resulting in dermatological responses [99].

2.10.7 Fluid Retention and Gout

Thiazolidinediones may induce sodium retention, resulting in oedema and elevated fluid volume, which can cause swelling in the legs, ankles, or feet. SGLT2 inhibitors enhance uric acid excretion, precipitating an acute gout episode in susceptible patients, which causes intense joint pain, frequently in the big toe [30].

2.11 Medicinal Flora as a Substitute for Antidiabetic Pharmaceuticals

Conventional antidiabetic medications exhibit constraints owing to their detrimental effects and economic inefficacy. Due to their accessibility, cost-effectiveness,

and minimal side effects, plants possessing antidiabetic qualities have become an alternative to conventional therapies. In scientific research, they are becoming recognized as a source for discovering innovative pharmaceutical templates. Research has confirmed that more than 410 medicinal plants possess anti-diabetic properties. The phytochemicals present in these plants, including tannins, alkaloids, flavonoids, and phenolic, are essential for optimizing pancreatic tissue function by regulating glucose absorption and insulin secretion [32].

The antioxidants present in holy basil, betel leaf, neem, and aloe Vera assist in regulating blood glucose levels and body weight. Berries, stone fruits, and citrus fruits diminish oxidative stress and enhance satiety. Specific phytochemicals included in olives and amla enhance insulin sensitivity. Seeds such as tamarind, cashew, almond, walnut, cumin, cocoa, and coconut provide essential fatty acids and minerals. Fiber-rich grains, including quinoa, maize, and oats, assist in regulating obesity and blood glucose levels [32–34].

Vegetables notable for their abundant nutritional profiles and low caloric content encompass bitter gourds, snake gourds, ridge gourds, bottle gourds, sweet potatoes, centella twigs, fungi, potatoes, cauliflower, kale, radish root, carrots, tomatoes, cucumbers, spinach, lettuce, okra, asparagus, eggplants, beetroot, and moringa leaves. The herbs and spices with antidiabetic properties that enhance metabolic rate include curry leaves, bay leaves, cloves, saffron, cinnamon bark, peppers, turmeric root, ginger, garlic, mint extract, parsley, celery stalks, rosemary oil, and thyme.

The herbs and spices with antidiabetic properties that enhance metabolic rate include curry leaves, bay leaves, cloves, saffron, cinnamon bark, peppers, turmeric root, ginger, garlic, mint extract, parsley, celery stalks, rosemary oil, and thyme.

Additional foods that assist with weight management and glucose metabolism encompass grapevines, Chinese rose, coffee beans, and onions. Incorporating these items into a balanced diet might enhance insulin sensitivity, provide better glycaemic control, and promote weight reduction, hence aiding in the management of type 2 diabetes and obesity [35].

2.11.1 Importance of Phytochemicals in the Management and Treatment of Diabetes Complications

Phytochemicals are naturally occurring chemical compounds found in cereal grains, fruits, vegetables, and plant-derived liquids. They exist in many plant components and are classified as primary and secondary metabolites. Plant-based diets contain classes of phytocompounds such as tannin, polyphenol, carotenoid, anthocyanin, flavonoid, and saponin which are essential for diabetes management.

By a number of methods, such as increasing insulin sensitivity, blocking the enzymes involved in breaking down carbohydrates, and lowering the liver's synthesis of glucose, these substances aid in blood sugar regulation. They also help prevent diabetes and enhance overall metabolic function by reducing inflammation, reducing oxidative stress, promoting the production of glucoregulatory or satiating gut hormones, and improving gut health. They also help prevent diabetes and enhance overall metabolic function by reducing inflammation, reducing oxidative stress, promoting the production of glucoregulatory or satiating gut hormones, and improving gut health [36].

Studies have shown that antidiabetic parameters can be modulated in phytochemical - based diets. Flavonoid-rich okra can block enzymes that break down carbohydrates and promote GLUT-4 translocation, whereas polyphenols found in pineapple have anti-inflammatory properties.

Moreover, tea's high tannin content may have anti-inflammatory and insulin-sensitizing effects. Rich in saponin, oats can help with insulin resistance and lipid profiles.

The powerful antidiabetic effects of saffron, which is enhanced by advantageous phytochemicals, include lowering mitochondrial malfunction, cytokines associated with inflammation, and triglyceride levels. Fruit polyphenols can inhibit carbohydrate disintegration, and increase the absorption of glucose hence improving insulin sensitivity. The anthocyanin found in berries can improve the sensitivity to insulin, protect β-cells, and inhibit carbohydrate-digesting enzymes [37].

2.11.2 Experimental Procedures Demonstrating the Effectiveness of Phytocompounds as Antidiabetic Agents

Prior investigations utilizing experimental models demonstrate the effectiveness of plant phytocompounds as antidiabetic agents. Rutin, a natural flavonoid glycoside present in various vegetables and fruits, alters gluconeogenic and glycolytic enzymes to enhance glucose homeostasis and facilitate glucose absorption. It improved glucose absorption in rats by activating the pathways of conventional protein kinase C, mitogen-activated protein kinase (MAPK), and phosphoinositide 3-kinase. Morin, a pentahydroxyflavone, is recognized for its ability to activate and sensitize insulin receptors, hence enhancing metabolic processes and ameliorating endothelial dysfunction [38].

Gallotannins diminish glucokinase activity and elevate glucose-6-phosphatase activity, hence stimulating insulin secretion from pancreatic beta cells. Furthermore, they elevate the phosphorylation of insulin receptor substrate-1 in muscle, along with the expression of PI3K and GLUT4 in RNA [39].

Gallic acid has demonstrated the ability to lower blood glucose levels in diabetic rats and improve glucose uptake by mobilizing GLUT4 in adipocytes derived from streptozotocin-treated rats through the upregulation of PI3K signaling[40]. The elevation of glucose absorption by cells results from mangiferin's promotion of glucose transfer protein synthesis and subsequent translocation to adipocytes. In 3T3-L1 adipocytes, berberine, arecoline, and vanillic acid can enhance glucose absorption by as much as thrice in the micromolar range [40].

Astragalus polysaccharide therapy may partially repair the insulin-induced translocation of GLUT4 mediated by protein kinase B in the skeletal muscles of diabetic mice . Daidzein is a chemical shown to enhance glucose absorption [41]. Verminoside was shown to enhance GLUT4 translocation to the cell surface in skeletal muscle cells without impacting cell viability. In L6 cells, lupeol and lupeol-trifluoroacetate markedly enhanced glucose absorption. This was linked to GLUT4 translocation and the activation of the IRS-1/PI3K/Akt signaling pathway [42].

Ursolic acid may enhance the glucose uptake capacity of the PI3K pathway [43]. Naringenin has been shown to improve liver function markers, reduce membrane lipid peroxidation, restore lipid profiles, promote antioxidant activity, and decrease hyperglycemia and hyperinsulinemia in diabetic rats via modulating the production of TNF-α and GLUT4 [93].

The skin of Chum salmon is rich in marine collagen peptides, which enhance insulin sensitivity in diabetic rats by promoting GLUT4 expression and reducing adipocytokines, oxidative stress indicators, and inflammatory cytokines. The bevachin in adipocytes from chum salmon enhances insulin sensitivity in diabetic rats by facilitating GLUT4 translocation and activating AMPK and Akt pathways, which subsequently stimulate adipogenic transcription factors.

Administration of rosmarinic acid results in elevated GLUT4 expression in the skeletal muscles of both streptozotocin-induced and high-fat diet-induced diabetic rats. Gluconeogenic genes such as glucose-6-phosphatase (G6Pase), glucose transporter 2 (GLUT2), and phosphoenolpyruvate carboxykinase (PEPCK) may be suppressed by baicalin and its metabolites, which have been shown to enhance glucose uptake. Ishige foliacea includes pterosin A, which can ameliorate insulin resistance, reduce Akt and AMPK phosphorylation, impair muscle GLUT4 translocation, and counteract increased PEPCK expression in diabetic rats [44].

Piceatannol, a natural analogue and metabolite of resveratrol, promotes AMPK activation, enhances glucose absorption, and facilitates GLUT4 translocation. Resveratrol activates AMPK and its downstream targets, resulting in reduced hepatic glycogen levels and decreased blood HbA1c. Chlorogenic acid suppresses hepatic G6Pase expression and activity, improves lipid profiles, and mitigates hepatic steatosis. In L6 myotubes, it facilitates GLUT4 translocation and activates the IRS-1-PI3K-Akt pathway [56]. The oral administration of honokiol to T2DM diabetic mice can markedly decrease fasting blood glucose levels and enhance the phosphorylation of Akt and IRβ . Kaempferol, a PTP1B inhibitor, improves peripheral insulin sensitivity by ameliorating hyperglycemia, hyperinsulinemia, and the circulating lipid profile [55].

In HepG2 cells, caempferol A, a sesquiterpenoid derived from the Caragana intermedia plant, increases the levels of insulin receptor substrate and phosphorylates the protein kinase Akt. In skeletal muscles, galangin, a naturally occurring DPP-4 inhibitor, reduces glucose levels more effectively than insulin administered to cells alone [45]. The data indicate that most phytochemicals enhance GLUT4 activity and translocation via the insulin signaling pathway.

2.12 *Azadirachta indica*

Azadirachta indica, usually referred to as neem, is a rapidly growing evergreen tree that is a member of the Meliaceae family. Indigenous to the Indian subcontinent and certain areas of Southeast Asia, it has been extensively disseminated throughout tropical and subtropical climates globally. *Azadirachta indica* trees often attain heights of 15–20 meters, while extraordinary individuals may reach 35–40 meters and can survive for almost 200 years in ideal conditions. The tree possesses a vertical trunk with deeply grooved bark, and its crown is thick and rounded, frequently reaching a diameter of up to 20 meters. *Azadirachta indica* flourishes in arid and semi-arid areas, exhibiting exceptional drought resilience and frequently losing leaves during extended dry spells. The durability and swift proliferation of *Azadirachta indica* provide it a significant asset in agroforestry, traditional medicine, and sustainable agriculture [46].

FIGURE 2.8: *Azadirachta indica* tree.

2.13 Phytochemical Profile

The therapeutic efficacy of the neem tree, *Azadirachta indica*, is primarily based on its unusually rich and diversified phytochemical composition, a complex array of natural substances that the review paper thoroughly elucidates. This botanical collection comprises a diverse range of secondary metabolites, classified as isoprenoids and non-isoprenoids, which are systematically located in its many components—leaves, seeds, bark, flowers, and fruits.

The most notable and well researched of these chemicals are limonoids, a highly oxidized category of tetranortriterpenoids recognized for their significant biological activity. Primarily, azadirachtin is a chemical largely located in the seeds, functioning as a potent antifeedant, insect growth regulator, and pesticide by interfering with the endocrine systems of pests.

This limonoid is associated with a group of related compounds, including azadirachtin M, N, and 11-epi-azadirachtin H, all of which enhance the tree's robust defensive systems. Other essential limonoids encompass nimbin and its crude variant nimbidin, which primarily contribute to *Azadirachta indica*'s notable anti-inflammatory, antipyretic, and antifungal attributes; salannin, a powerful antifeedant; gedunin, recognized for its antimalarial and antifungal effects; and nimbolide, a compound derived from leaves and flowers exhibiting significant antibacterial and anticancer capabilities, particularly via its inhibition of the NF-κB signaling pathway. Compounds such as epoxyazadiradione and azadiradione enhance this limonoid richness, demonstrating antioxidant, anti-inflammatory, and anticancer properties [47].

In addition to this renowned family of limonoids, *Azadirachta indica* generates a diverse array of other essential phytochemicals. The tree serves as a notable source of diverse triterpenoids, including azadirone, zafaral, and meliacinahydride in the leaves, as well as nimbilin and nimolinin in the root bark. Common plant sterols, such as β-sitosterol and stigmasterol, are present and may contribute to cholesterol reduction and cardioprotective benefits. The volatile essential oils extracted

from leaves and flowers via hydro-distillation are abundant in hydrocarbons and oxygenated compounds such as β-elemene, germacrene D, caryophyllene, and pentacosane, which significantly contribute to *Azadirachta indica*'s notable antibacterial and larvicidal properties. Flavonoids and polyphenolic chemicals represent a significant aspect of *Azadirachta indica*'s bioactivity, providing robust antioxidant properties that mitigate oxidative stress. This category includes prominent antioxidants like as quercetin and rutin derived from leaves, along with catechin derivatives such (-)-epicatechin and genistein-7-O-glucoside extracted from seeds. The flowers are an abundant source of distinctive prenylated flavanones, which exhibit antimutagenic properties against some carcinogens. Moreover, *Azadirachta indica* seed oil is abundant in fatty acids such as oleic acid, linoleic acid, and α-linolenic acid, which enhance its moisturizing, anti-inflammatory, and wound-healing properties in topical formulations. The seeds contain pungent organosulfur compounds, which likely contribute to the unique odor and antibacterial properties, while polysaccharides isolated from the seed tegument have strong anti-inflammatory action, corroborating traditional use. The distribution of these compounds is distinctly specialized; seeds and kernels serve as the principal reservoirs of potent limonoids, leaves and flowers are abundant in flavonoids and particular triterpenoids, bark contains anti-ulcer compounds, and fruits possess a unique array of tetranortriterpenoids. The phytochemical composition of *Azadirachta indica* is characterized by significant complexity and synergy, with the combined effects of limonoids, flavonoids, terpenoids, fatty acids, and volatile oils establishing its reputation as a multifaceted therapeutic agent, serving as a natural basis for pharmaceuticals, pesticides, and nutraceuticals.

TABLE 2.1: Phytochemical Compounds and their Medicinal Properties

Phytochemical Compound	**Class of Compound**	**Medicinal Properties & Biological Activities**
Azadirachtin	Limonoid (Triterpenoid)	- Potent Insecticidal & Anti-feedant: Disrupts insect molting and reproduction [48]. - Anticancer: Induces apoptosis (cell death) in various cancer cell lines [51]. - Antiviral: Shows activity against certain viruses [52].

Table 2.1 continued from previoust page

Phytochemical Compound	**Class of Compound**	**Medicinal Properties & Biological Activities**
Nimbin	Limonoid (Triterpenoid)	- Antipyretic: Reduces fever [49]. - Antihistamine: Helps alleviate allergic reactions. Anti-inflammatory: Reduces swelling and inflammation [100]. - Antifungal: Effective against various fungi [101].
Nimbidin	Limonoid (Triterpenoid)	- Anti-inflammatory & Anti-arthritic: Potently reduces joint inflammation and pain. - Antipyretic: Fever-reducing. - Antihistaminic: Anti-allergic properties. - Antibacterial: Active against various bacteria. - Antiucler: Helps protect the gastric lining [102].
Gedunin	Limonoid (Triterpenoid)	- Antimalarial: Effective against the Plasmodium falciparum malaria parasite [103]. - Antifungal: Strong activity against fungi. - Anticancer: Demonstrates cytotoxic effects on cancer cells [51].
Salannin	Limonoid (Triterpenoid)	- Insect Repellent: Deters insect feeding. - Anticancer: Shows growth inhibitory effects on tumors [104]. - Antifungal: Active against fungal pathogens.
Quercetin	Flavonoid	- Antioxidant: Powerful free radical scavenger [105]. - Anti-inflammatory: Modulates inflammatory pathways [102]. - Anticancer: Can inhibit cancer cell proliferation [106]. - Cardioprotective: Supports heart health [107].
Catechin	Flavonoid (Polyphenol)	- Antioxidant: Contributes to the overall antioxidant capacity [105]. - Anti-inflammatory: Helps reduce inflammation [108].
Gallocatechin	Flavonoid (Polyphenol)	- Antioxidant: Strong radical scavenging activity [105].

Table 2.1 continued from previoust page

Phytochemical Compound	**Class of Compound**	**Medicinal Properties & Biological Activities**
Myricetin	Flavonoid	- Antioxidant: Protects cells from oxidative damage[105]. - Antidiabetic: May help improve insulin sensitivity. Anticancer: Exhibits pro-apoptotic effects.
Azadiradione	Limonoid (Triterpenoid)	- Anti-inflammatory: Reduces inflammation [108]. - Antioxidant: Displays free radical scavenging ability [105].
Epoxyazadiradione	Limonoid (Triterpenoid)	- Antimicrobial: Active against bacteria and fungi [50]. - Anti-inflammatory: Potent anti-inflammatory agent [108].
Nimbolide	Limonoid (Triterpenoid)	- Potent Anticancer: One of the most promising neem compounds for inducing apoptosis and inhibiting metastasis in cancer cells. - Anti-inflammatory: Strong anti-inflammatory effects [108]. - Antibacterial: Effective against certain bacteria [50].
Mahmoodin	Limonoid (Triterpenoid)	- Antimicrobial: Effective against pathogenic bacteria and fungi [50].
Sodium Nimbidate	Derivative of Limonoid	- Anti-arthritic: Used in studies for its efficacy against arthritis.
Polysaccharides (e.g., Arabinogalactan)	Complex Carbohydrate	- Immunomodulatory: Stimulates the immune system. Antioxidant: Contributes to cellular protection by destroying ROS [105].

2.14 Medicinal Uses of *Azadirachta indica*

Azadirachta indica widely recognized as neem, is fundamental to traditional medicinal practices throughout the Indian subcontinent and beyond. Esteemed for more

than four thousand years, it is sometimes referred to as "the village pharmacy" because of the medicinal properties of its entire structure—leaves, seeds, bark, blossoms, and roots. Contemporary scientific research has thoroughly substantiated these conventional applications, demonstrating that *Azadirachta indica*'s effectiveness arises from a diverse array of bioactive chemicals. Prominent among them are limonoids such as azadirachtin, nimbin, nimbidin, nimbolide, and gedunin, in addition to flavonoids, tannins, and sterols. This note outlines the extensive pharmacological properties of *Azadirachta indica*, as evidenced by current research.

2.14.1 Antimicrobial Efficacy

Azadirachta indica demonstrates extensive antibacterial efficacy, rendering it a formidable weapon against bacteria, fungi, and viruses. Its antibacterial efficacy is efficient against both Gram-positive and Gram-negative bacteria, including multidrug-resistant strains of Staphylococcus aureus and Escherichia coli. The processes involve the breakdown of bacterial cell wall production and the interference with cellular signaling.

Azadirachta indica mouthwash has been clinically demonstrated to be as efficient as chlorhexidine in diminishing dental plaque and gingivitis, highlighting its practical utility. Its antifungal capabilities are notable against infections such as Candida albicans and different dermatophytes, while its antiviral potential has been investigated against viruses including dengue and coxsackie B, where it may impede viral reproduction [50].

2.14.2 Anti-inflammatory and Analgesic Properties

The anti-inflammatory and analgesic effects of *Azadirachta indica* are well - documented. Compounds like nimbidin and sodium nimbinate serve as principal mediators of this action, chiefly by inhibiting prostaglandin production and modulating

the nuclear factor-kappa B (NF-κB) pathway, a crucial regulator of inflammation. *Azadirachta indica* extracts in animal models have demonstrated effectiveness akin to traditional non-steroidal anti-inflammatory medicines (NSAIDs) such as indomethacin in alleviating edema and pain responses, hence substantiating its application in the treatment of illnesses including arthritis and fever [54].

2.14.3 Antidiabetic and Hypoglycemic Efficacy

Azadirachta indica is a notable herbal treatment for controlling diabetes mellitus. Extracts from leaves and seeds have exhibited substantial hypoglycemic effects in experimental diabetes models generated by alloxan and streptozotocin.

The postulated processes are numerous, encompassing the enhancement of insulin production from pancreatic β-cells, increased peripheral glucose consumption, and the suppression of intestinal α-glucosidase, hence diminishing carbohydrate absorption from the gut. Moreover, *Azadirachta indica* extract therapy has demonstrated an enhancement of the lipid profile in diabetic individuals, providing a twofold protective advantage against hyperglycemia and hyperlipidemia [54].

2.14.4 Antioxidant Efficacy

The elevated levels of flavonoids and phenolic chemicals in *Azadirachta indica*, including quercetin and catechin, provide significant free radical scavenging capabilities. The antioxidant capacity is essential for alleviating oxidative stress, a prevalent pathogenic element in chronic conditions such as diabetes, cancer, and cardiovascular illnesses.

Azadirachta indica leaf extract has demonstrated the ability to augment the activity of natural antioxidant enzymes such as superoxide dismutase (SOD), catalase (CAT), and glutathione in vivo, therefore safeguarding tissues against oxidative damage [53].

2.14.5 Antineoplastic and Anti-proliferative Activity

This is a very promising domain within *Azadirachta indica* research. Bioactive limonoids, specifically nimbolide and azadirachtin, have exhibited significant chemo preventive and anticancer properties in many in vitro and in vivo investigations. The anticancer mechanisms are multifaceted, encompassing the activation of apoptosis via the mitochondrial route, inhibition of cell growth, suppression of angiogenesis, and prevention of metastasis.

The anticancer mechanisms are multifaceted, encompassing the activation of apoptosis via the mitochondrial route, inhibition of cell growth, suppression of angiogenesis, and prevention of metastasis. Nimbolide has demonstrated significant effectiveness against cancer cell lines of the breast, prostate, colon, and cervix [1].

2.14.6 Hepatoprotective and Nephroprotective Efficacy

Azadirachta indica extracts provide substantial protection to the liver and kidneys against damage caused by numerous chemical poisons and pharmaceuticals. The hepatoprotective action against chemicals such as carbon tetrachloride and paracetamol is primarily ascribed to its antioxidant capabilities, which stabilize hepatocyte membranes and augment the activity of detoxifying enzymes, so reducing necrosis. *Azadirachta indica* has been demonstrated to mitigate nephrotoxicity caused by agents such as cisplatin, hence preserving renal function and structural integrity [109].

2.14.7 Immunomodulatory Activity

Azadirachta indica functions as a natural immunomodulatory, adept at both boosting and inhibiting the immune system as required. Research indicates that *Azadirachta indica* leaf extracts can augment the immune response by activating both cellular and humoral immunity, namely through the stimulation of macrophages and lymphocytes.

The immunostimulant effect may be advantageous in fighting infections. Conversely, some *Azadirachta indica* fractions have demonstrated immunosuppressive effects, which may be beneficial in the management of autoimmune illnesses and the prevention of organ transplant rejection; however, this needs additional clinical exploration [110].

2.15 Global Shift Toward Natural Remedies

The worldwide resurgence of natural medicines, sometimes referred to as a "return to nature," is not only a unique movement but a multifaceted confluence of historical, cultural, economic, and scientific influences. It signifies a significant reassessment of our connection to health, medicine, and the environment.

This transition fundamentally responds to the constraints and perceived shortcomings of the prevailing allopathic medical approach. Although contemporary medicine has accomplished remarkable feats, especially in acute care, surgical procedures, and infectious illnesses, its deficiencies have become more evident. The emergence of chronic, multifaceted ailments such as autoimmune disorders, metabolic syndrome, and certain malignancies, which resist a straightforward "one-pill-one-cure" solution, has prompted several individuals to pursue more holistic approaches.

The concerning crisis of antibiotic resistance, primarily caused by the excessive use of pharmaceutical antibiotics, has compelled both the public and the scientific community to seek alternatives; plant-based antimicrobials present a promising, multi-targeted solution that may mitigate resistance. The apprehension regarding significant adverse effects from synthetic medications exacerbates the situation. The prominent withdrawal of drugs and extensive descriptions of potential side effects in marketing have diminished unquestioning belief in pharmaceuticals. Numerous persons currently see natural medicines, due to their longstanding historic application, as milder and intrinsically safer, despite this belief not necessarily being scientifically substantiated [111].

A significant cultural and intellectual shift is concurrently occurring. We inhabit a period characterized by unparalleled access to knowledge and an expanding culture of self-advocacy. Patients have transitioned from being passive users of care to active participants in their health journeys. The internet enables individuals to investigate their ailments and possible treatments, prompting them to consider alternatives outside recommended ones. This corresponds with a wider societal trend emphasizing wellness, preventive, and holistic living. Individuals are progressively focusing on techniques that promote holistic well-being—such as mindfulness, organic nutrition, and natural supplements—rather than only addressing illness post-occurrence. This comprehensive worldview perceives the body as an interconnected system, a viewpoint that ancient healing practices such as Ayurveda and ancient Chinese Medicine have always upheld, and which profoundly resonates with individuals experiencing disconnection due to the specialization of contemporary healthcare [112].

This cultural transformation is supported by a robust and expanding body of scientific evidence. The phrase "return to nature" is rather deceptive since it suggests a withdrawal from scientific inquiry. The trend is progressively propelled by modern science. Pharmacognosy, the examination of medicinal substances obtained from natural sources, is a substantial discipline. Scientists can now isolate, analyze, and comprehend the processes of active chemicals in plants using advanced methods. The identification of the antimalarial agent artemisinin from sweet wormwood (Artemisia annua) and ongoing investigations into the anticancer attributes of chemicals such as curcumin and the *Azadirachta indica* limonoid nimbolide furnish a substantial evidentiary foundation. This study frequently substantiates that the synergistic interaction of several substances in a complete plant extract can be more efficacious and result in fewer adverse effects than a singular, isolated synthetic molecule, a principle referred to as polypharmacology [113].

Ultimately, economic and environmental factors are of considerable importance. In several low- and middle-income nations, pharmaceutical medications are prohibitively costly or unattainable. Locally developed natural medicines serve as a

vital and economical primary healthcare option for a significant segment of the global population. In affluent countries, the escalating expenses of healthcare and drugs are prompting people to choose more economical options for controlling chronic ailments. The development of synthetic medicines has a considerable ecological impact, encompassing chemical synthesis and pollution from unmetabolized medications in aquatic systems. A rising belief exists that plant-based medications are more sustainable and environmentally harmonious [113].

Chapter 3

Materials and Methods

3.1 Collection, Drying and Extract Preparation

The leaves of *Azadirachta indica* were obtained from the local market and thoroughly washed with tap water. The leaves were cleaned and then allowed to dry for 15–17 days at room temperature. To get a uniformly coloured powder, dried leaves were pulverised using a grinder. For extract preparation, the 5:1 ratio of methanol and dry powder was taken in reagent bottles and shaken for a whole day. The solution was then centrifuged, followed by filtration, and poured into petri dishes until it had evaporated. The final yield of the dried extract was calculated and it was stored at 4°C [114].

3.2 Phytochemical Screening

The phytochemical screening provides valuable information about the bioactive compounds present in *Azadirachta indica*. For identification, thin-layer chromatography (TLC) analysis was performed on silica gel plates. For fractionation, column chromatography was performed on silica gel and Diaion HP-20. The fractions obtained were mixed to super-fractions based upon TLC analysis and checked for their phenolic count and antioxidant potential by performing total

phenolic content and radical scavenging assay. Moreover, their anti-diabetic effectiveness was assessed by performing alpha-glucosidase and alpha-amylase assays. The ESIMS was performed for quantification of these super-fractions to ensure the phytochemicals present in them. All the organic solvents for the chromatographic separations and extractions were distilled before use and performed following the standard protocol with slight modifications [115].

3.2.1 Thin Layer Chromatography

Thin-layer chromatography is a widely used technique for separating and analyzing compounds in a mixture. The procedure began with the preparation of a TLC plate coated with silica gel. A small amount of the sample solution, i.e., methanolic extract of *Azadirachta indica* was applied as a spot near the bottom of the plate using a capillary tube. Care was taken to ensure that the spot is small and concentrated. Once the sample is applied, the plate is placed upright in a developing chamber containing a shallow layer of solvent or mobile phase that is appropriate for the compounds being analyzed [116].

Different solvent systems were tried to check whether the compounds show polar or non-polar behaviour. One of them is n-hexane: ethyl acetate. In this solvent system, n-Hexane is non-polar, and ethyl acetate is moderately polar. This mixture is used to achieve a balance between non-polar and moderately polar compounds. It helps in separating compounds that range in polarity, allowing for effective resolution of mixtures containing both polar and non-polar substances. Different ratios were tried to fine-tune the separation [117].

Dichloromethane: Methanol was also used as a solvent system. Dichloromethane is moderately polar and effective for separating a range of compounds, particularly non-polar to moderately polar substances, while methanol is highly polar, which enhances the separation of polar compounds [118]. In n-hexane: chloroform, n-hexane is a non-polar solvent, effective for separating non-polar compounds. It has low interaction with polar stationary phases, while chloroform is moderately polar, which helps in separating compounds that exhibit some polarity [119]. In

chloroform: methanol, chloroform is moderately polar, and methanol is highly polar. This combination is particularly effective for separating polar compounds. The increasing polarity of methanol enhances the movement of polar analytes, while chloroform aids in moderating interactions with the stationary phase. This mixture is useful for compounds that exhibit strong polar characteristics [120]. The selected solvent systems for TLC of *Azadirachta indica*, along with ratios and usefulness based upon separation of polar, moderate or non-polar substances, are shown in table 3.1.

TABLE 3.1: TLC solvent systems used for *Azadirachta indica* along with ratios and usefulness [121]

S.No	Solvent Systems Used	Ratios	Usefulness of the selected ratios
1	n-hexane: ethyl acetate	5:05	A balanced polarity that can separate moderately polar compounds
2	n-hexane: ethyl acetate	1:10	More polar, suitable for separating polar compounds that require a stronger solvent to move
3	n-hexane: ethyl acetate	10:01	Less polar, ideal for non-polar compounds
4	Dichloromethane: Methanol	5:05	This ratio creates a solvent system that is neither too polar nor too non-polar, providing a balanced environment for the separation of a wide variety of compounds
5	n-hexane: Chloroform	9:01	The 9:1 ratio favors n-hexane, making the solvent system predominantly non-polar. This is beneficial for separating non-polar compounds
6	Chloroform: Methanol	100% M	Methanol is highly polar, making it excellent for separating very polar compounds
7	Chloroform: Methanol	1:01	This ratio allows both polar and non-polar compounds to be separated. It's useful for compounds that have intermediate polarity
8	Chloroform: Methanol	5:01	This ratio leans towards non-polarity while still allowing some interaction with polar compounds. It is effective for moderately polar substances

Table 3.1 continued from previous page

S.No	Solvent Systems Used	Ratios	Usefulness of the selected ratios
9	Chloroform: Methanol	9:01	It provides a slight preference towards non-polarity, useful for separating a range of moderately polar to non-polar compounds
10	Chloroform: Methanol	10:01	This ratio can effectively resolve a wide range of polarities, facilitating better resolution of polar compounds
11	Chloroform: Methanol	15:01	It is useful for separating compounds with higher polar interactions
12	Chloroform: Methanol	20:01	It is suitable for compounds with low to moderate polarity. It allows for slower movement, which can help achieve better separation of compounds
13	Chloroform: Methanol	30:01:00	Very non-polar, useful for separating non-polar compounds or those with minimal polarity
14	Chloroform: Methanol	1:05	This ratio favors polar interactions, effectively separating polar compounds while reducing the mobility of non-polar substances
15	Chloroform: Methanol	1:10	This ratio enhances the separation of polar analytes, making it ideal for compounds with strong polar characteristics
16	Chloroform: Methanol	1:20	This is best for very polar compounds. The high proportion of methanol ensures that polar analytes are effectively mobilized
17	Chloroform: Methanol	100% C	Chloroform is moderately polar, using it in 100% allows for the separation of non-polar compounds

These solvents gradually ascended the plate through capillary action, carrying the sample with them. As the solvent moved, the different components of the sample separated based on their affinities for the stationary phase (the silica gel) and the mobile phase (the solvent). Once the solvent front reached a predetermined

height, the plate was removed and allowed to dry. Visualization of the separated compounds was achieved using UV light and by applying Wagner's and Dragendorff staining reagents. The positions of the compounds were marked, and the retention factor (Rf value) was calculated by measuring the distance traveled by each compound relative to the solvent front [122].

3.2.2 Column Chromatography

Column chromatography was performed by preparing the column by cleaning it thoroughly and adding a small amount of the mobile phase to the bottom to prevent the stationary phase from drying out. Next, the column was packed with the stationary phase, such as silica gel, by using a funnel to ensure a uniform layer formation. The mobile phase was added continuously to saturate the stationary phase and to eliminate air bubbles. The sample was prepared by dissolving it in a small amount of the mobile phase and filtering it to remove insoluble particles. Carefully sample was loaded onto the stationary phase and adsorbed for a few minutes. Elution began by adding the mobile phase at a steady flow rate, collecting the eluent in fractions using test tubes. Separation was monitored with TLC to track the progress and identify distinct components. Fractions were collected and combined to make super-fractions based on TLC analysis [123].

3.2.2.1 Bioactivity Assays

i. Radical Scavenging Assay

The antioxidant activity of column chromatography super-fractions of *Azadirachta indica* was evaluated using the DPPH free radical scavenging assay [124]. The experiment was conducted by using 0.004% (w/v) DPPH solution prepared in methanol. For this purpose, 1mg/1ml dilution of each super-fraction was prepared by taking 1mg of dried fraction in 1ml of methanol. 100μL of each dilution was mixed with 3ml DPPH. The methanolic leaf extract of *Azadirachta indica* was gradually added to the DPPH solution, resulting in gradual shift in the solution's

color to pale yellow from deep violet. The reduction of DPPH's purple color in test samples indicates the antioxidant action. The DPPH solution was left undisturbed for thirty minutes in order to verify its stability. Throughout the experiment, the solution's color remained unchanged, indicating that DPPH's maximal stability had occurred. The absorption intensity of the solution was measured using a spectrophotometer at 517 nm. The antioxidant activity percentage was calculated using the following formula.

$$Scavengingpercentage = [(A_{control} - A_{sample})/A_{control}] \times 100$$

A_{sample} is the treatment with plant fraction absorbance is at 517 nm. $A_{control}$ is the sample's absorbance at 517 nm without plant fraction.

ii. Total Phenolic Assay

Phenolic compounds are family of antioxidant agents that may both adsorb and neutralize free radicals. The method used to observe the TPC of the *Azadirachta indica* super-fractions was FC [125]. Gallic acid was used as standard. 10% FC reagent was mixed with 7.5% Na_2CO_3. It was further mixed with gallic acid (0-12 ppm) and incubated at 45°C for 45 minutes in incubator. It was followed by measuring absorbance at 765 nm. By using gallic acid a calibration curve was created. The standard curve was used to create a regression equation, which was then used to quantify the amount of gallic acid in the *Azadirachta indica* super-fractions. Phenolic concentrations were measured by mixing 270 μL of each super-fraction dilution with 10% FC reagent and 7.5% Na_2CO_3. The absorbance was again measured at 765 nm.

iii. Inhibition of Alpha-amylase

Alpha-amylase is involved in starch digestion, and its inhibition can have significant implications for diabetes management and food processing. Here we investigated the inhibitory effects of super-fractions of *Azadirachta indica* against

alpha amylase activity by mixing 125 μL phosphate buffer (pH 6.9), 250 μL super-fraction dilution and 250 μL alpha-amylase enzyme (0.5 mg/mL).

It was pre-incubated at 25°C for 10 minutes. Then 250 μL of 1% starch in 0.02 M sodium phosphate buffer (pH 6.9) was added and incubated again at 25°C for 10 minutes. Reaction was stopped by adding 0.5ml DNSA reagent, After five minutes of incubation in a boiling water bath, it was allowed to cool to room temperature. Five milliliters of distilled water were then added to the reaction mixture to dilute it. Acarbose was used as the positive control [126]. Absorbance was measured at 540 nm and percentage of inhibition was calculated using the following formula.

Absorbance was measured at 540 nm and percentage of inhibition was calculated using the following formula.

$$Alpha - amylaseinhibitionpercentage = [(A_{control} - A_{sample})/A_{control}] \times 100$$

A_{sample} is the treatment with plant fraction absorbance is at 540 nm. $A_{control}$ is the sample's absorbance at 540 nm without plant fraction.

iv. Inhibition of Alpha-glucosidase

To perform alpha-glucosidase assay, a mixture of 50 μl of each *Azadirachta indica* super-fraction and 100 μL of 0.1 M phosphate buffer (pH 6.9) containing 50 μL α-glucosidase solution was taken in a cuvette and incubated at 25°C for 10 min. After preincubation, 50 μL of 5 Mm PNPG solution in 0.1 M phosphate buffer (pH 6.9) was added to each cuvette. The reaction mixtures were incubated at 25°C for 5 min. Before and after incubation, absorbance was recorded at 405 nm by a spectrophotometer. Acarbose was used as the positive control [127]. The percentage of inhibition was calculated using the following formula.

$$Alpha - glucosidase\ inhibition\ percentage = [(A_{control} - A_{sample})/A_{control}] \times 100$$

A_{sample} is the treatment with plant fraction absorbance is at 405 nm. $A_{control}$ is the sample's absorbance at 405 nm without plant fraction.

3.2.3 Electrospray Ionization Mass Spectrometry

ESIMS works by applying a high voltage to a liquid sample to produce charged droplets, which lose solvent and release gas-phase ions that are analyzed according to their mass-to-charge ratio, allowing soft ionization of polar and thermally unstable compounds [128].

The apparatus used for LCMS analysis was a Triple Quadrupole Mass Spectrometer, model: TSQ Quantis (Thermo Electron Scientific, USA) equipped with a heated electrospray ionization (H-ESI) source. In this method, methanol was employed as the solvent for sample preparation, and samples were introduced through a direct insertion technique. The capillary voltage was set to 80 kV to optimize ion generation. The sheath gas flow rate was configured at 15 units, complemented by an auxiliary gas flow rate of 5 units. Scanning occurred at a rate of 30 to 1500 m/z, and the capillary temperature is held at 275 °C.

Ionization was achieved using heated electro spray ionization, which effectively converts the samples into ions for detection. During the fragmentation phase of the MS/MS operation, multiple peaks were selected for analysis, with collision energies varying between 10 to 40 V. Xcalibur software was used for data collection. Samples were prepared with meticulous care, and the instrument was calibrated beforehand to ensure both accuracy and repeatability in the results. Data analysis was performed by carefully observing relative abundances and verifying fragmentation patterns of both positive and negative modes of MS/MS spectra for each super-fraction by using ChemDraw Ultra 12.0 software [128].

3.3 In silico Evaluation of *Azadirachta indica* Phytocompounds

The phytochemicals obtained from each super-fraction that underwent LC-MS analysis were evaluated for their anti-diabetic potential. It was done by checking

their binding affinity against selected target proteins that are involved in the impairment of normal glucose metabolism. Ligands were taken from Pubchem (pubchem.ncbi.nlm.nih.gov/) and refined in Chem3D pro while proteins were accessed through PDB (www.rcsb.org) and Alphafold (alphafold.ebi.ac.uk) and prepared in PyMol (pymol.org). The Protparam (web.expasy.org/protparam/) was used for protein's physicochemical properties, while ligand's druglikeness attributes were checked by online server pkCSM (omictools.com/pkcsm-tool). Active sites of proteins were checked by the DogSiteScorer (proteins.plus/dogsite). Molecular docking was performed by using the CB Dock server (clab.labshare.cn/blinddock.php) and receptor-ligand interactions were analyzed by Discovery Studio 2025 Client [129]. It was followed by identification of lead compound which was further compared with standard anti-diabetic drug.

Chapter 4

Results

4.1 Collection and Drying of *Azadirachta indica*

The leaves of *Azadirachta indica* were obtained from the local market and thoroughly washed with tap water. The leaves were cleaned and then allowed to dry for 15–17 days at room temperature. To obtain a uniformly colored powder, the dried leaves were pulverized using a grinder. The weight of dried powder was 628 grams.

4.2 Extract Preparation

The effect of three extraction process factors: the methanol concentration, powder concentration and extraction time was evaluated. The protocol criteria were taken into consideration when selecting the factorial levels. In multiple reagent bottles, methanol and plant powders were mixed in a 5:1 ratio, and these bottles were placed on a shaker for 24 hours, respectively. Then the solutions were filled in 50mg falcon tubes for centrifugation which was carried out at 4000 rpm for 10 minutes. The supernatants (extracts) were separated from the pellet through filtration. The filtered extracts of *Azadirachta indica* were taken in large petri dishes and placed at room temperature for the given period of time. It took 5-7 days to evaporate

the solvent at room temperature and a greenish-black dry extract was obtained. The yield of total extract is 22.09 grams, while the percentage yield is 3.51 grams. Then up to the time of additional testing, these extracts were stored at 4°C. Figure 4.1 (a-f) represents all steps of extract preparation.

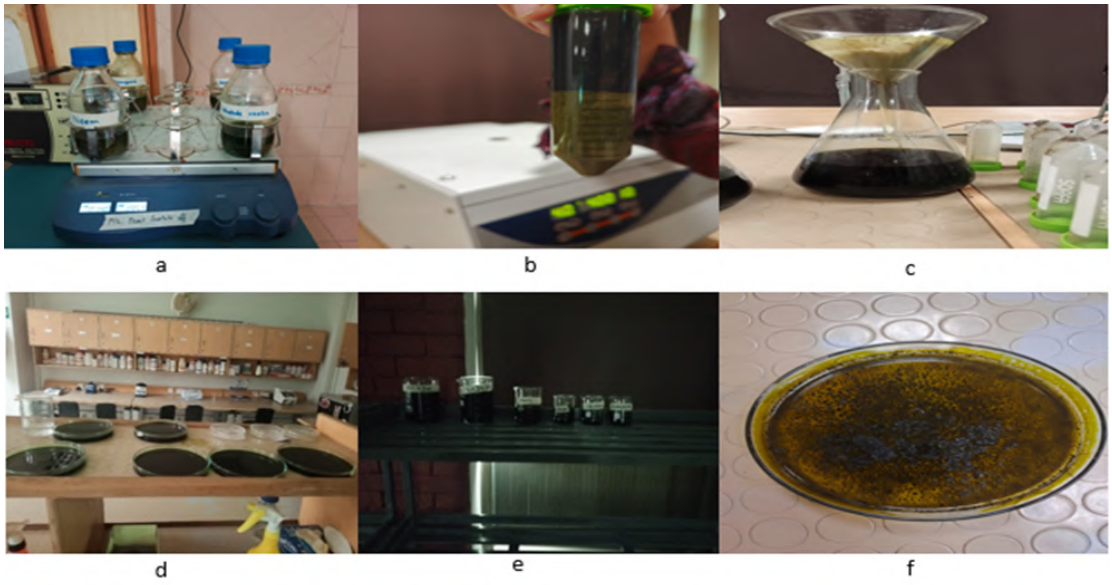

FIGURE 4.1: Extract preparation (a) Shaking (b) centrifugation (c) filtration (d) evaporation (e) dark-greenish extract (f) concentrated extract for use in experiments

4.3 Phytochemical Screening

For phytochemical screening of *Azadirachta indica*, thin layer chromatography, column chromatography, and LCMS were performed.

4.3.1 Thin Layer Chromatography

Thin-layer chromatography of *Azadirachta indica* was performed by taking different concentrations of the solvent systems, i.e., chloroform/methanol, n-hexane/chloroform, dichloromethane/methanol and n-hexane/ethyl acetate. The plant's response to these varying solvents was observed in visible light, UV366nm, UV254 nm and staining reagent. TLC bands detection after dye treatment was also analyzed. Compounds having Rf values between 0.01-0.2 are highly polar while

0.3-0.6 are moderately polar. Compounds having Rf values between 0.7 and 0.8 are considered less polar, while Rf values above 0.8 are non-polar compounds. The chromatograms with all these observations are shown in the figures below.

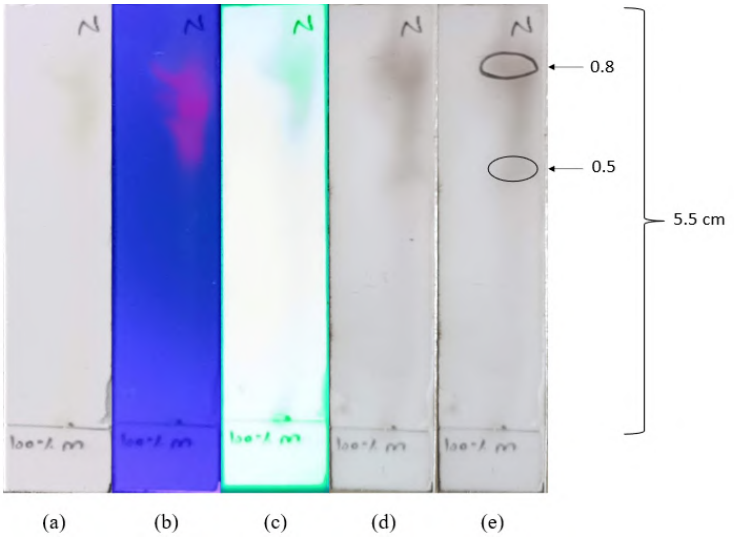

FIGURE 4.2: TLC chromatogram of *Azadirachta indica* 100% methanol (a) visible light (b) UV 360nm (c) UV 254nm (d) dye-treated plate (e) detection of bands with Rf value

Representative silica TLC separations of *Azadirachta indica* extract are shown in figure 4.2. Separation of the extract in 100% methanol over 5.5 cm resulted in two bands with Rf values of 0.5 and 0.8, indicating the presence of moderately polar to less polar compounds.

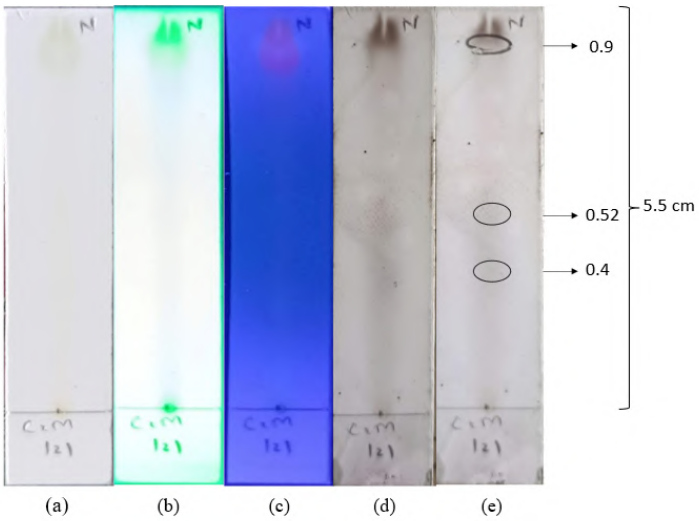

FIGURE 4.3: TLC chromatogram of *Azadirachta indica* with chloroform:methanol of ratio 1:1 (a) visible light (b) UV 360nm (c) UV 254nm (d) dye-treated plate (e) detection of bands with Rf value

Figure 4.3 shows that separation of the extract in chloroform:methanol 1:1 over 5.5 cm resulted in three bands with Rf value 0.4, 0.52 and 0.9, indicating the presence of moderately polar to non- polar compounds.

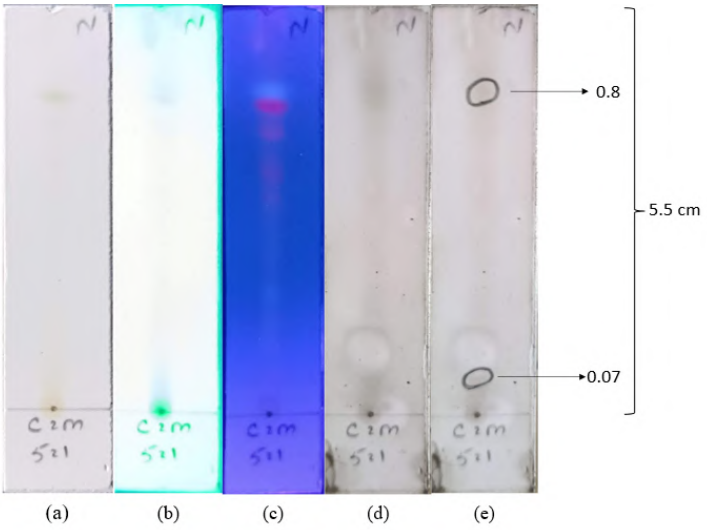

FIGURE 4.4: TLC chromatogram of *Azadirachta indica* with chloroform:methanol of ratio 5:1 (a) visible light (b) UV 360nm (c) UV 254nm (d) dye-treated plate (e) detection of bands with Rf value

Figure 4.4 shows that separation of the extract in chloroform:methanol 5:1 over 5.5 cm resulted in two bands with Rf values 0.07 and 0.8, indicating the presence of polar and less polar compounds.

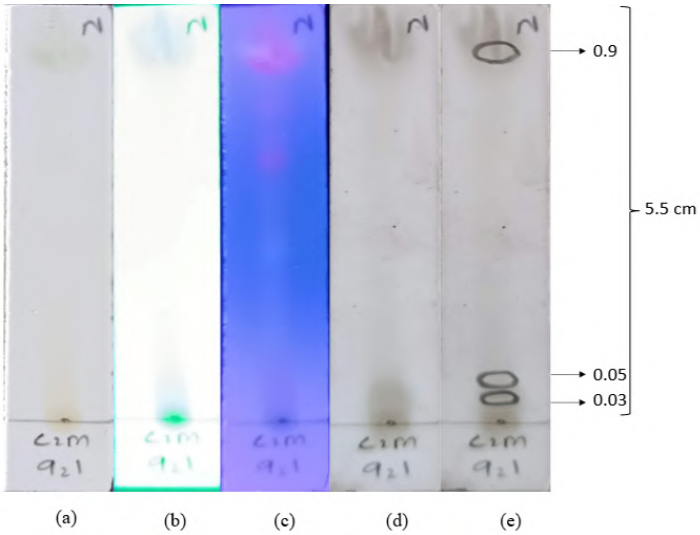

FIGURE 4.5: TLC chromatogram of *Azadirachta indica* with chloroform:methanol of ratio 9:1 (a) visible light (b) UV 360nm (c) UV 254nm (d) dye-treated plate (e) detection of bands with Rf value

Figure 4.5 shows that separation of the extract in chloroform:methanol 9:1 over 5.5 cm resulted in three bands with Rf values 0.03, 0.05 and 0.9, indicating the presence of highly polar and non-polar compounds.

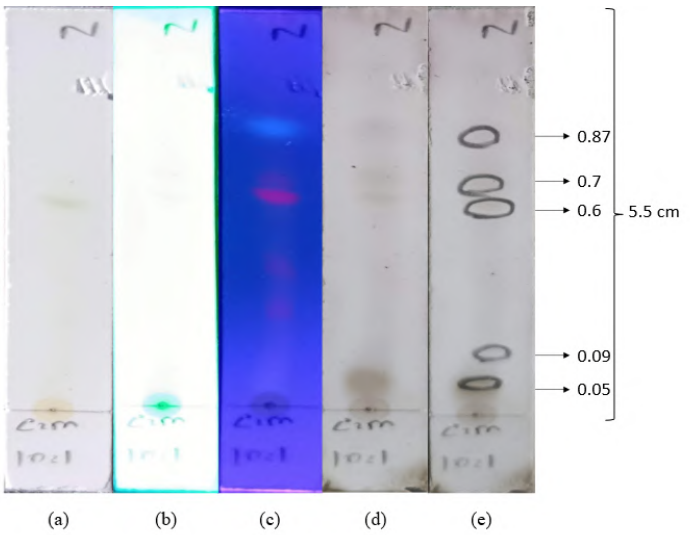

FIGURE 4.6: TLC chromatogram of *Azadirachta indica* with chloroform:methanol of ratio 10:1 (a) visible light (b) UV 360nm (c) UV 254nm (d) dye-treated plate (e) detection of bands with Rf value

Figure 4.6 shows that separation of the extract in chloroform:methanol 10:1 over 5.5 cm resulted in five bands with Rf values 0.05, 0.09, 0.6, 0.7 and 0.87, indicating the presence of highly polar to moderate and less polar compounds.

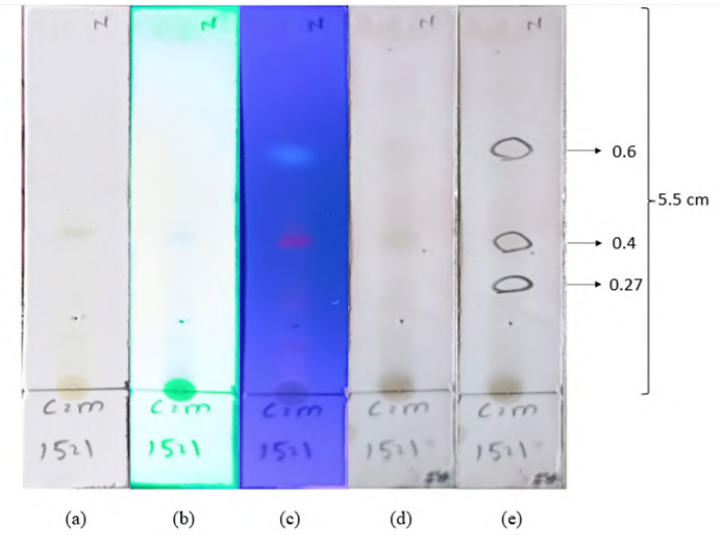

FIGURE 4.7: TLC chromatogram of *Azadirachta indica* with chloroform:methanol of ratio 15:1 (a) visible light (b) UV 360nm (c) UV 254nm (d) dye-treated plate (e) detection of bands with Rf value

Figure 4.7 shows that separation of the extract in chloroform:methanol 15:1 over 5.5 cm resulted in three bands with Rf values 0.27, 0.4 and 0.6, indicating the presence of polar to moderate polar compounds.

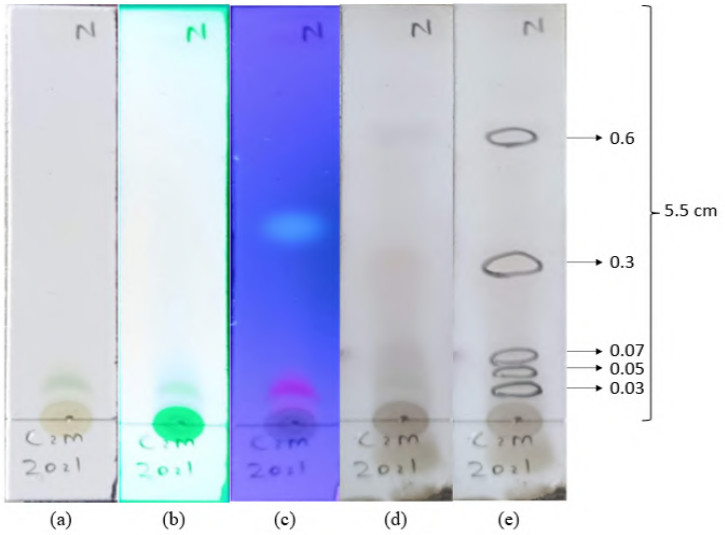

FIGURE 4.8: TLC chromatogram of *Azadirachta indica* with chloroform:methanol of ratio 20:1 (a) visible light (b) UV 360nm (c) UV 254nm (d) dye-treated plate (e) detection of bands with Rf value

Figure 4.8 shows that separation of the extract in chloroform:methanol 20:1 over 5.5 cm resulted in five bands with Rf values 0.03, 0.05, 0.07, 0.3 and 0.6, indicating the presence of highly polar to moderate polar compounds.

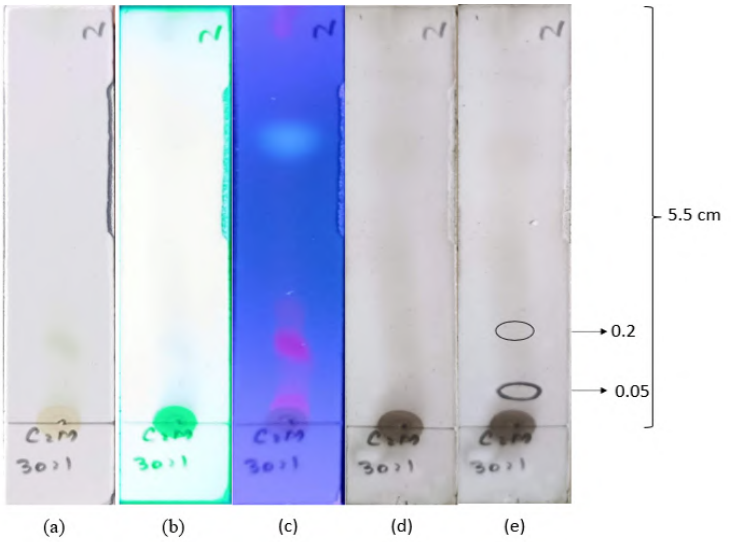

FIGURE 4.9: TLC chromatogram of *Azadirachta indica* with chloroform:methanol of ratio 30:1 (a) visible light (b) UV 360nm (c) UV 254nm (d) dye-treated plate (e) detection of bands with Rf value

Figure 4.9 shows that separation of the extract in chloroform:methanol 30:1 over 5.5 cm resulted in two bands with Rf value 0.05 and 0.2, indicating the presence of highly polar compounds.

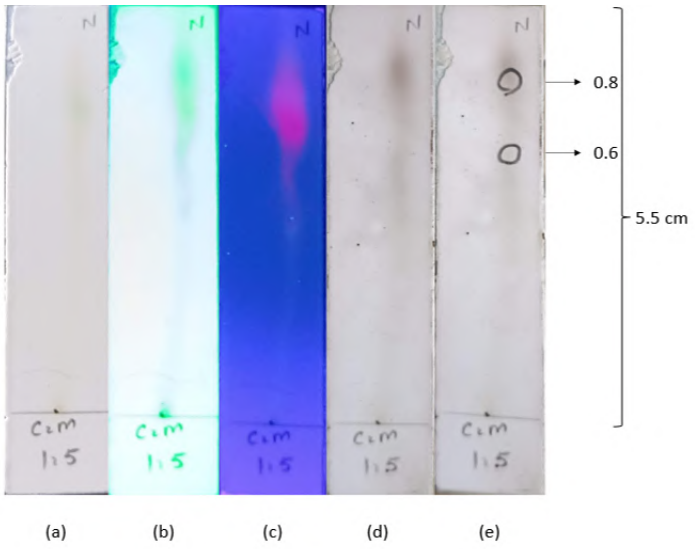

FIGURE 4.10: TLC chromatogram of *Azadirachta indica* with chloroform:methanol of ratio 1:5 (a) visible light (b) UV 360nm (c) UV 254nm (d) dye-treated plate (e) detection of bands with Rf value

Figure 4.10 shows that separation of the extract in chloroform:methanol 1:5 over 5.5 cm resulted in two bands with Rf values 0.6 and 0.8, indicating the presence of moderately polar to less polar compounds.

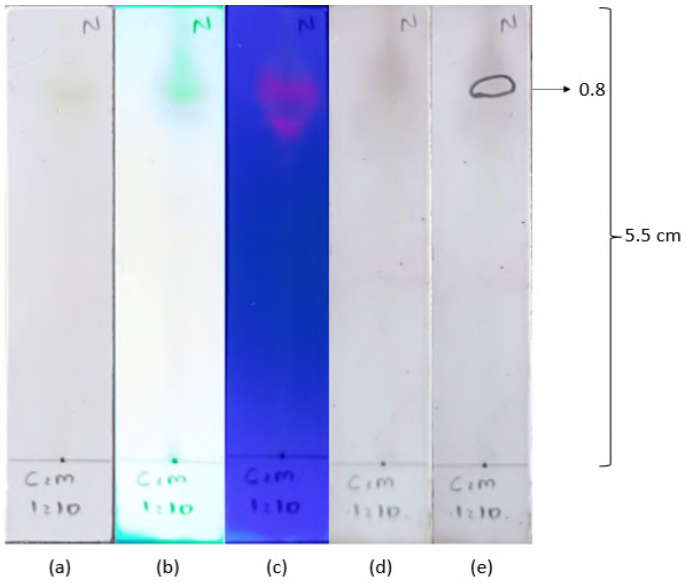

FIGURE 4.11: TLC chromatogram of *Azadirachta indica* with chloroform:methanol of ratio 1:10 (a) visible light (b) UV 360nm (c) UV 254nm (d) dye-treated plate (e) detection of bands with Rf value

Figure 4.11 shows that separation of the extract in chloroform:methanol 1:10 over 5.5 cm resulted in one band with Rf value 0.8, indicating the presence of less polar compound.

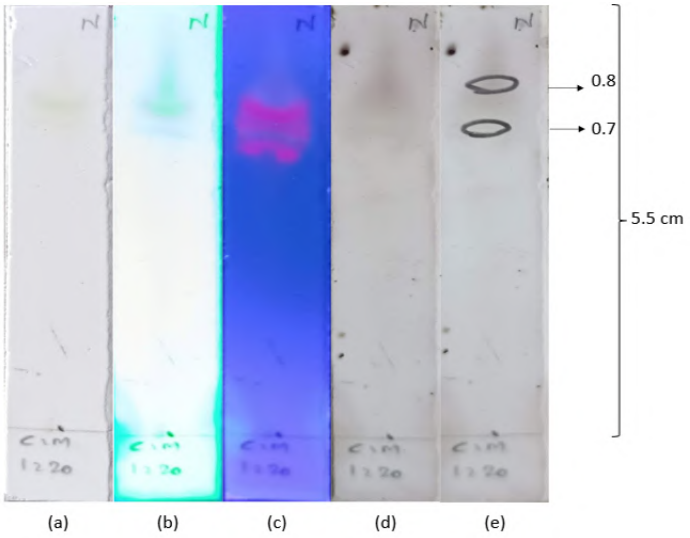

FIGURE 4.12: TLC chromatogram of *Azadirachta indica* with chloroform:methanol of ratio 1:20 (a) visible light (b) UV 360nm (c) UV 254nm (d) dye-treated plate (e) detection of bands with Rf value

Figure 4.12 shows that separation of the extract in chloroform:methanol 1:20 over 5.5 cm resulted in two bands with Rf values 0.7 and 0.8, indicating the presence of less polar compounds.

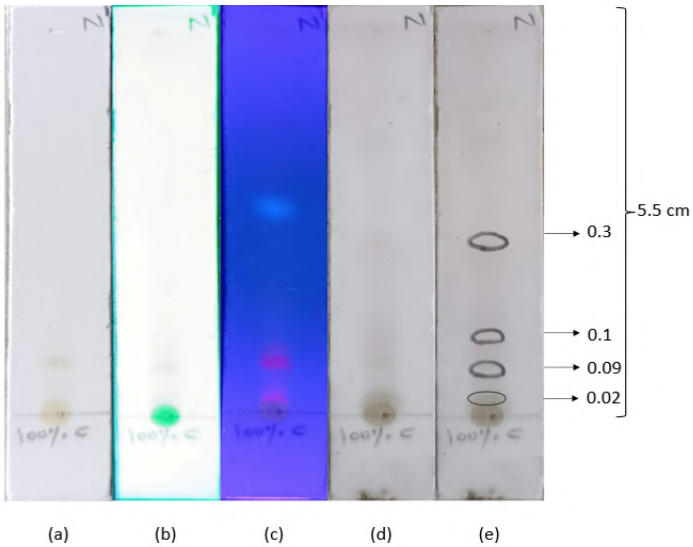

FIGURE 4.13: TLC chromatogram of *Azadirachta indica* with 100% chloroform (a) visible light (b) UV 360nm (c) UV 254nm (d) dye-treated plate (e) detection of bands with Rf value

Figure 4.13 shows that separation of the extract in 100% chloroform over 5.5 cm resulted in four bands with Rf values 0.02, 0.09, 0.1 and 0.3, indicating the presence of highly polar to polar compounds.

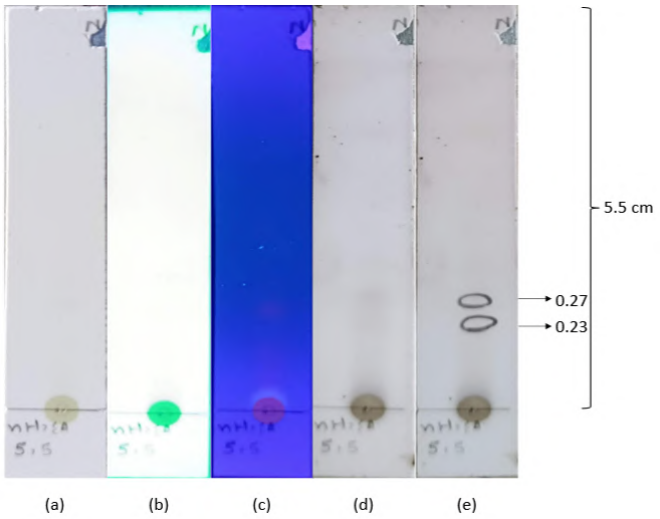

FIGURE 4.14: TLC chromatogram of *Azadirachta indica* with n-hexane:ethyl acetate of ratio 5:5 (a) visible light (b) UV 360nm (c) UV 254nm (d) dye-treated plate (e) detection of bands with Rf value

Figure 4.14 shows that separation of the extract in n-hexane:ethyl acetate 5:5 over 5.5 cm resulted in two bands with Rf values 0.23 and 0.27, indicating the presence of polar compounds.

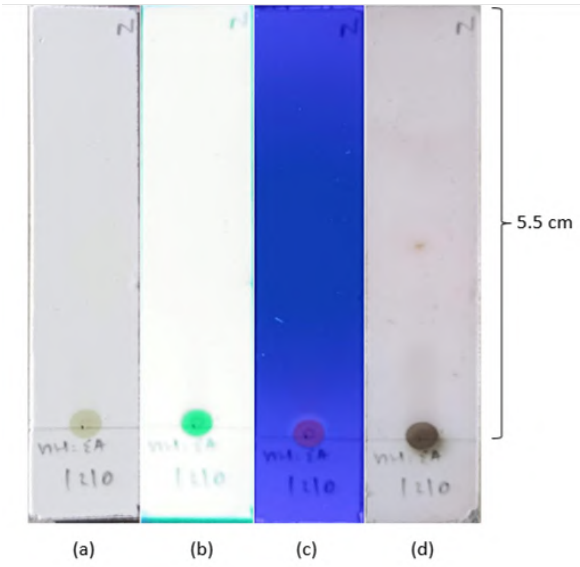

FIGURE 4.15: TLC chromatogram of *Azadirachta indica* with n-hexane:ethyl acetate of ratio 1:10 (a) visible light (b) UV 360nm (c) UV 254nm (d) dye-treated plate

Figure 4.15 shows that in n-hexane:ethyl acetate 1:10 over 5.5 cm distance, there is no separation of compounds as no band is visible in any UV light or dye-treated TLC plate, indicating that the n-hexane:ethylacetate with 1:10 is not suitable for *Azadirachta indica* extract.

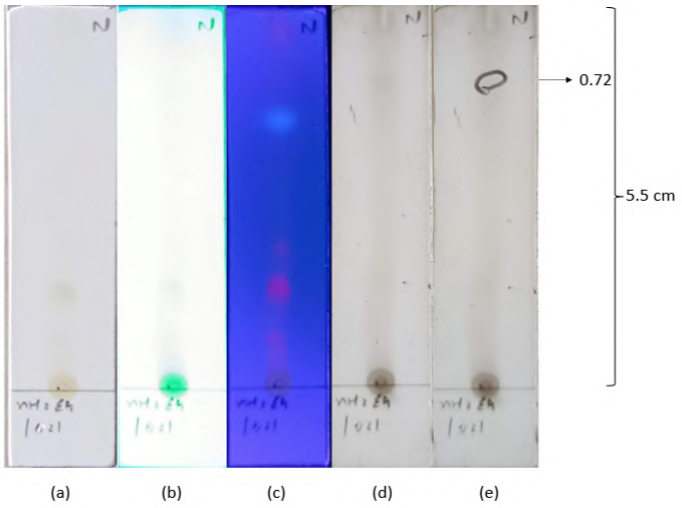

FIGURE 4.16: TLC chromatogram of *Azadirachta indica* with n-hexane:ethyl acetate of ratio 10:1 (a) visible light (b) UV 360nm (c) UV 254nm (d) dye-treated plate (e) detection of bands with Rf value

Figure 4.16 shows that separation of the extract in n-hexane:ethyl acetate 10:1 over 5.5 cm resulted in only one band with Rf value 0.72, indicating the presence of less polar compound.

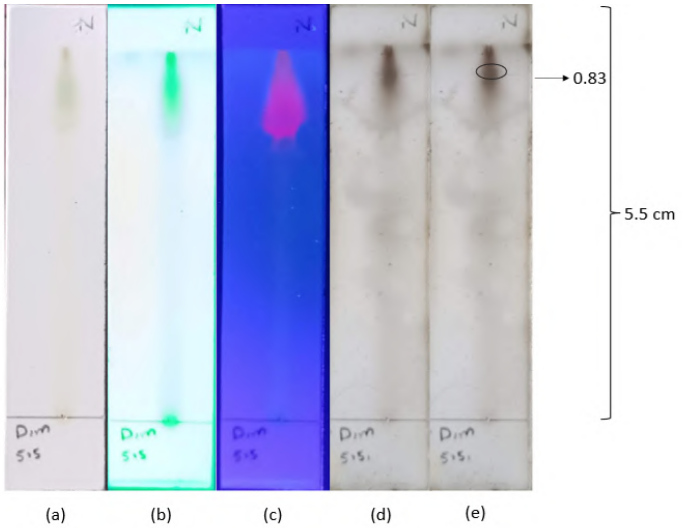

FIGURE 4.17: TLC chromatogram of *Azadirachta indica* with di chloro methane : methanol of ratio 5:5 (a) visible light (b) UV 360nm (c) UV 254nm (d) dye-treated plate (e) detection of bands with Rf value

Figure 4.17 shows that separation of the extract in dichloromethane:methanol 5:5 over 5.5 cm resulted in only one band with Rf value 0.83, indicating the presence of less polar compound.

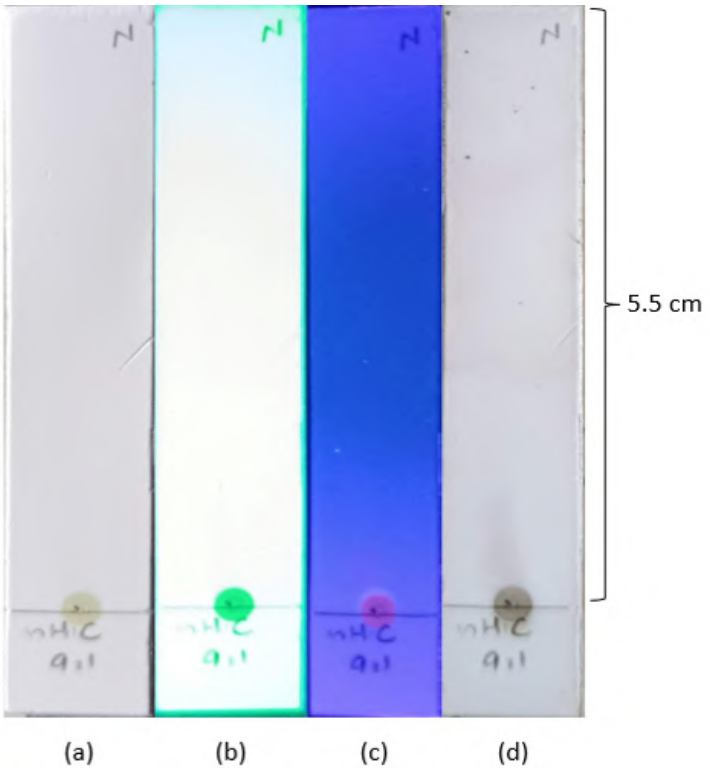

FIGURE 4.18: TLC chromatogram of *Azadirachta indica* with n-hexane: chloroform of ratio 9:1 (a) visible light (b) UV 360nm (c) UV 254nm (d) dye-treated plate

Figure 4.18 shows that in n-hexane:chloroform 9:1 over 5.5 cm distance, there is no separation of compounds as no band is visible in any UV light or dye-treated TLC plate, indicating that the n-hexane:chloroform with 9:1 is not suitable for *Azadirachta indica* extract.

A detailed analysis of the above chromatograms shows that different ratios of n-hexane/chloroform, dichloromethane/methanol, and n-hexane/ethyl acetate were tried, but they didn't show any variety of compounds, and some showed no bands, thus indicating that these are not suitable solvent systems for compound analysis of *Azadirachta indica*. The chloroform/methanol proved as good solvent system for *Azadirachta indica*, as its different ratios gave potential results with a variety of highly polar to moderately polar and less polar compounds, showing that this

solvent system can be used for further analysis of *Azadirachta indica* phytocompounds.

4.3.2 Column Chromatography

After performing the TLC of *Azadirachta indica* with several solvent systems, column chromatography was initiated. As *Azadirachta indica* showed good results with chloroform/methanol ratios, so this solvent system was used further for column chromatography. 10 grams of *Azadirachta indica* concentrated extract was used for the column chromatography and different combinations of chloroform/methanol were used i.e., 100% methanol, C:M 1:5, 1:10, 1:20, 5:1, 10:1, 20:1, 1:1 and 100% chloroform. The mobile phase of different proportions of this solvent system was allowed to flow down and was collected as fractions as shown in the figure 4.19.

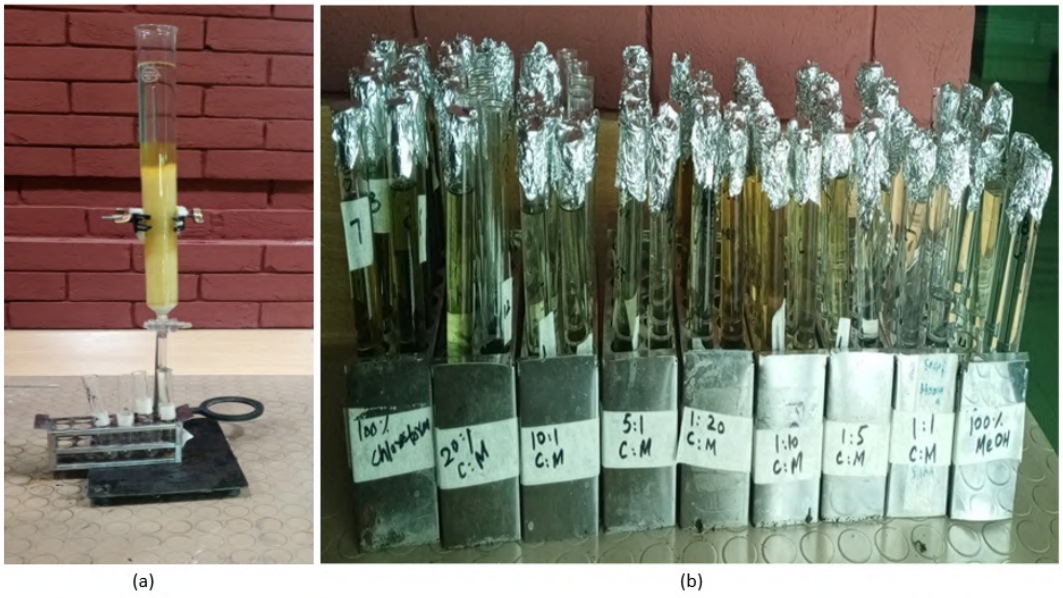

FIGURE 4.19: Column chromatography of *Azadirachta indica* (a) column packed with solvent system (b) fractions of all combinations

As nine combinations were used to run the column, there was a total of nine fractions obtained. Each fraction consists of four 20ml test tubes. These fractions were further analyzed by TLC with a solvent system of chloroform/methanol with

a ratio of 10:1. The chromatograms obtained were visualized in visible light, UV 360 and UV 254. Band detection was done by application of dye and Rf values were calculated as shown in figures below.

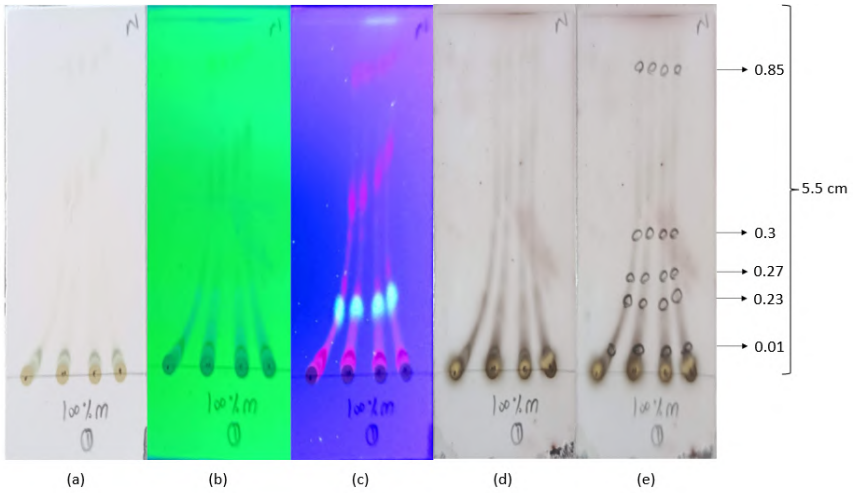

FIGURE 4.20: TLC chromatogram of *Azadirachta indica* with 100% methanol (a) visible light (b) UV 360nm (c) UV 254nm (d) dye-treated plate (e) detection of bands with Rf value

Figure 4.20 shows that separation of the extract in 100% methanol over 5.5 cm resulted in five bands with Rf values 0.01, 0.23, 0.27, 0.3 and 0.85, indicating the presence of highly polar to less polar compounds.

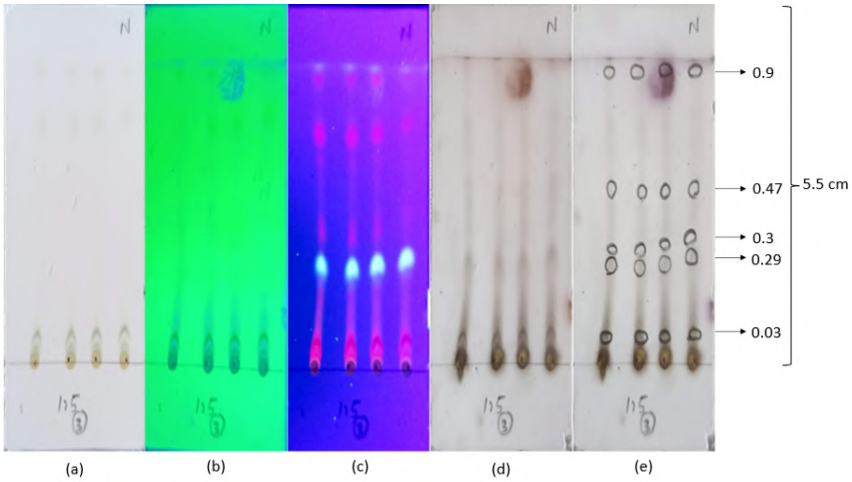

FIGURE 4.21: TLC chromatogram of *Azadirachta indica* with chloroform:methanol of ratio 1:5 (a) visible light (b) UV 360nm (c) UV 254nm (d) dye-treated plate (e) detection of bands with Rf value

Figure 4.21 shows that separation of the extract in chloroform:methanol 1:5 over 5.5 cm resulted in five bands with Rf values 0.03, 0.29, 0.3, 0.47 and 0.9, indicating the presence of highly polar to moderately polar and non-polar compounds.

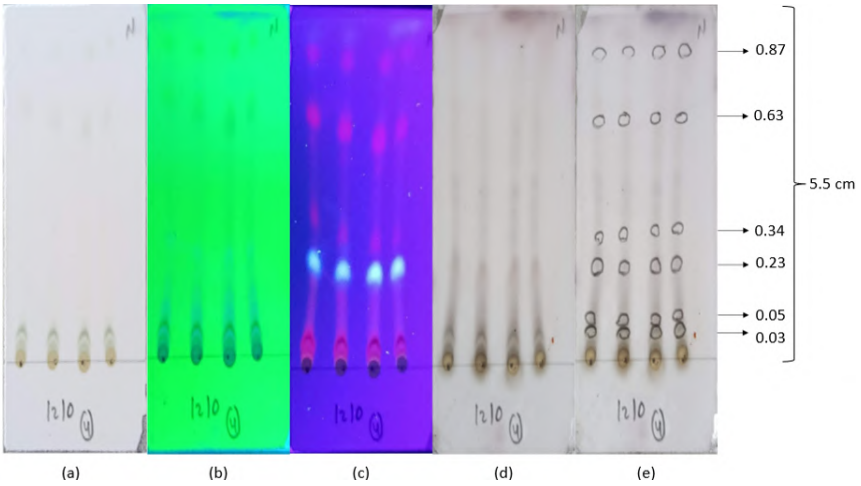

FIGURE 4.22: TLC chromatogram of *Azadirachta indica* with chloroform:methanol of ratio 1:10 (a) visible light (b) UV 360nm (c) UV 254nm (d) dye-treated plate (e) detection of bands with Rf value

Figure 4.22 shows that separation of the extract in chloroform:methanol 1:10 over 5.5 cm resulted in six bands with Rf values 0.03, 0.05, 0.23, 0.34, 0.63 and 0.87, indicating the presence of highly polar to moderately polar and non-polar compounds.

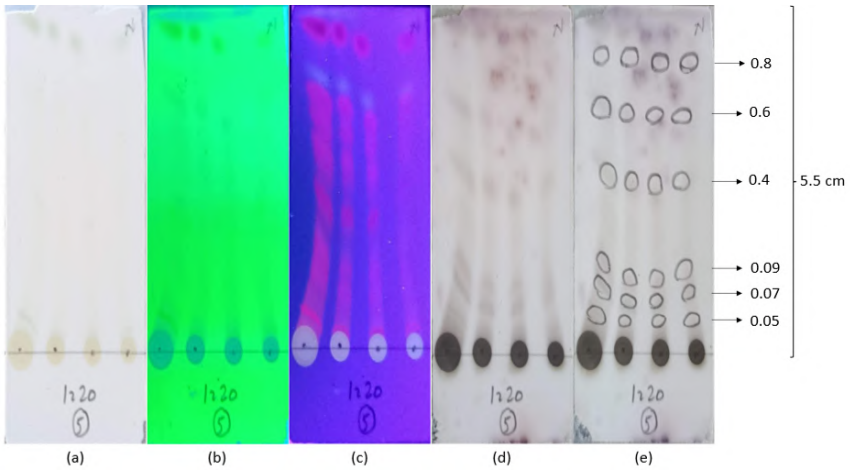

FIGURE 4.23: TLC chromatogram of *Azadirachta indica* with chloroform:methanol of ratio 1:20 (a) visible light (b) UV 360nm (c) UV 254nm (d) dye-treated plate (e) detection of bands with Rf value

Figure 4.23 shows that separation of the extract in chloroform:methanol 1:20 over 5.5 cm resulted in six bands with Rf values 0.05, 0.07, 0.09, 0.4, 0.6 and 0.8, indicating the presence of highly polar to moderately polar and less polar compounds.

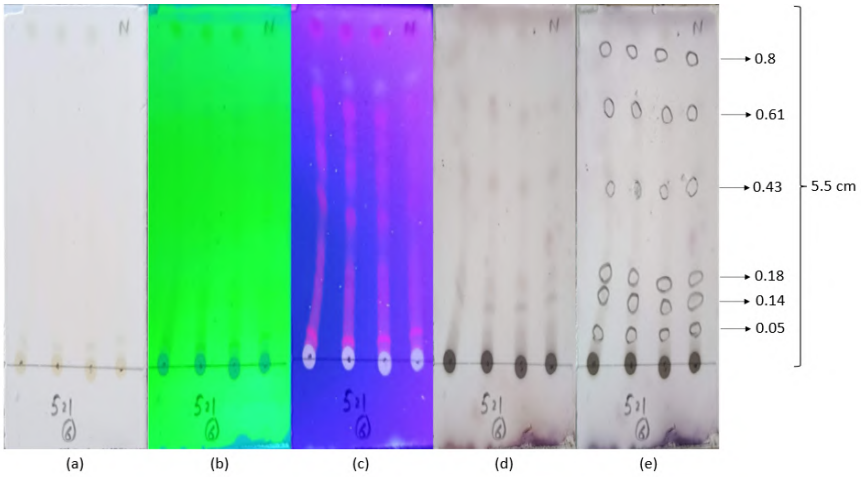

FIGURE 4.24: TLC chromatogram of *Azadirachta indica* with chloroform:methanol of ratio 5:1 (a) visible light (b) UV 360nm (c) UV 254nm (d) dye-treated plate (e) detection of bands with Rf value

Figure 4.24 shows that separation of the extract in chloroform:methanol 5:1 over 5.5 cm resulted in six bands with Rf values 0.05, 0.14, 0.18, 0.43, 0.61 and 0.8, indicating the presence of highly polar to moderately polar and less polar compounds.

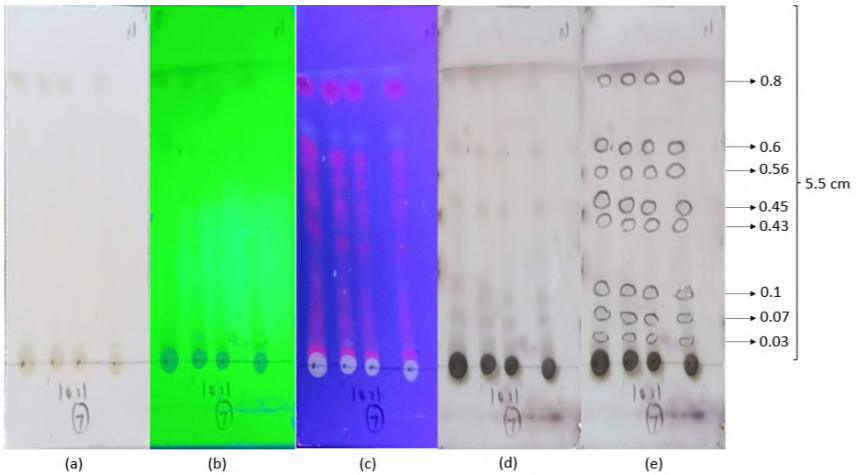

FIGURE 4.25: TLC chromatogram of *Azadirachta indica* with chloroform:methanol of ratio 10:1 (a) visible light (b) UV 360nm (c) UV 254nm (d) dye-treated plate (e) detection of bands with Rf value

Figure 4.25 shows that separation of the extract in chloroform:methanol 10:1 over 5.5 cm resulted in eight bands with Rf values 0.03, 0.07, 0.1, 0.43, 0.45, 0.56, 0.6 and 0.8, indicating the presence of highly polar to moderately polar and less polar compounds.

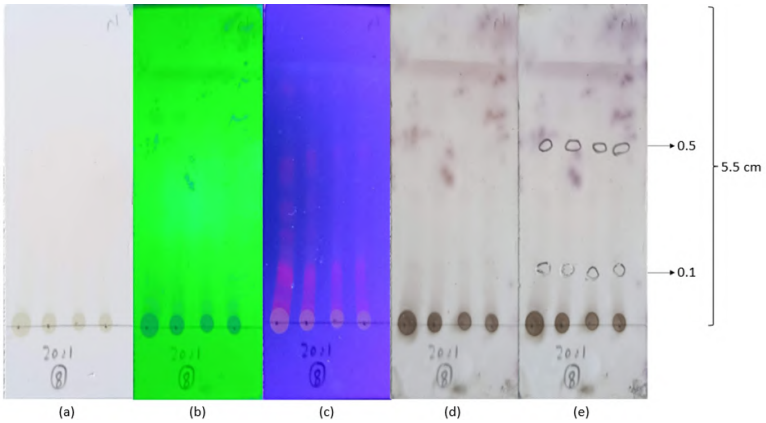

FIGURE 4.26: TLC chromatogram of *Azadirachta indica* with chloroform:methanol of ratio 20:1 (a) visible light (b) UV 360nm (c) UV 254nm (d) dye-treated plate (e) detection of bands with Rf value

Figure 4.26 shows that separation of the extract in chloroform:methanol 20:1 over 5.5 cm resulted in two bands with Rf values 0.1 and 0.5 indicating the presence of polar to moderately polar compounds.

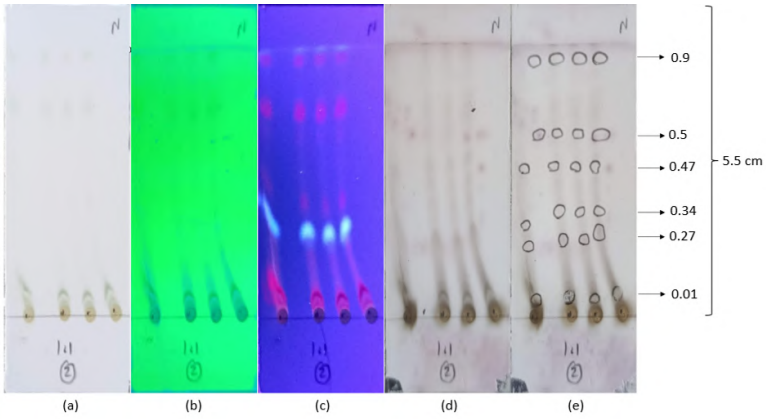

FIGURE 4.27: TLC chromatogram of *Azadirachta indica* with chloroform:methanol of ratio 1:1 (a) visible light (b) UV 360nm (c) UV 254nm (d) dye-treated plate (e) detection of bands with Rf value

Figure 4.27 shows that separation of the extract in chloroform:methanol 1:1 over 5.5 cm resulted in six bands with Rf values 0.01, 0.27, 0.34, 0.47, 0.5 and 0.9, indicating the presence of highly polar to moderately polar and non- polar compounds.

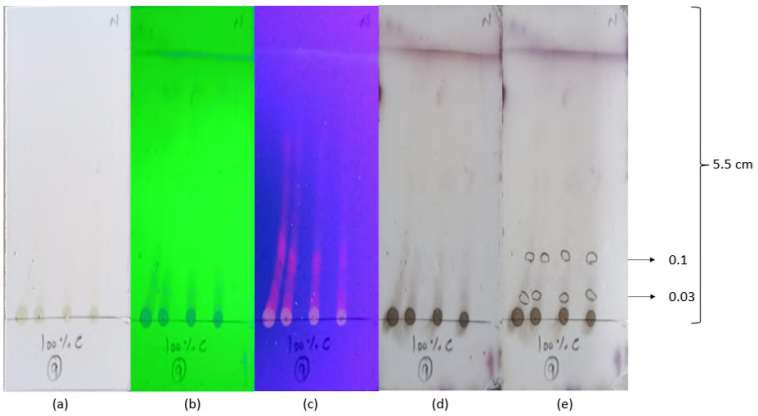

FIGURE 4.28: TLC chromatogram of *Azadirachta indica* with 100% chloroform (a) visible light (b) UV 360nm (c) UV 254nm (d) dye-treated plate (e) detection of bands with Rf value

Figure 4.28 shows that separation of the extract in 100% chloroform over 5.5 cm resulted in two bands with Rf values of 0.03 and 0.1, indicating the presence of highly polar compounds.

The analysis of chromatograms of the above combinations shows that all four elutes in a single combination share the same number and Rf value of bands, so these four elutes of all individual combinations were mixed to a single fraction. So there were a total of nine fractions named as F1, F2, F3, F4, F5, F6, F7, F8 and F9. These individual fractions were analyzed by TLC as shown in figure 4.29.

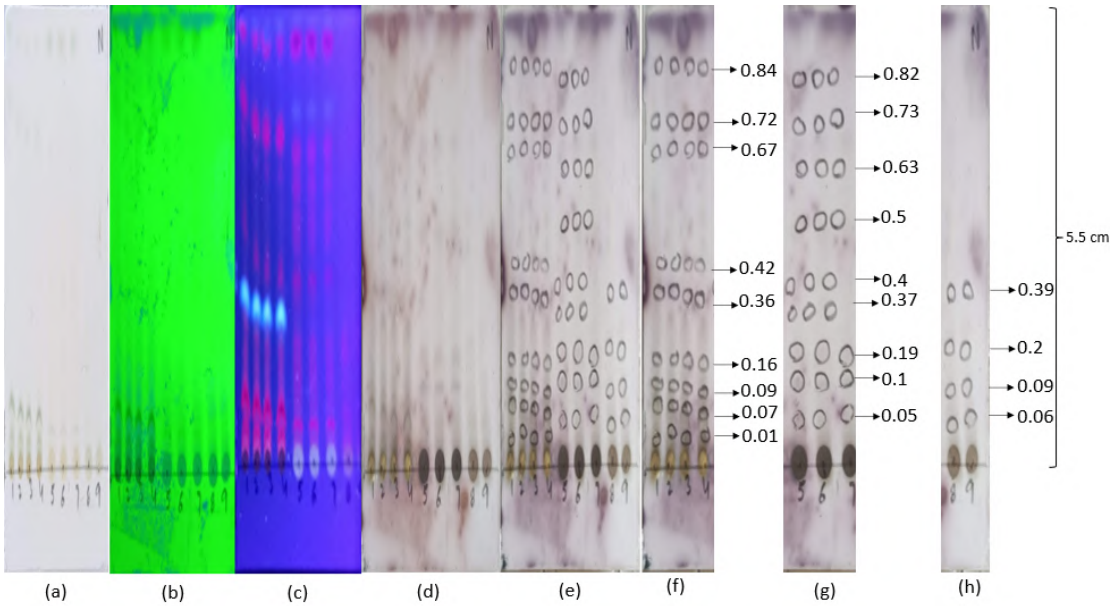

FIGURE 4.29: TLC chromatogram of *Azadirachta indica* with all combined fractions (a) visible light (b) UV 360nm (c) UV 254nm (d) dye-treated plate (e) detection of bands with Rf value (f) Rf value of fractions 1,2,3,4 (g) Rf value of fractions 5,6,7 (h) Rf value of fractions 8 and 9

Figure 4.29 shows that TLC analysis of nine combined fractions showed that first four fractions F1, F2, F3 and F4 showed nine similar bands with Rf values of 0.01, 0.07, 0.09, 0.16, 0.36, 0.42, 0.67, 0.72 and 0.84. indicating the presence of highly polar to moderately polar and less polar compounds.

Similarly F5, F6 and F7 also showed nine similar bands with Rf values 0.05, 0.1, 0.19, 0.37, 0.4, 0.5, 0.63, 0.73 and 0.82, indicating the presence of highly polar to moderately polar and less polar compounds. F8 and F9 shared four similar bands with Rf values 0.06, 0.09, 0.2 and 0.39, indicating the presence of highly polar to moderately polar compounds. On basis of similarity of bands fractions were combined to form super-fractions.

F1, F2, F3 and F4 were combined to form neem super-fraction 1 and named as NF1. F5, F6 and F7 were combined as neem super-fraction 2 and named as NF2, while F8 and F9 were combined to form neem super-fraction 3 and named as NF3. These super-fractions were further analyzed by TLC, as shown in figure 4.30.

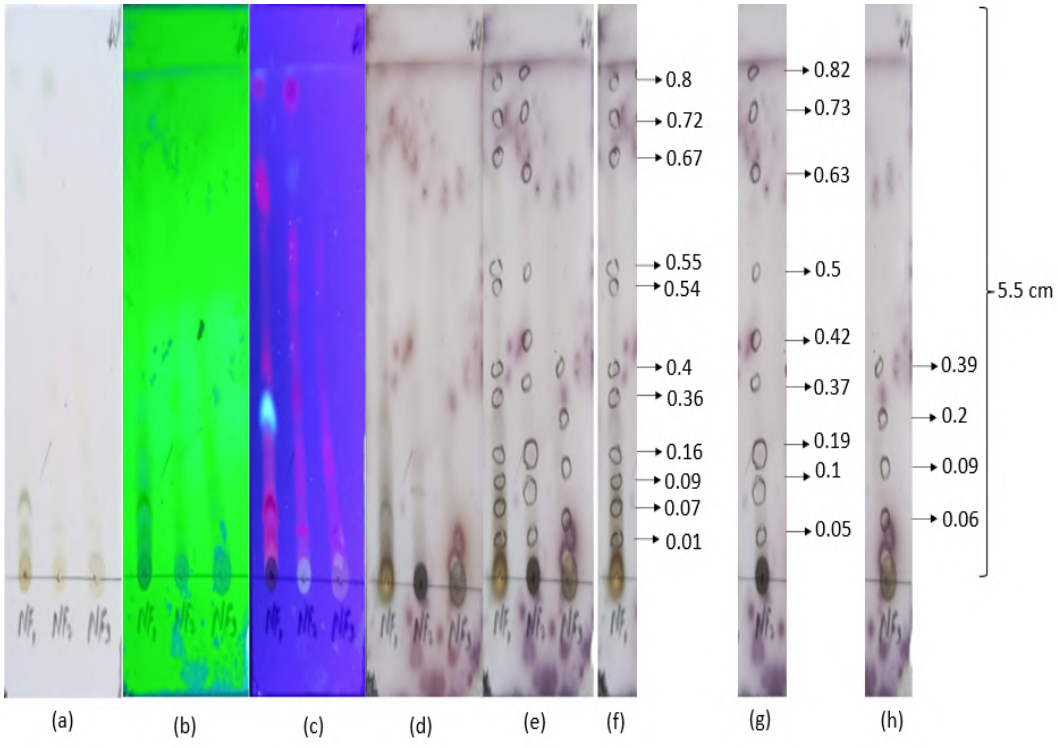

FIGURE 4.30: TLC chromatogram of *Azadirachta indica* with super fractions (a) visible light (b) UV 360nm (c) UV 254nm (d) dye-treated plate (e) detection of bands with Rf value (f) neem super-fraction 1, NF1 (g) neem super-fraction 2, NF2 (h) neem super-fraction 3, NF3

TABLE 4.1: Details of column chromatography

Name of Plant	**Amount used for column(g)**	**Solvent system**	**Proportions of mobile phase to run the column**	**No of elutes collected in test tube**	**Number of fractions obtained**	**TLC Solvent system along with proportion**	**Fractions mixed on basis of TLC**	**Mixed fractions TLC solvent systems with proportion**	**Mixing of fractions to make super-fraction**	**Mass of each super-fraction (g)**	**Yield of each super-fraction (%)**
Azadirachta indica	10	Chloroform : methanol	100% methanol	4	9	Chloroform : methanol	F1	Chloroform : methanol 10:1	F1 + F2 + F3 + F4 = AF1	NF1 = 4.8	NF1 = 45
			1:01	4		10:01	F2		F5 + F6 + F7 = NF2	NF2 = 2.7	AF2 = 27
			1:5	4			F3		F8 + F9 = NF3	AF3 = 2.1	NF3 = 15
			1:10	4			F4				
			1:20	4			F5				
			5:01	4			F6				
			10:01	4			F7				
			20:01	4			F8				
			100% chloroform	4			F9				

The concentrated super-fractions were stored at 4℃ and used for further HPLC-MS, in vivo and in vitro experimentation.

Figure 4.30 shows the TLC analysis of super-fractions. NF1 showed nine bands with Rf values of 0.01, 0.07, 0.09, 0.16, 0.36, 0.4, 0.54, 0.55, 0.67, 0.72 and 0.8. indicating the presence of highly polar to moderately polar and less polar compounds. Similarly, NF2 showed nine bands with Rf values 0.05, 0.1, 0.19, 0.37, 0.42, 0.5, 0.63, 0.73 and 0.82, indicating the presence of highly polar to moderately polar and less polar compounds. NF3 showed four bands with Rf values 0.06, 0.09, 0.2 and 0.39, indicating the presence of highly polar to moderately polar compounds. These super-fractions were evaporated and concentrated. The mass of NF1 is 4.5, the mass of NF2 is 2.7 and the mass of NF3 is 1.5. The yield of super-fraction NF1 is 45, for NF2 it is 27 and for NF3 it is 15 as shown in figure 4.31.

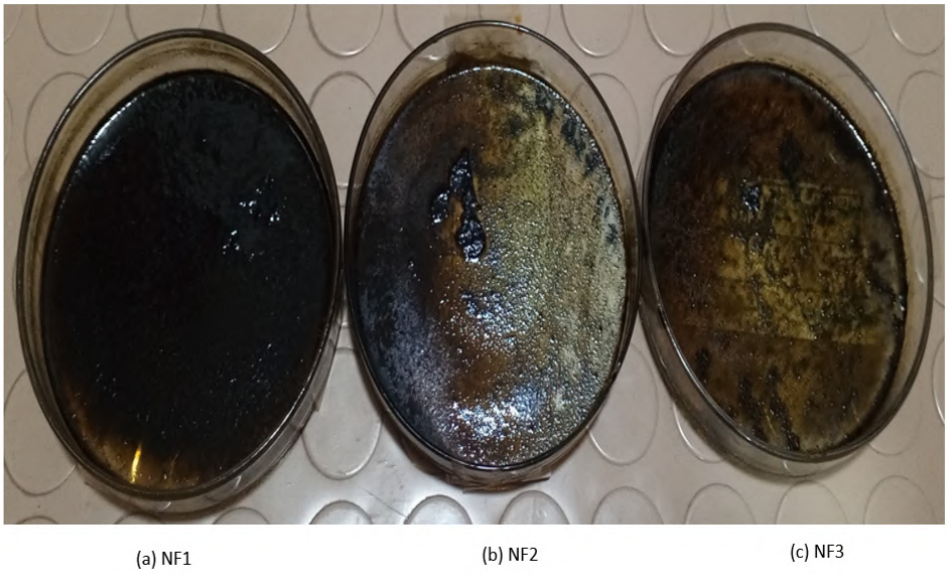

FIGURE 4.31: Concentrated super-fractions (a) NF1 (b) NF2 (c) NF3

4.3.2.1 Bioactivity Assays of Super-fractions

i. 2, 2 - Diphenyl - 1 - Picrylhydrazyl Radical Scavenging Assay

The DPPH free radical scavenging assay was used to assess the antioxidant activity of *Azadirachta indica* super-fractions. For every super-fraction, 100µl was

combined with 3ml of DPPH solution to create a dilution of 1mg/1ml. Antioxidant activity was demonstrated by the color shift from deep violet to pale yellow brought on by the methanolic leaf extract, as shown in figure 4.32.

FIGURE 4.32: DPPH assay of *Azadirachta indica* super-fractions

Following thirty minutes of stabilization, the absorbance at 517 nm was measured, and the antioxidant activity percentage was computed using the formula $[(Ac - As)/Ac] \times 100]$. The experiment was repeated in triplicate. All readings along with average and percentage scavenging inhibition, are given in table 4.1.

TABLE 4.2: Add caption

Plant name	**Control**	**Name of super-fraction**	**DPPH Value 1**	**DPPH Value 2**	**DPPH Value 3**	**Average DPPH**	**Scavenging activity (%)**
Azadirachta indica	0.701	NF1	0.217	0.219	0.22	0.218	68.9
		NF2	0.237	0.236	0.237	0.236	66.3

Table 4.2 – continued from previous page

Plant name	Control	Name of super-fraction	DPPH Value 1	DPPH Value 2	DPPH Value 3	Average DPPH	Scavenging activity (%)
		NF3	0.29	0.295	0.296	0.293	58.2

The results show that NF1 has the highest scavenging activity, i.e., 68.9%, followed by NF2, which has 66.3%, and NF3, which has 58.2% scavenging activity. This trend is shown in the graph below.

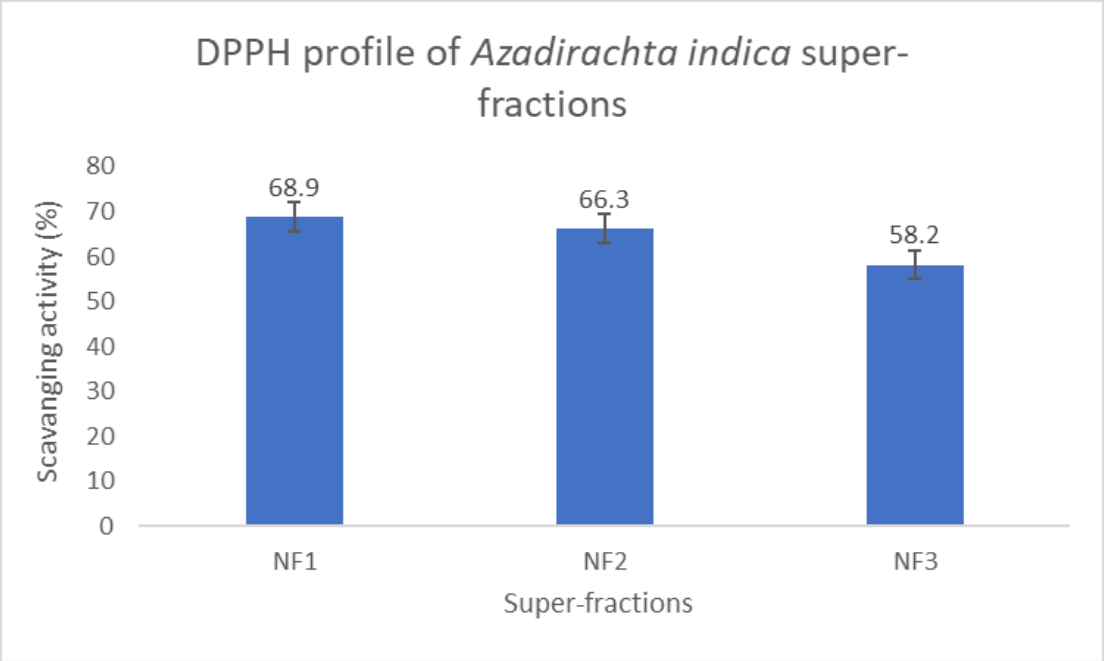

FIGURE 4.33: DPPH profile of *Azadirachta indica* super-fractions

ii. Total Phenolic Concentration

The total phenolic content of the *Azadirachta indica* super-fractions was ascertained using the FC method, and gallic acid was utilized to generate a calibration curve.The standard curve was used to create a regression equation, which was then used to quantify the amount of gallic acid in the super-fractions: y= 0.0632x+0.2211, R2 = 0.8958, where x is the equivalent gallic acid (mg/ml) and y is the absorbance. The absorbance values (0.189, 0.321, 0.592, 0.489, 0.479, 0.653, 0.691, 0.654, 0.778, 0.784, 0.896, 1.057) increase as the concentration of Gallic acid

increases (0 to 12 mg/ml). This implied that the amount of light absorbed at 765 nm and the concentration of gallic acid in the solution were directly correlated as shown in figure 4.34 below.

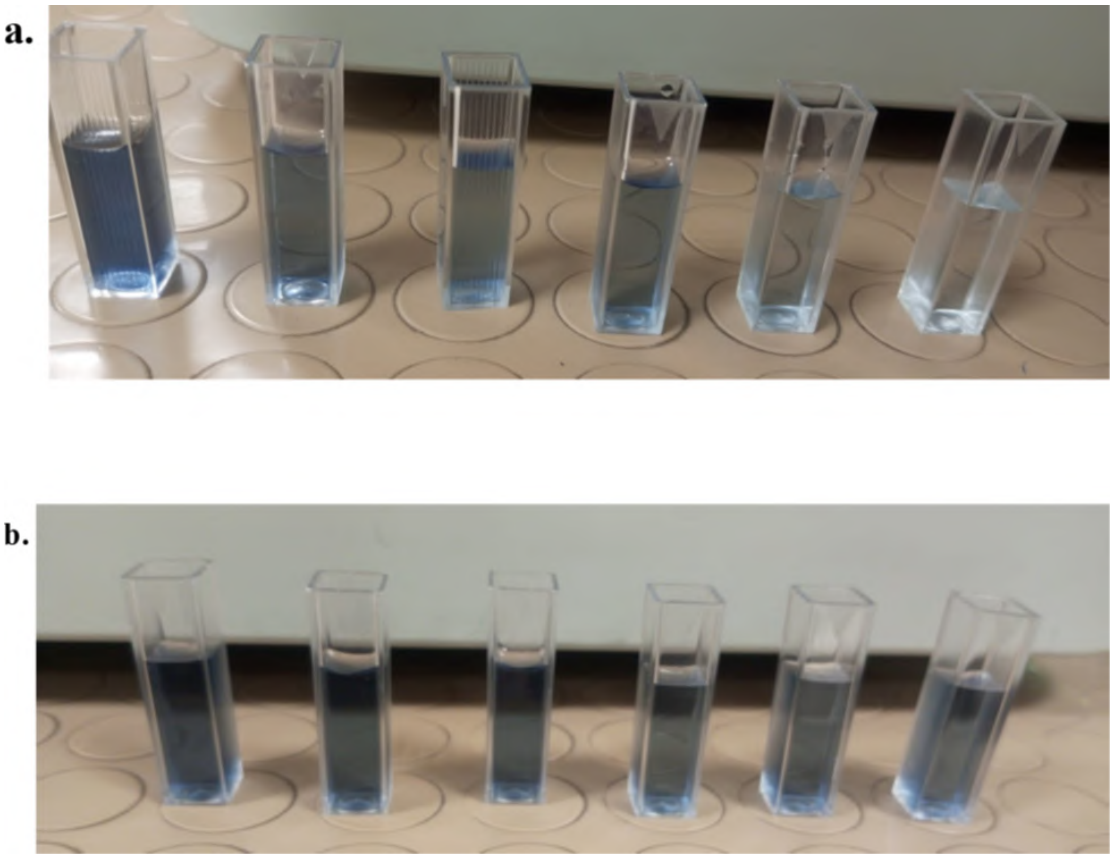

FIGURE 4.34: (a, b) Gallic acid concentrations

The curve formed by plotting the absorbance values against different concentrations of gallic acid is shown in the graph below.

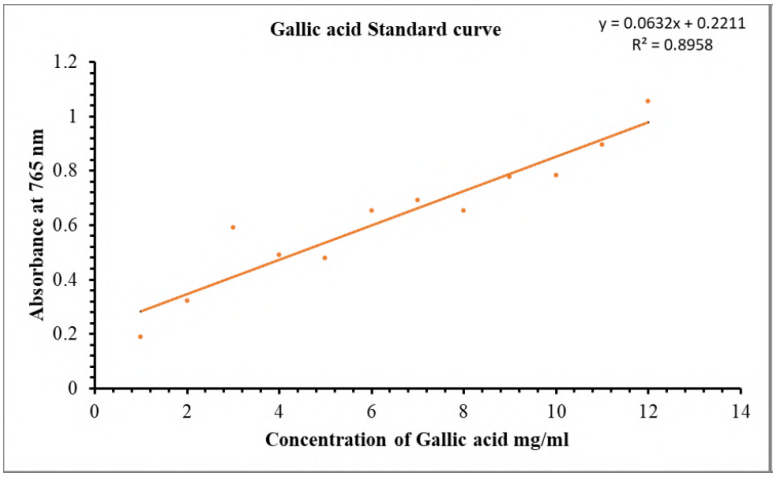

FIGURE 4.35: Graph plot of gallic acid results

Phenolic concentrations were measured by mixing 270 μL of each super-fraction dilution with 10% FC reagent and 7.5% Na_2CO_3 as shown in figure 4.36 and the absorbance was again measured at 765 nm.

FIGURE 4.36: TPC assay of *Azadirachta indica* super-fractions

Phenolic concentrations were observed in the super-fractions of *Azadirachta indica* and shown in table **??**. NF1 exhibited absorbance up to 0.697. NF2 exhibited absorbance up to 0.327 while NF3 exhibited absorbance up to 0.373.

TABLE 4.3: Absorbance of *Azadirachta indica* super-fractions at 765 nm

Plants name	**Name of Super-fractions**	**TPC 1**	**TPC 2**	**TPC 3**	**Average TPC**
Azadirachta indica	NF1	15:38	0.701	0.743	0.697
	NF2	7:35	7:46	0.361	0.327
	NF3	7:29	0.346	0.373	0.341

The curve shown in figure 4.35 above helps quantify the total phenolic content in *Azadirachta indica*'s super-fractions.

By measuring the absorbance of the sample at the same wavelength (765 nm) and comparing it to the standard curve, the concentration of phenolic compounds in *Azadirachta indica*'s super-fractions could be estimated. The absorbance values of 0.743, 0.361, and 0.373 for NF1, NF2 and NF3, respectively, were calibrated using the Gallic acid standard curve and it indicated the concentration of phenolic content as shown in graph below.

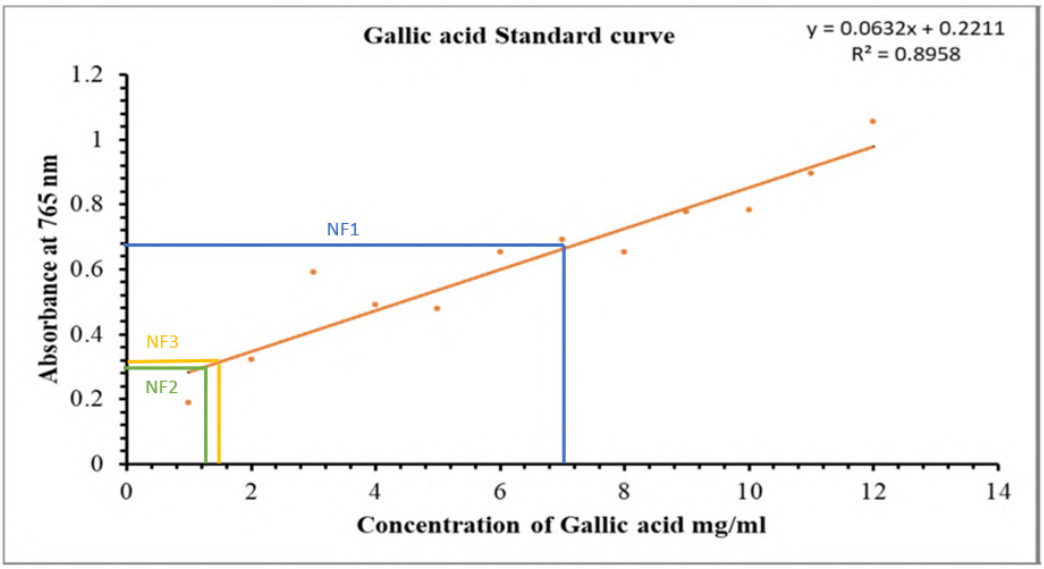

FIGURE 4.37: Phenolic concentration in *Azadirachta indica* super-fractions

It was found that the phenolic concentration in NF1 with an absorbance of 0.697 was 7.6 mg GAE/g. Similarly, the phenolic concentration in NF2 with an absorbance of 0.327 was 1.5 mg GAE/g, and the phenolic concentration in NF3 with an absorbance of 0.341 was 1.7 mg GAE/g. The table 4.4 shows the concentration of phenolic acids in *Azadirachta indica* super-fractions.

TABLE 4.4: Phenolic concentration in *Azadirachta indica* super-fractions

Sample	**Absorbance**	**Phenolic concentration**
		(mg GAE/g)
NF1	0.697	14:24
NF2	0.327	12:00
NF3	0.341	16:48

According to table, NF1 has the highest phenolic content, i.e., 7.6 mg GAE/g, followed by NF3, which has 1.7 mg GAE/g, and NF2, which has 1.5 mg GAE/g. This trend is shown in the graph below.

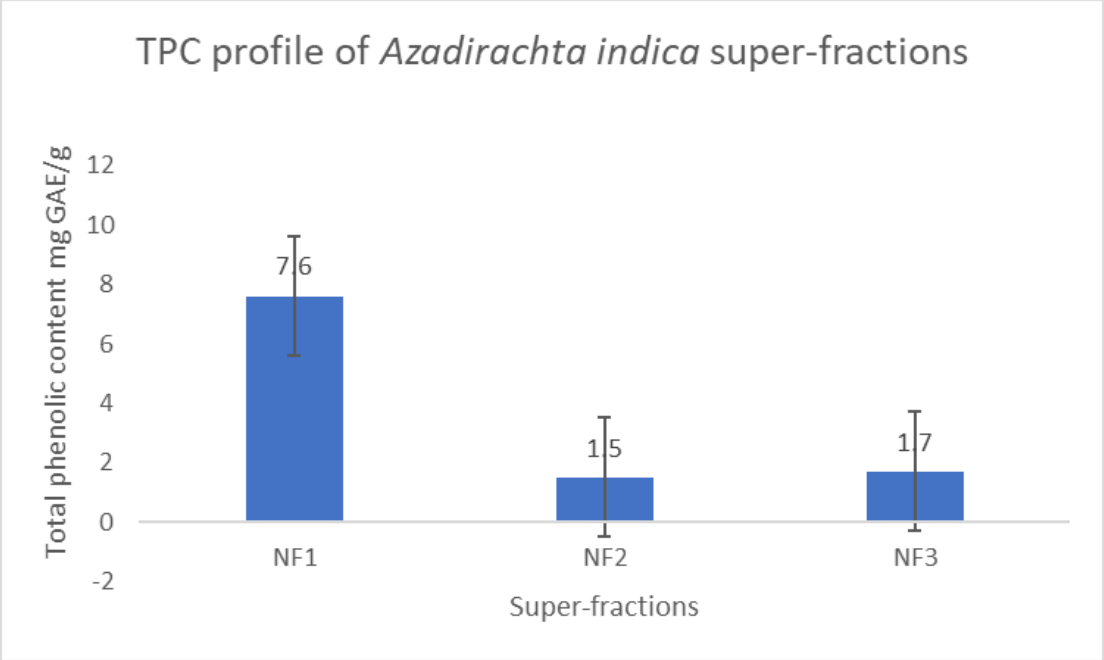

FIGURE 4.38: TPC profile of *Azadirachta indica* super-fractions

iii. Inhibition of Alpha-amylase

Inhibiting alpha-amylase is vital for diabetes management and starch digestion. This study explored the effects of *Azadirachta indica* super-fractions on alpha-amylase using a specific assay, where phosphate buffer, super-fraction dilution, and the alpha-amylase were combined with starch as shown in figure 4.39.

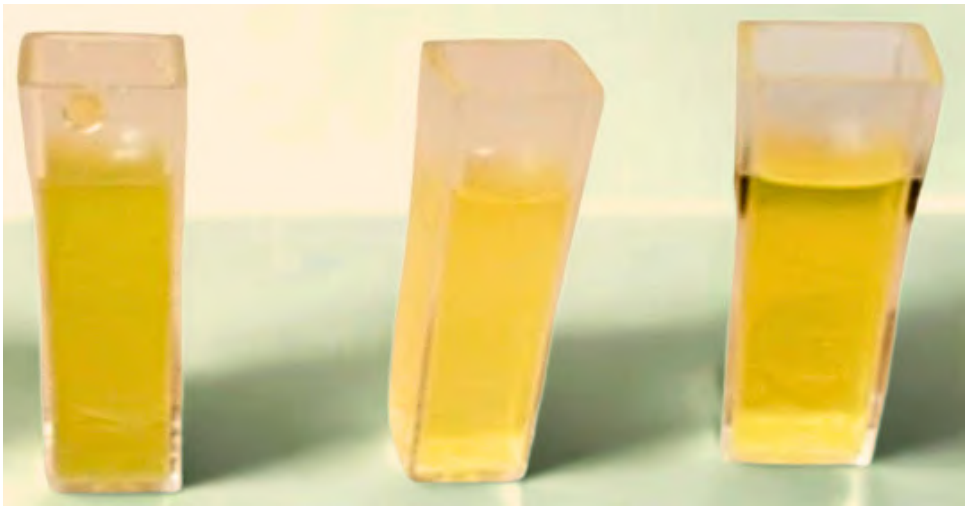

FIGURE 4.39: Alpha-amylase assay of *Azadirachta indica* super-fractions

Acarbose served as the positive control, with the reaction halted using the DNSA reagent. The absorbance was measured at 540 nm and the inhibition percentage was calculated as shown in table 4.5.

TABLE 4.5: Alpha-amylase inhibition of *Azadirachta indica* super-fractions

Plant name	**Control**	**Name of super-fractions**	**Alpha-amylase 1**	**Alpha-amylase 2**	**Alpha-amylase 3**	**Avg**	**Alpha-amylase inhibition (%)**
Azadirachta indica	0.971	NF1	0.7	0.539	0.511	0.583	39.9
		NF2	0.655	0.595	0.565	0.605	37.7
		NF3	15:38	0.684	0.695	15:04	35.4

According to the percentage inhibition value, the NF1 showed 39.9% inhibition, indicating it is the most effective at inhibiting alpha-amylase activity among the three samples. NF2 has 37.7% alpha-amylase inhibition, while NF3 has 35.4% alpha-amylase inhibition. This trend is shown in the graph below.

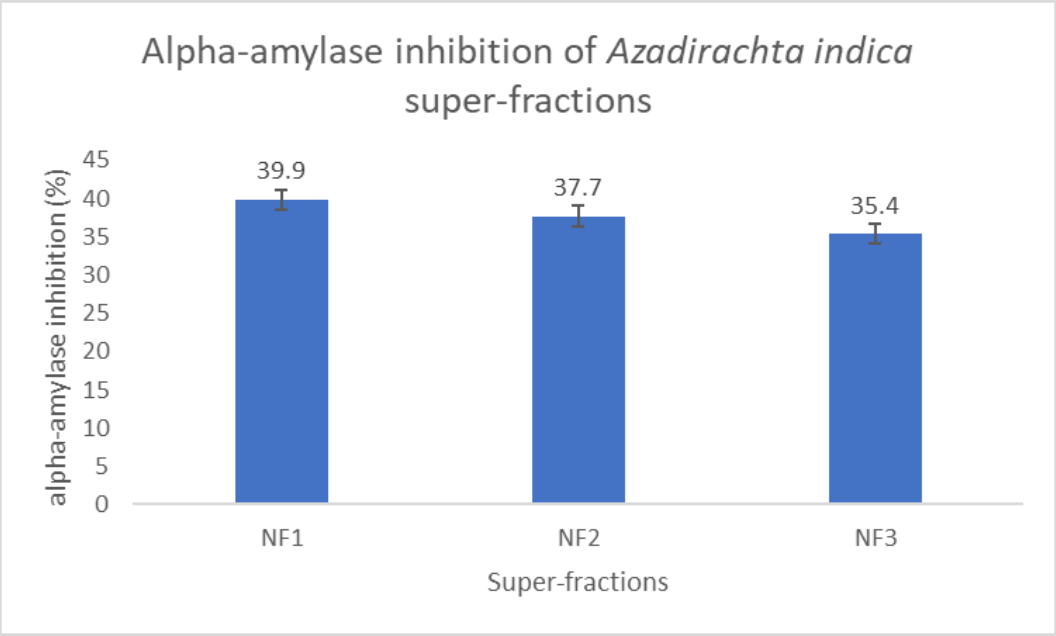

FIGURE 4.40: Alpha-amylase inhibition of *Azadirachta indica* super-fractions

iv. Alpha-glucosidase Inhibition

To conduct the alpha-glucosidase assay, super-fraction dilution, phosphate buffer (pH 6.9), and α-glucosidase solution were mixed, followed by the addition of PNPG solution and incubation as shown in the figure 4.41.

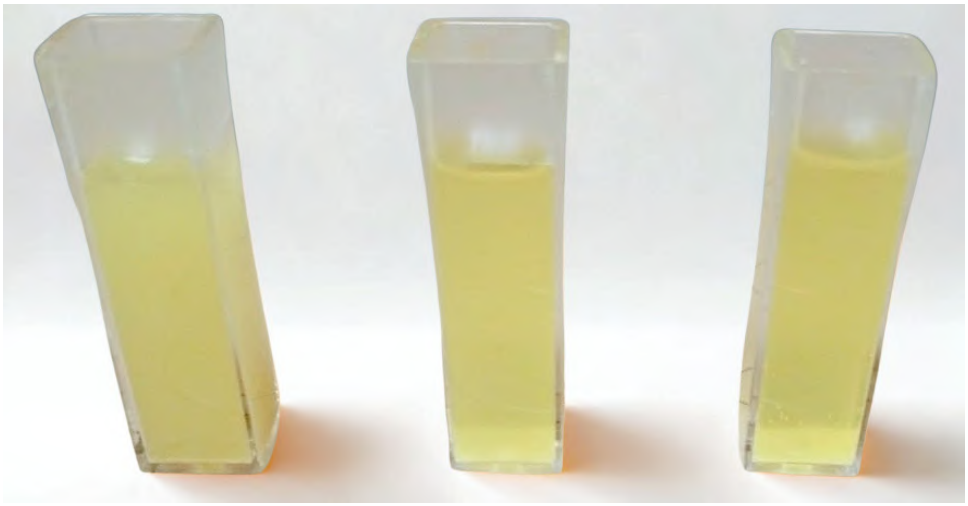

FIGURE 4.41: Alpha-glucosidase assay of *Azadirachta indica* super-fractions

Absorbance was measured at 405 nm using a spectrophotometer before and after incubation, using acarbose as a positive control, and the inhibition percentage was calculated as shown in table 4.6.

TABLE 4.6: Alpha-glucosidase inhibition of *Azadirachta indica* super-fractions

Plant name	**Control**	**Name of super-fractions**	**Alpha glucosi-dase 1**	**Alpha glucosi-dase 2**	**Alpha glucosi-dase 3**	**Avg**	**Alpha-glucosidase inhibition (%)**
Azadirachta indica	0.531	NF1	0.429	0.341	0.328	0.366	31.1
		NF2	11:12	0.445	0.371	10:14	19.6
		NF3	0.451	0.462	0.473	0.461	13.2

According to the percentage inhibition value, the NF1 showed 31.1% inhibition, indicating it is the most effective at inhibiting alpha-glucosidase activity among

the three samples. NF2 has 19.6% alpha-glucosidase inhibition, while NF3 has 13.2% alpha-glucosidase inhibition. This trend is shown in the graph below.

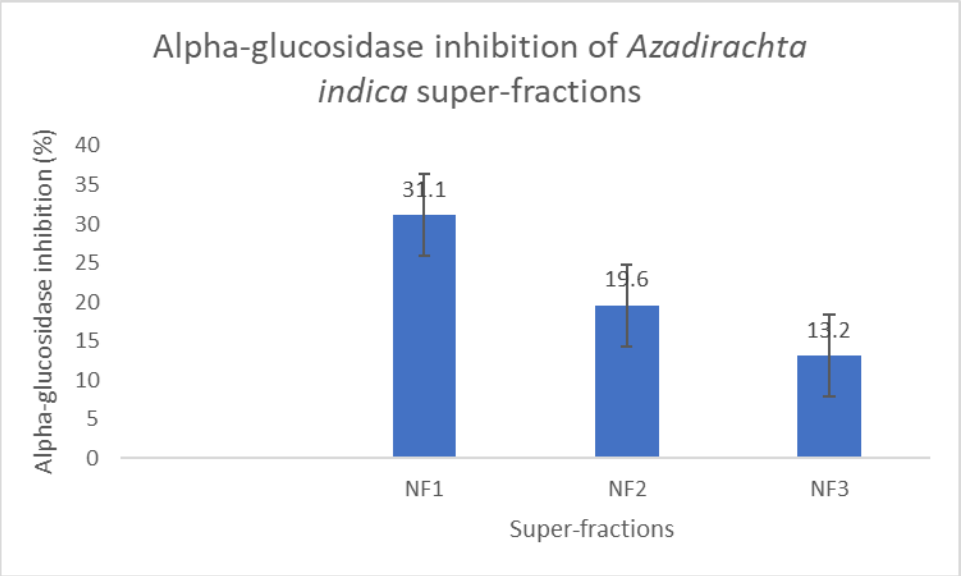

FIGURE 4.42: Alpha-glucosidase inhibition of *Azadirachta indica* super-fractions

4.3.3 High-Performance Liquid Chromatography - Mass Spectrometry

The LCMS analysis used a Triple Quadrupole Mass Spectrometer with a heated electrospray ionization source. Samples were prepared using methanol and introduced through a direct insertion technique. Multiple peaks were selected for analysis during the fragmentation phase. The compounds obtained after LC-MS data analysis in positive and negative mode along with molecular weight, fragmentation peaks and structure are given in table 4.7 below.

TABLE 4.7: Compounds obtained after LC-MS data analysis

Molecular Weight	**Fragmentation Peaks**	**Compound**	**Structure**
NF1 Positive Mode			
104.08	60.05 57.83 57.5	GABA	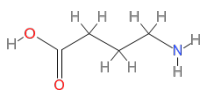

Table 4.7 continued from previous page

Molecular Weight	Fragmentation Peaks	Compound	Structure
NF1 Negative Mode			
255	152.92	Purpurin	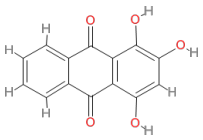
	151.08		
	146.58		
	137.92		
	124.83		
	96.08		
NF2 Positive Mode			
105.08	64.17, 63.92, 63.75, 62.75	Cyclopropanecarbonyl chloride	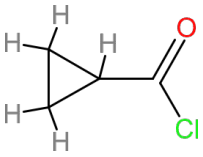
NF2 Negative Mode			
265.08	119.17	Honokiol	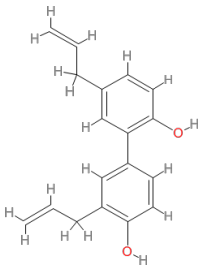
	103.25		
	89.17,89.00,88.83		
	71.17		
	59.25,59.00		
NF3 Positive Mode			
146.25	100.17, 99.75	Spermidine	
	82.00, 81.83		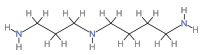
	72		
	67.25		
NF3 Negative Mode			
132.75	114.75	Aspartic acid	
	73.08,72.75		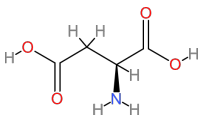
	70.75, 68.92		
	59.25		

Above table shows the compounds obtained after LC-MS data analysis. These compounds were selected on the basis of molecular weight and fragmentation pattern. GABA was obtained in NF1 positive mode while purpurin was present in NF1 negative mode. In NF2 positive mode, cyclopropanecarbonyl chloride and in

negative mode, honokiol was present. In NF3 positive mode, spermidine and in negative mode aspartic acid was present.

4.4 In silico Evaluation of *Azadirachta indica* Phytocompounds

4.4.1 3D Structure Prediction and Refinement of Selected Proteins

The peroxisome proliferator-activated receptor-γ (PPAR-γ), pancreatic and duodenal homeobox 1 (PDX-1), insulin receptor substrate-2 (IRS-2), phosphatidylinositol 3-kinase alpha (PI3K-α), and protein kinase B (Akt2) were selected as target proteins for their potential roles in the development of Type 2 Diabetes. 3D structure and FASTA sequence of target proteins i.e. PI3K-α, Akt2 and PPAR-γ was taken from PDB under PDB IDs 5M6U, 8Q61 and 5GTN respectively. While the 3D structure and FASTA sequence of PDX-1 and IRS-2 were obtained from AlphaFold under IDs P52945 and Q9YAH2, respectively.

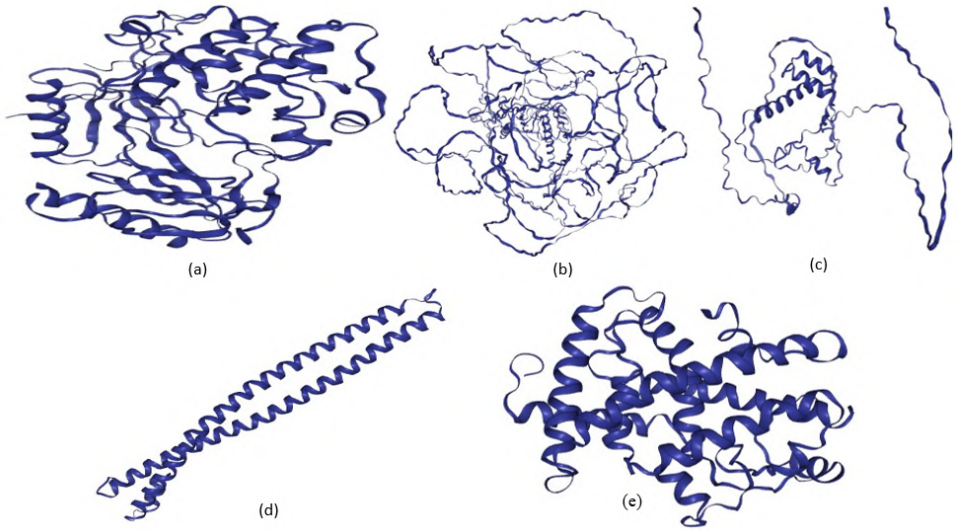

FIGURE 4.43: Structures of refined target proteins (a) Akt2 (b) IRS-2 (c) PDX-1 (d) PI3K-α (e) PPAR-γ

Using PyMol, the protein structures were refined by eliminating any ligands and water molecules. To obtain a stable conformation the absent polar hydrogens were

added, and other atoms were removed to prevent overlaps and the modified file was saved in PDB format. The refined structures of target proteins are shown in figure 4.43 above.

4.4.2 Physicochemical Characterization of Target Proteins

We utilized an online tool called ProtParam to forecast a variety of parameters, including the molecular and structural properties of specific proteins. Table 4.8 lists the physicochemical characteristics of target proteins.

TABLE 4.8: The target proteins' physicochemical characteristics

S. No.	Target Proteins	MW	PI	NR	PR	Ext Co1.	Ext Co2.	Instability Index	Aliphatic Index	GRAVY
1	Akt2	55897.90	5.89	74	66	67185	66810	34.81	76.89	-0.468
2	PI3K-α	83557.30	5.77	109	96	999505	99130	48.33	81.34	-0.712
3	PPAR-γ	32242.41	5.36	40	32	11920	11920	44.57	105.80	-0.117
4	IRS-2	137334.06	8.90	105	121	94880	93630	70.45	58.54	-0.506
5	PDX-1	30770.99	7.10	31	31	39545	39420	78.54	61.87	-0.671

All proteins exhibit molecular weights ranging from approximately 30 kDa to 137 kDa, with isoelectric points varying from 5.36 to 8.90, suggesting they are likely soluble under physiological conditions.

The instability index values are relatively out of range except for Akt2. Moreover, the proportionate volume of the aliphatic side chains is represented by the aliphatic index, and this index is high for all proteins, indicating the tendency to be thermostable.

Additionally, the GRAVY value is negative, indicating that the proteins are hydrophilic and help in interactions with the aqueous environment. Overall, these properties suggest that the proteins are well-suited for their biological roles.

4.4.3 Active Site Identification

The dogsitescorer software, which determines the number of pockets that can be bound and gives details on their surface area and volume, was utilized to

determine the active sites of the proteins. Figure 4.44 below illustrates the areas and volumes of target proteins. The coloured areas depict the active sites available for a particular protein.

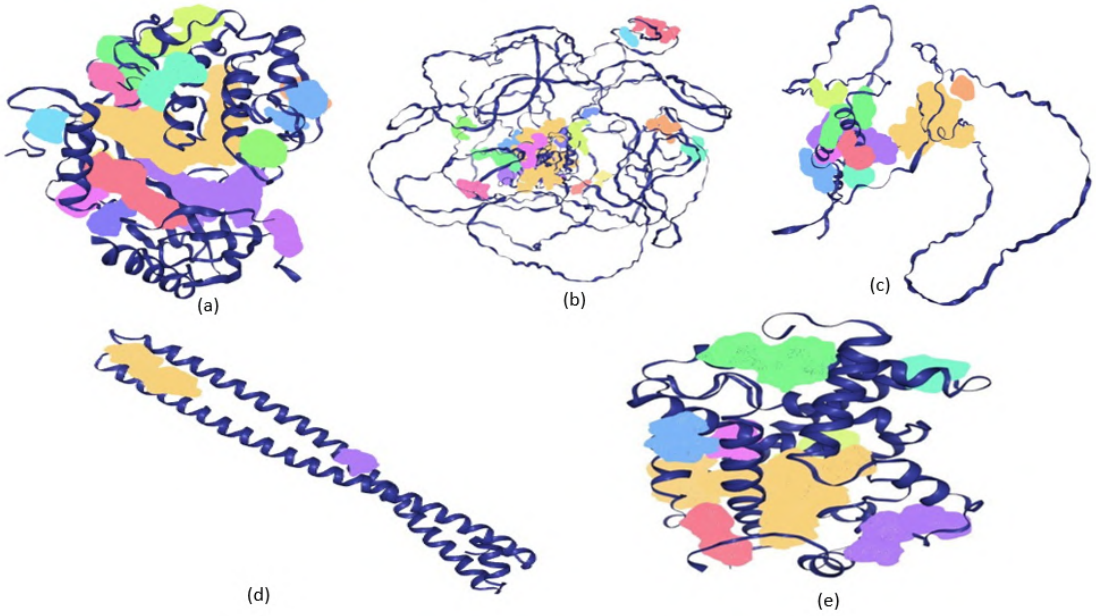

FIGURE 4.44: Active sites of refined target proteins (a) Akt2 (b) IRS-2 (c) PDX-1 (d) PI3K-α (e) PPAR-γ

Dogsitescorer data depict different numbers of pockets for each protein. Every pocket has different surface area and volume. According to this data, the Akt2 consists of fifteen pockets, PDX-1 consists of nine pockets. PI3K-α consists of two pockets, PPAR-γ consists of eighteen pockets, and IRS-2 consists of eight pockets.

4.4.4 Retrieval of Chemical Structure of the Ligands

The largest chemical database in the world, PubChem, was searched for ligands. These ligands' 3D structures were extracted in SDF format from the PubChem database. After downloading the structures, the next step performed was minimizing the energy of these ligands. This step is an important one as we can't use simply the downloaded structure as the ligands are unstable and it can directly affect the docking vina scores. The refined structures of ligands obtained after energy minimization along with other information are given in table 4.9.

TABLE 4.9: Chemical structure of ligands

Ligand Names	**Mol weights**	**Formulas**	**Mol Structures**	**Canonical Smiles**
Purpurin	256.209	$C_{14}H_8O_5$	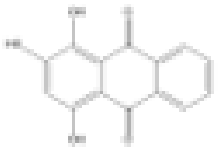	C1=CC=C2C(=C1)C(=O)C3=C(C2=O)C(=C(C=C3O)O)O
GABA	103.12	$C_4H_9NO_2$	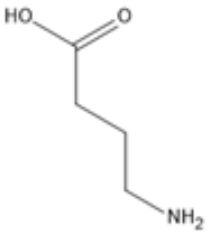	C(CC(=O)O)CN
Cyclo propane carbonyl chloride	104.53	C_4H_5ClO	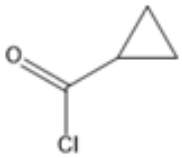	C1CC1C(=O)Cl
Honokiol	266.3	$C_{18}H_{18}O_2$	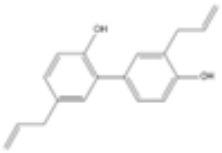	C=CCC1=CC(=C(C=C1)O)C2=CC(=C(C=C2)O)CC=C
Spermidine	145.25	$C_7H_{19}N_3$		C(CCNCCCN)CN
Aspartic acid	133.1	$C_4H_7NO_4$	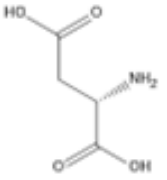	C([C@@H](C(=O)O)N)C(=O)O

4.4.5 Virtual Screening of Ligands

For compounds to be separated as both drug-like and nondrug-like virtual screening and pharmacokinetic properties are followed. The Lipinski rule addresses specific parameters, including molecular weight ($\leq$ 500), log P ($\leq$ 5), H-bond donors

(≤ 5), H-bond acceptors (≤ 10), and rotatable bonds (≤ 10). Orally active chemicals must adhere to these guidelines. The manner of administration affects the drug-like. When a chemical satisfies three or more requirements, it is classified as a drug; if it violates more than two, its absorption is poor [130]. Virtual screening of ligands is shown is table 4.10.

TABLE 4.10: Virtual screening of ligands

S. No	**Ligand Name**	**Mol Weight**	**Log P value**	**Rotatable Bonds**	**H-bond Acceptors**	**H-bond Donors**
1.	GABA	103.121	-0.1901	3	2	2
2.	Purpurin	256.209	1.5788	0	5	3
3.	Cyclopropane carbonyl chloride	104.53	1.1618	1	1	0
4.	Honokiol	266.3	4.2218	5	2	2
5.	Spermidine	145.25	-0.3363	7	3	3
6.	Aspartic acid	133.1	-1.127	3	3	3

According to table 4.10, the molecular weight, log P value, hydrogen bond donors, acceptors and rotatable bonds are in range for all ligands. Overall, all ligands are following all lipinski rules so they can be processed further.

4.4.6 ADMET Analysis of Ligands

A second investigation was conducted utilizing the online program pkCSM to ascertain ligands' ADMET characteristics as a pharmacokinetic metric following the Lipinski rule. There are two general words in pharmacology: pharmacodynamics and pharmacokinetics. Within the field of pharmacology, pharmacodynamics examines how medications affect the body. In pharmacokinetics, we investigate how medications are absorbed, distributed, metabolized, and excreted [131].

4.4.6.1 Absorption Properties of Ligands

The absorption parameters reveal important criteria for evaluating the bioavailability of compounds. For water solubility, the higher the number, the better

the solubility, helping with absorption. In the case of $CaCO_2$ permeability, a desirable number should be above 0, and when above 1, permeability and absorption are high. For intestinal absorption, desirable values should be above 50%, representing good absorption in human metabolism. For skin permeation, desirable values should be above -2, helping with absorption. Finally, being an P-Glycoprotein substrate is desirable when "Yes" as it can be preferably transported by P-Glycoprotein, depending on the case. Ideally, for P-glycoprotein inhibitors, a "No" status is preferred to avoid potential drug interactions that could compromise therapeutic efficacy [132]. The absorption properties of ligands are given in table 4.11.

TABLE 4.11: Absorption properties of ligands

Ligand Name	**Water solubility**	**$CaCO_2$ Permeability**	**Intestinal absorption (human)**	**Skin permeability**	**P - glycoprotein substrate**	**P - glycoprotein I inhibitor**	**P - glycoprotein II inhibitor**
GABA	-2.63	0.581	77.806	-2.741	No	No	No
Purpurin	-2.901	-0.198	68.97	-2.736	Yes	No	No
Cyclopropanecarbonyl chloride	-1.3	1.503	100	-2.263	Yes	No	No
Honokiol	-4.106	1.584	92.564	-2.735	Yes	No	No
Spermidine	-0.492	0.9	69.32	-2.849	Yes	No	No
Aspartic acid	-2.0891	-0.498	17.945	-2.735	No	No	No

According to table 4.11, all ligands have good water solubility except spermidine. Caco2 permeability is in range for all ligands except aspartic acid and purpurin. Intestinal absorption for all ligands is above 50 except for aspartic acid. Skin permeability is also in range. No ligand is an inhibitor of P-glycoprotein while some ligands are identified as P-glycoprotein substrates, which could affect their systemic availability.

4.4.6.2 Distribution Properties of Ligands

The theoretical volume or VDss indicates the entire dosage of the medication that must be dispersed evenly to produce a concentration similar to that of blood

plasma. For VDss a good value is typically greater than 0.5 L/kg, indicating favorable distribution in body tissues. The fraction unbound (Fu) should ideally be above 0.1, which signifies a significant proportion of the drug is available for therapeutic action. The blood-brain barrier reduces the amount of exogenous substances that can reach the brain directly while protecting it. Regarding BBB permeability (log BB), values greater than 0 suggest the ability to cross the blood-brain barrier. For CNS permeability (log PS), values closer to 0, ideally above -2 are preferred, as they indicate potential for penetration into the central nervous system [133]. Table 4.12 shows the distribution properties of ligands. The table indicates all ligands have safe range which is given below.

TABLE 4.12: Distribution properties of ligands

	Distribution Properties			
Ligand Name	**VDss (human)**	**Fraction unbound (human) Fu**	**BBB permeability log BB**	**CNS permeability log PS**
GABA	-0.65	0.561	-0.364	-3.039
Purpurin	0.627	0.237	-0.769	-2.371
Cyclopropanecarbonyl chloride	0.025	0.647	0.026	-2.222
Honokiol	0.163	0.005	-0.112	-1.477
Spermidine	1.014	0.937	-0.275	-3.09
Aspartic acid	-0.428	0.458	-0.707	-3.544

The above table 4.12 shows that GABA and aspartic acid have negative VDSS values. The fraction unbound values, BBB and CNS permeability is approximately in range for all ligands.

4.4.6.3 Metabolism Properties of Ligands

The enzyme cytochrome P450 is in charge of the liver's detoxification process. Many drugs get deactivated by this enzyme but certain drugs are capable of activating. This enzyme's inhibitors can directly affect the metabolism of the drug

hence should not be used. Similarly, CYP2D6 and CYP3A4 are responsible for the drugs' metabolism. Inhibition of these affects the pharmacokinetics of the drug in use [134]. The ligand metabolism prediction is shown below. The metabolic characteristics of ligands are displayed in table 4.13.

TABLE 4.13: Metabolism properties of ligands

	Metabolism Properties						
Ligand Name	**CYP2D6 sub-strate**	**CYP3A4 sub-strate**	**CYP1A2 inhibitor**	**CYP2C19 inhibitor**	**CYP2C9 inhibitor**	**CYP2D6 in-hibitor**	**CYP3A4 in-hibitor**
GABA	No	No	No	No	No	No	No
Purpurin	No	No	No	No	No	No	No
Cyclopropane carbonyl chloride	No	No	No	No	No	No	No
Honokiol	No	No	Yes	Yes	Yes	No	Yes
Spermidine	No	No	No	No	No	No	No
Aspartic acid	No	No	No	No	No	No	No

The metabolic properties of the ligands as shown in table 4.13, indicate that none of the compounds are substrates for the CYP2D6 and CYP3A4 enzymes which suggests they are not metabolized by these pathways. This is beneficial as it reduces potential drug interactions that could arise from competition for these important metabolic enzymes.

This is beneficial as it reduces potential drug interactions that could arise from competition for these important metabolic enzymes. Honokiol shows inhibition of the CYP enzymes, which can lead to increased levels of drugs metabolized by this enzyme.

4.4.6.4 Excretion Properties of Ligands

Two organs are involved in drug excretion, the liver, which is engaged in biliary excretion, and the kidneys, which are involved in renal excretion. Excretion may also include other organs, such as the lungs in the case of volatile or gaseous substances.

Excretion may also include other organs, such as the lungs in the case of volatile or gaseous substances. Moreover, drugs can be expelled through tears, saliva, and perspiration [135]. The excretion values of the ligands are given in table 4.14.

TABLE 4.14: Excretion properties of ligands

	Excretion Properties	
Ligand Name	**Total Clearance**	**Renal OCT2 substrate**
GABA	0.571	No
Purpurin	0.018	No
Cyclopro panecarbonyl chloride	0.023	No
Honokiol	0.333	No
Spermidine	1.132	No
Aspartic acid	0.145	No

According to table 4.14, the total clearance values for the compounds are in range. Notably, all compounds are classified as non-substrates for renal OCT2, which implies that they do not rely on this renal transport mechanism for excretion. This is beneficial as it minimizes the risk of interactions with other drugs that may utilize the same pathway.

4.4.6.5 Toxicity Properties of Ligands

By using pkCSM we determined the toxicity of the ligands. AMES toxicity test is used to test the mutagenic potential of the compound by using bacteria. If it shows a positive response, then the ligand is mutagenic which can also act as a carcinogen. The toxicity of *T. Pyriformis* (protozoa bacterium) is used as a toxic endpoint in the *T. Pyriformis* toxicity method. Any value >-0.5 log ug/L is considered toxic [136]. The values predicted in the Minnow toxicity test are used to represent the concentration at which the compound could cause the death of 50% of the minnows. The value below 0.5 mM is regarded as acute toxic. The expected log value of the oral rat chronic toxicity test's lowest recorded adverse effect is correlated with the drug concentration that requires a specific duration of treatment, expressed in log mg/kg bw/day. A hepatotoxicity test predicts that if

a compound could affect liver functioning or not. Higher maximum tolerated dose (MRTD) values indicate better safety [137]. The toxicity values of all ligands are given in table 4.15.

TABLE 4.15: Toxicity values of ligands

	Toxicity Properties									
Ligand Name	**AMES toxicity**	**Max tolerated dose (human)**	**hERG I inhibitor**	**hERG II inhibitor**	**Oral rat acute toxicity (LD50)**	**Oral rat chronic toxicity (LOAEL)**	**Hepato toxicity**	**Skin sensitization**	***T. pyriformis* toxicity**	**Minnow toxicity**
GABA	No	1.267	No	No	1.642	2.928	No	No	-0.148	2.581
Purpurin	No	0.372	No	No	2.261	2.649	No	No	0.433	2.2
Cyclopropane carbonyl chloride	No	0.951	No	No	2.212	1.69	No	No	-0.026	1.758
Honokiol	No	0.305	No	No	2.184	1.791	No	No	0.749	0.14
Spermidine	No	1.281	No	No	2.062	0.556	No	No	-0.01	2.498
Aspartic acid	No	1.286	No	No	2.366	2.857	No	No	0.285	3.512

According to table 4.15, no inhibition of hERG I or hERG II was seen in any ligand. None of the ligands demonstrated hepatotoxicity, AMES toxicity, or skin sensitization. MRTD value is also positive for all ligands. *T. pyriformis* activity and minnow toxicity values are also in range for all ligands.

4.4.7 Molecular Docking

To carry out docking, the three-dimensional structures of the protein and ligands are used. An online blind auto docking program called CB dock is utilized for this. CB Dock computes the cavity sizes and predicts the protein binding locations. CB Dock provides us with the top five possess and receptor models upon docking.

Based on the cavity size and the vina score, the optimal position was chosen among these five [138]. Target proteins and ligands were used in molecular docking. Ligands are in SDF format, while the proteins are in PDB format. After verifying the input files, CB Dock uses Open Babel and MGL tools to transform them into files in the pdbqt format. Next, CB dock determines the receptor's cavities as well as the diameters and centers of the top five cavities. The protein-ligand interaction's high-affinity score determines which of the five optimal conformations is the best [139]. The scores obtained after the docking of proteins and ligands are shown in tables 4.16.

TABLE 4.16: Docking score of ligand-protein complexes

S. No	**Ligands**	**Target Proteins**				
		Akt2	**IRS-2**	**PDX-1**	**PI3K-α**	**PPAR-γ**
1.	GABA	-4.3	-3.3	-2.9	-3.5	-4.2
2.	Purpurin	-9.5	-7	-6.4	-6.4	-8.4
3.	Cyclopro panecarbonyl chloride	-4.1	-3.4	-3.2	-3.6	-4.3
4.	Honokiol	-8.1	-6	-6.1	-6.9	-8.3
5.	Spermidine	-4.6	-3.8	-3.2	-3.6	-4.3
6.	Aspartic acid	-1	-0.8	-0.8	-0.9	-1

Table 4.16 shows the docking result of receptors with ligands. It shows that purpurin has the highest binding score of -9.5 with Akt2, followed by -8.4 with PPAR-γ.

4.4.7.1 Analysis of Docked Complexes via Discovery Studio

To understand docking data, ligand and protein interaction was estimated. Hydrogen bonding, alkyl and van der waals interactions are the main types of interactions that were investigated. Discovery Studio 2025 Client was used to analyze these interactions between proteins and ligands. The saved conformations for the ligand-receptor complex of each molecule were analyzed in detail. This program creates schematic representations of the protein-ligand interactions between the

specified ligands in the PDB file automatically [140]. Numerous interactions between the ten ligands and the three target proteins were seen in the docked data, which were submitted in PDB format. The docked complexes and ligand-receptor interactions are depicted in the following diagrams. The (a) part of the figure represents the docking complex, while (b) part of the figure provides information about the interaction between protein and ligand.

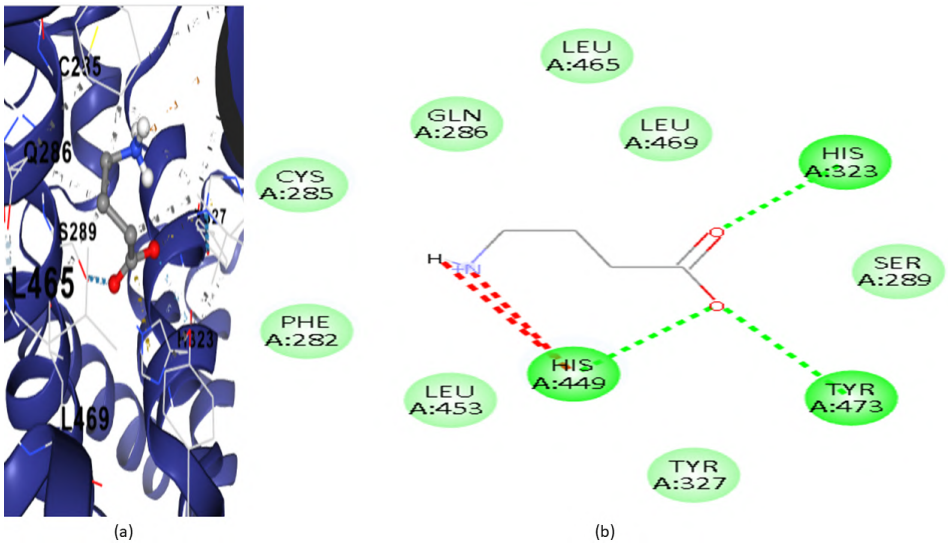

FIGURE 4.45: Analysis of dock complexes of GABA with PPAR-γ

Figure 4.45 shows the interaction of GABA with PPAR-γ. It shows there are three conventional hydrogen bonds, eight van der waals and two unfavorable interactions.

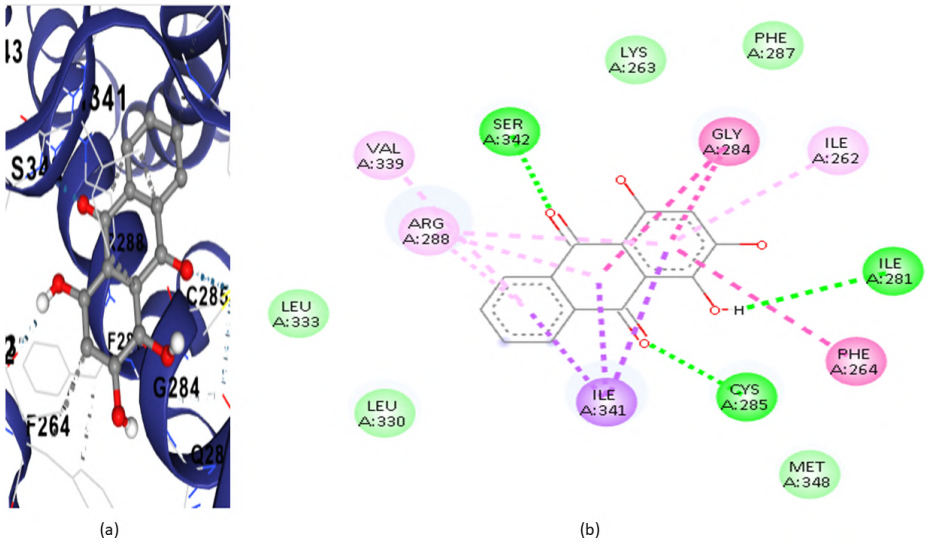

FIGURE 4.46: Analysis of dock complexes of purpurin with PPAR-γ

Figure 4.46 shows the interaction of purpurin with PPAR-γ. It displays five van der Waals contacts, three alkyl bonds, and three typical hydrogen bonds.

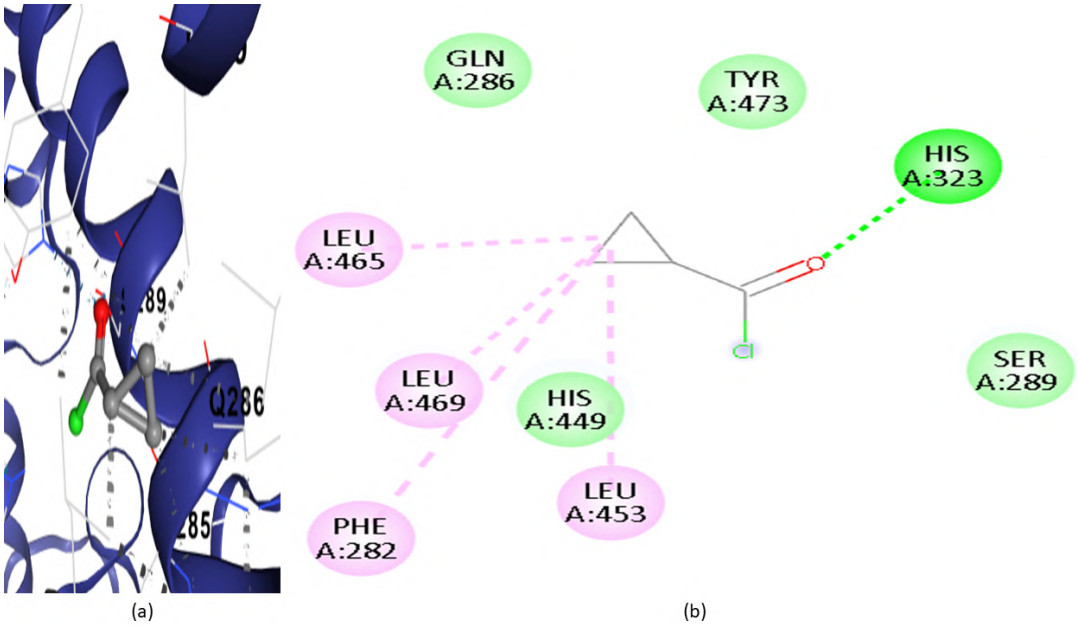

FIGURE 4.47: Analysis of dock complexes of cyclopropanecarbonyl chloride with PPAR-γ

Figure 4.47 shows the interaction of cyclopropanecarbonyl chloride with PPAR-γ. It displays four alkyl bonds, four van der Waals contacts, and one typical hydrogen bond.

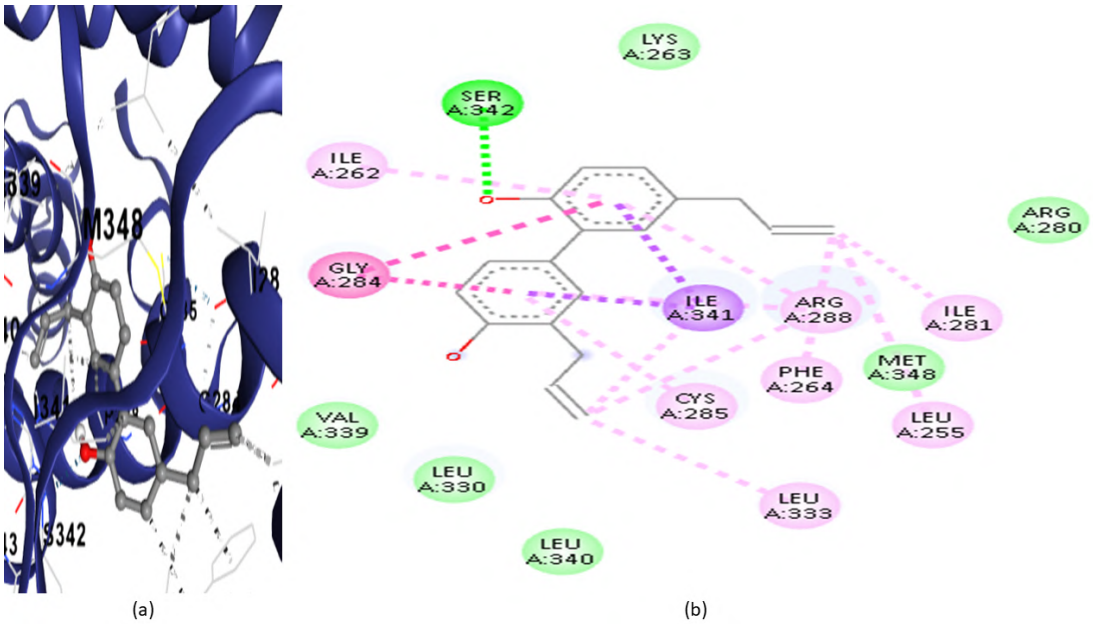

FIGURE 4.48: Analysis of dock complexes of honokiol with PPAR-γ

Figure 4.48 shows the interaction of honokiol with PPAR-γ. There are six van der Waals contacts, seven alkyl bonds, and one typical hydrogen bond, according to the data.

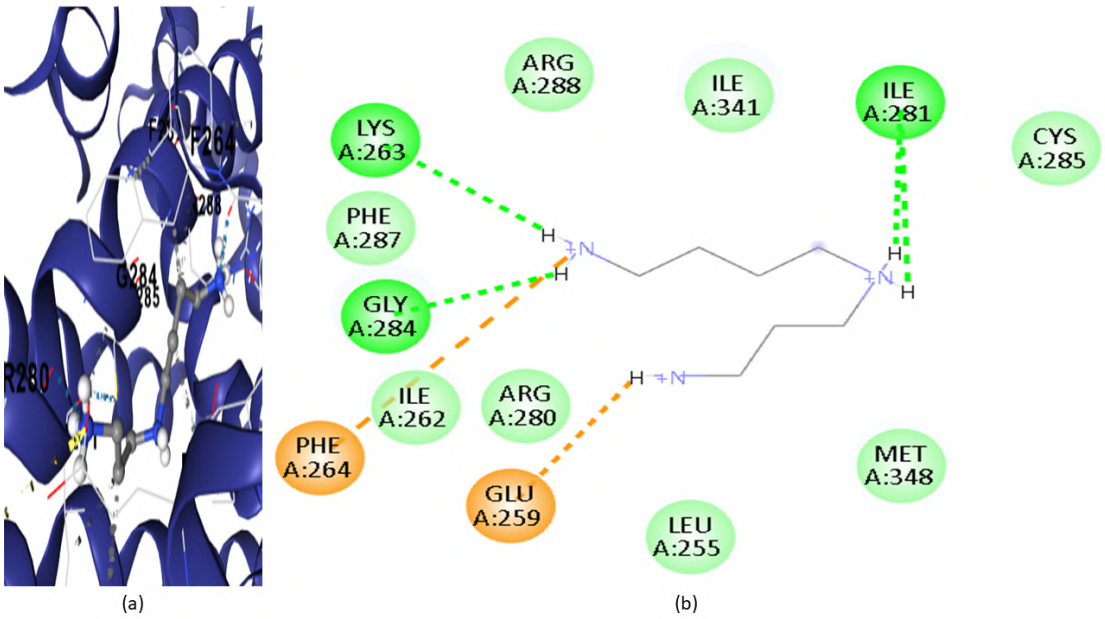

FIGURE 4.49: Analysis of dock complexes of spermidine with PPAR-γ

Figure 4.49 shows the interaction of spermidine with PPAR-γ. It reveals eight van der Waals interactions in addition to three traditional hydrogen bonds.

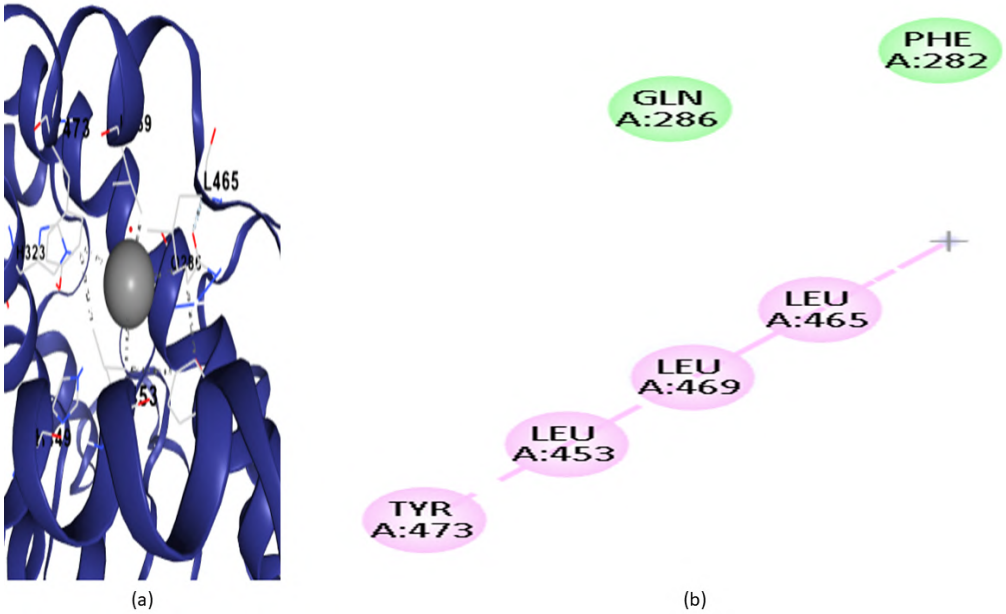

FIGURE 4.50: Analysis of dock complexes of aspartic acid with PPAR-γ

Figure 4.50 shows the interaction of aspartic acid with PPAR-γ. It shows there is four alkyl bonds and two van der waals interactions.

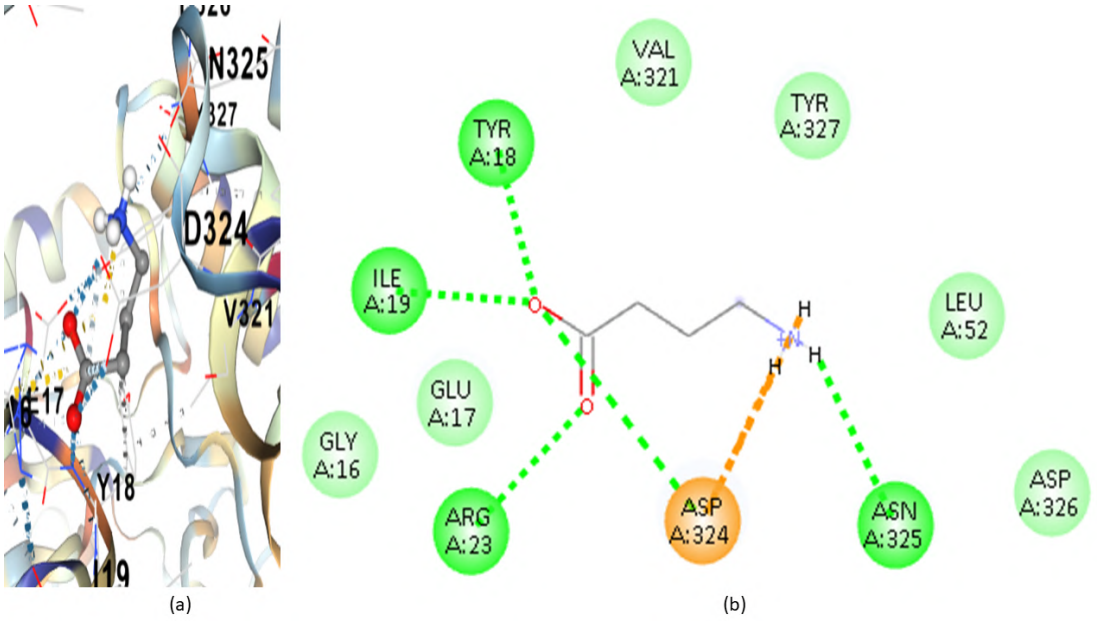

FIGURE 4.51: Analysis of dock complexes of GABA with Akt2

Figure 4.51 shows the interaction of GABA with Akt2. It shows there are five conventional hydrogen bonds and six van der waals interactions.

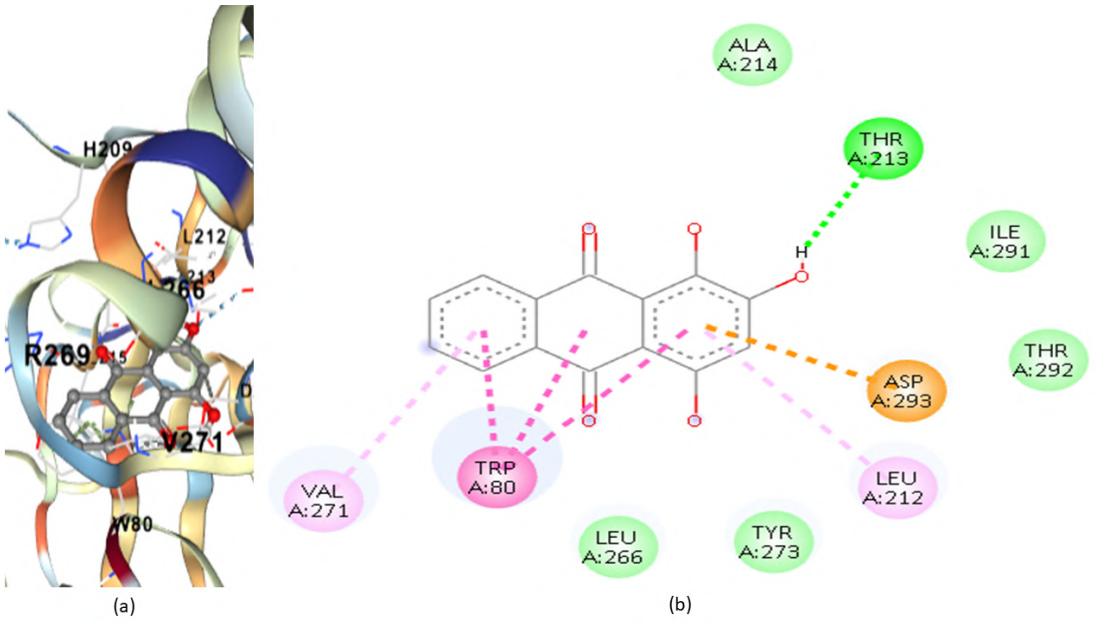

FIGURE 4.52: Analysis of dock complexes of purpurin with Akt2

Figure 4.52 shows the interaction of purpurin with Akt2. Two alkyl bonds, one traditional hydrogen bond, and five van der Waals interactions are visible.

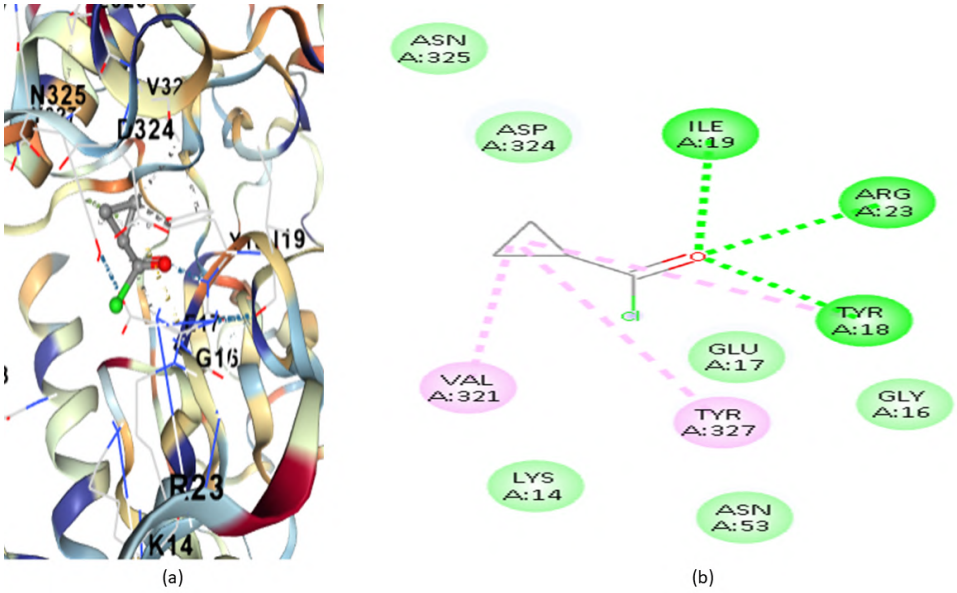

FIGURE 4.53: Analysis of dock complexes of cyclopropanecarbonyl chloride with Akt2

Figure 4.53 shows the interaction of cyclopropanecarbonyl chloride with Akt2. It displays six van der Waals contacts, three traditional hydrogen bonds, and two alkyl bonds.

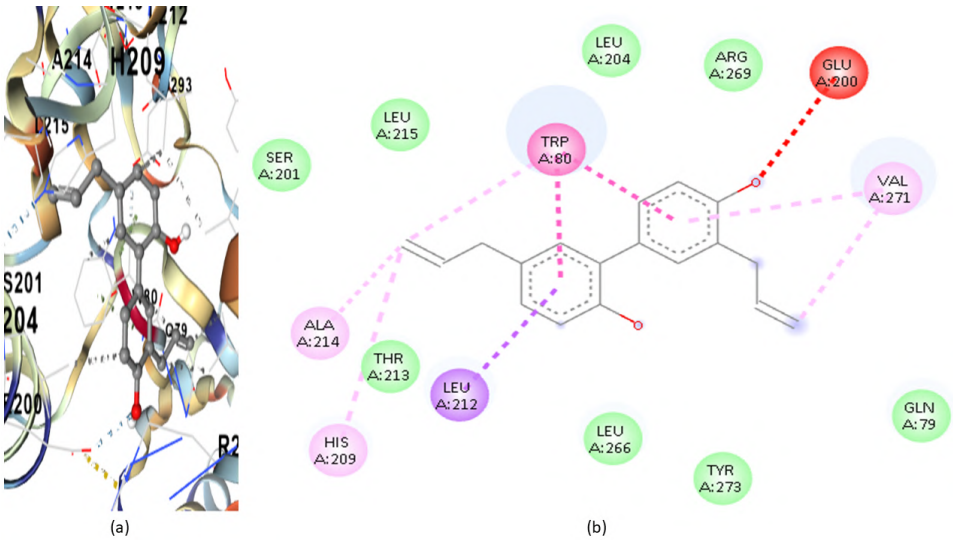

FIGURE 4.54: Analysis of dock complexes of honokiol with Akt2

Figure 4.54 shows the interaction of honokiol with Akt2. It displays eight van der Waals contacts and three alkyl bonds.

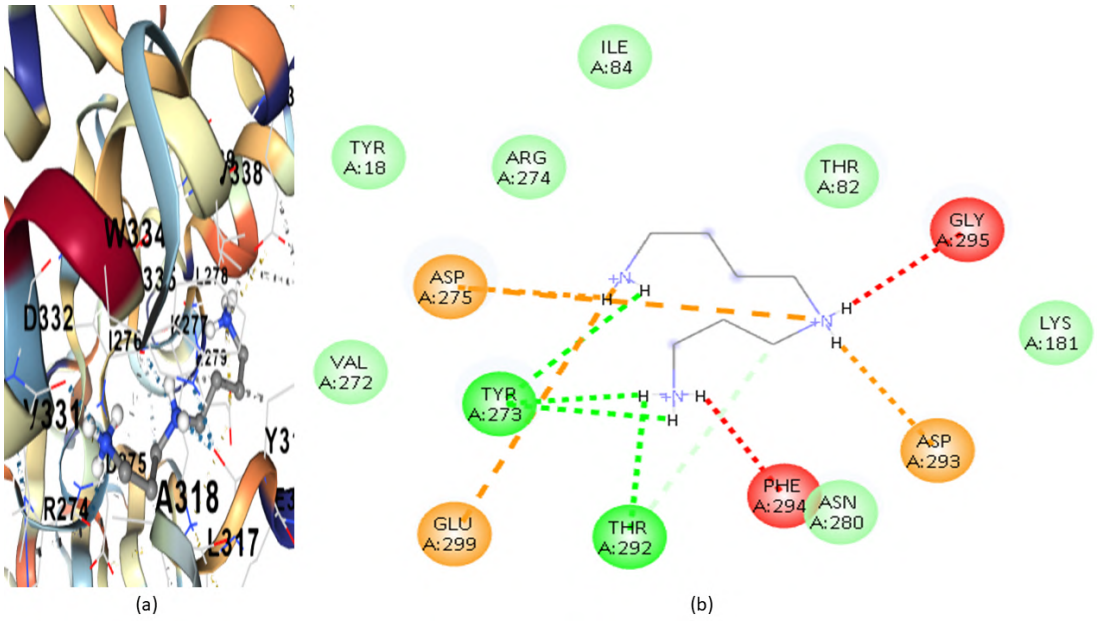

FIGURE 4.55: Analysis of dock complexes of spermidine with Akt2

Figure 4.55 shows the interaction of spermidine with Akt2. It demonstrates that there are seven van der Waals interactions and three traditional hydrogen bonds.

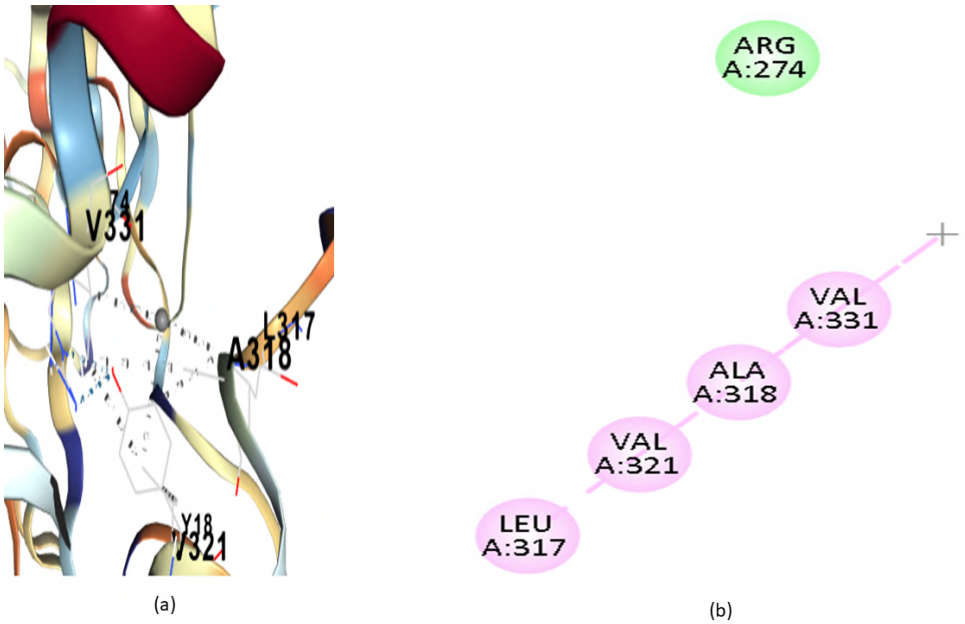

FIGURE 4.56: Analysis of dock complexes of aspartic acid with Akt2

Figure 4.56 shows the interaction of aspartic acid with Akt2. It shows there are four alkyl bonds and one van der waals interactions.

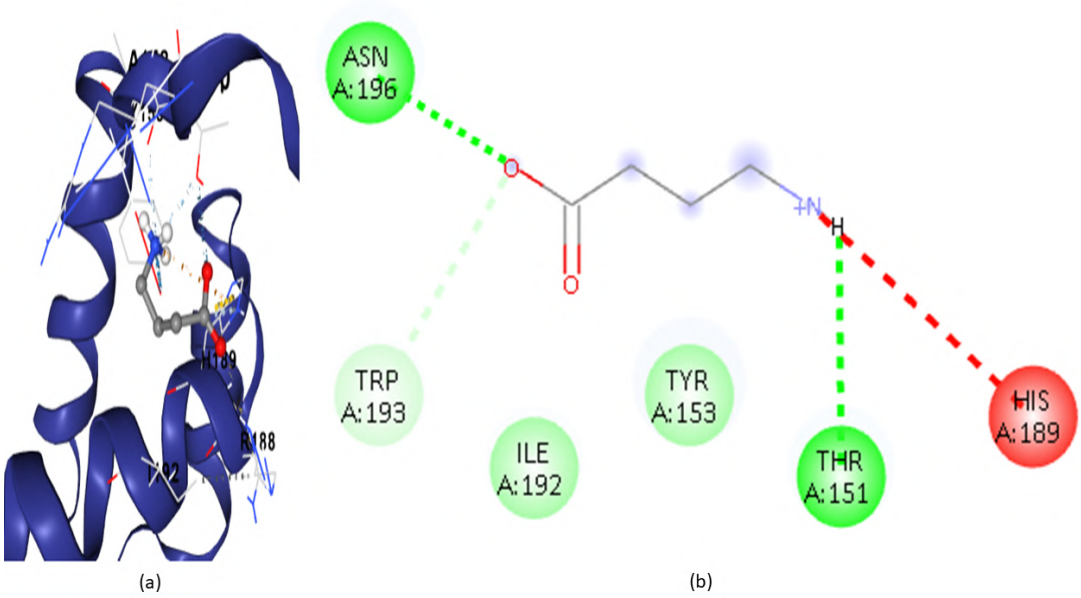

FIGURE 4.57: Analysis of dock complexes of GABA with PDX-1

Figure 4.57 shows the interaction of GABA with PDX-1. It shows there are two conventional hydrogen bonds, one carbon hydrogen bond and two van der waals interactions.

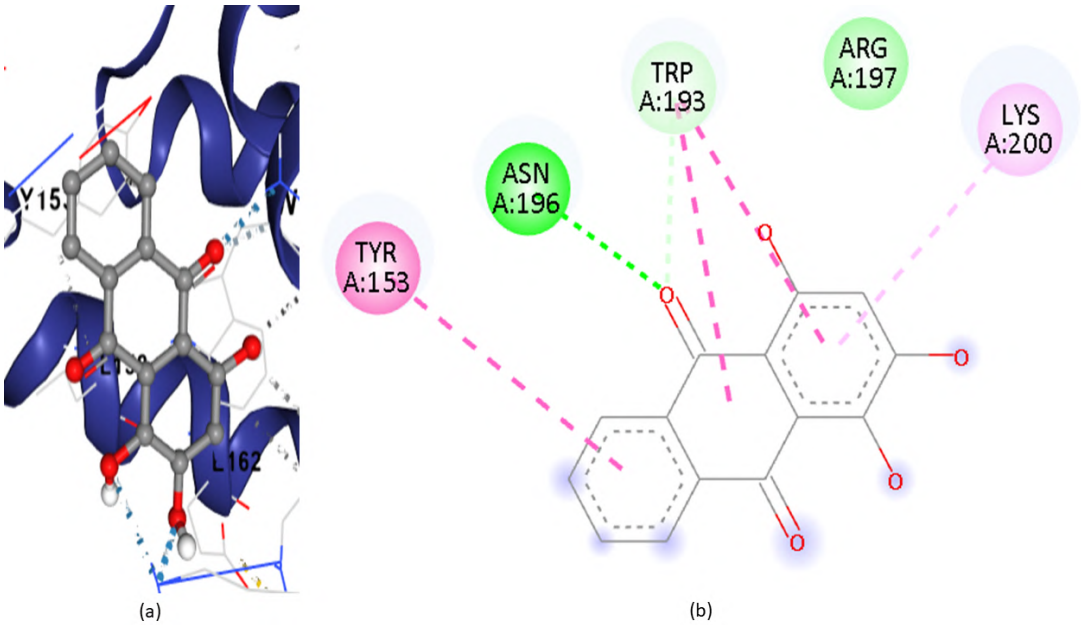

FIGURE 4.58: Analysis of dock complexes of purpurin with PDX-1

Figure 4.58 shows the interaction of purpurin with PDX-1. It shows there is one alkyl bond, one conventional hydrogen bond, one C & H bond and one van der waals interaction.

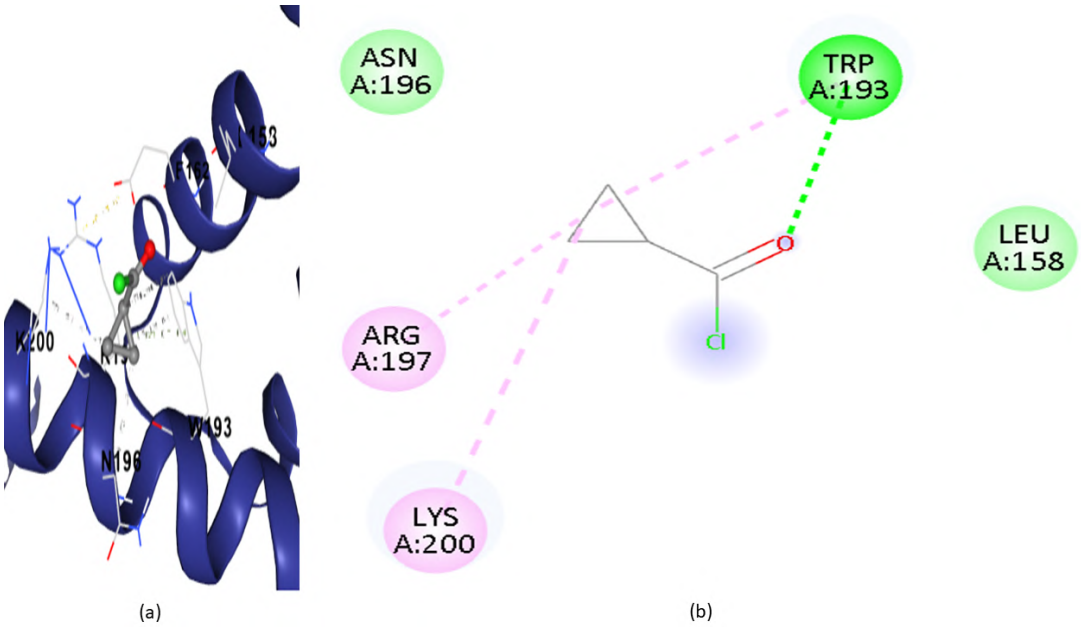

FIGURE 4.59: Analysis of dock complexes of cyclopropanecarbonyl chloride with PDX-1

Figure 4.59 shows the interaction of cyclopropanecarbonyl chloride with PDX-1. It shows there are two alkyl bonds, one conventional hydrogen bond and two van der waals connections.

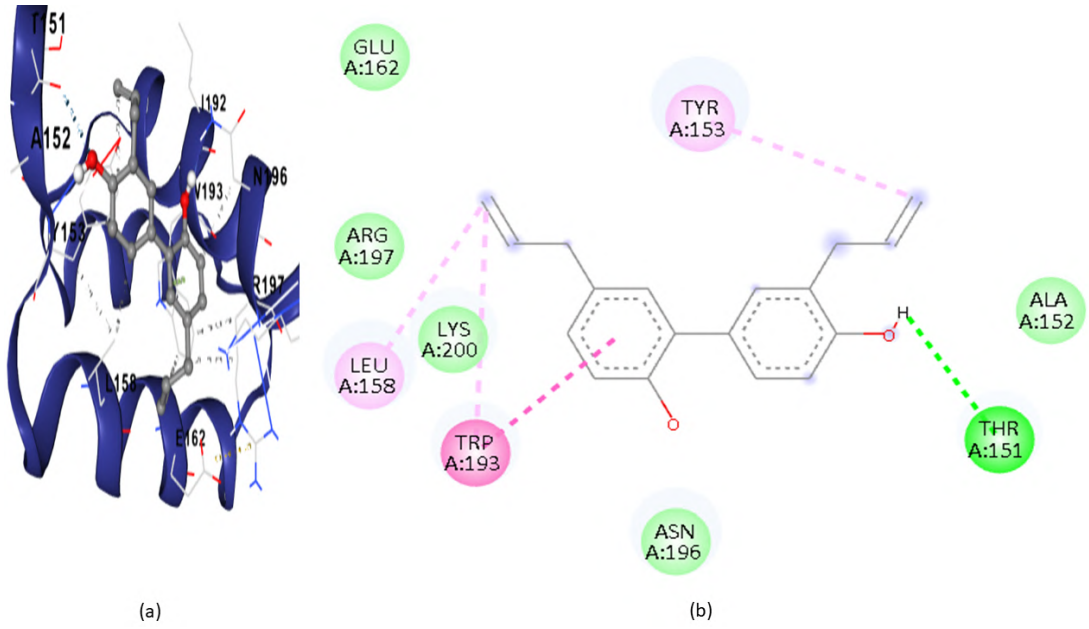

FIGURE 4.60: Analysis of dock complexes of honokiol with PDX-1

Figure 4.60 shows the interaction of honokiol with PDX-1. It shows there are two alkyl bonds, one conventional hydrogen bond and five van der waals interactions.

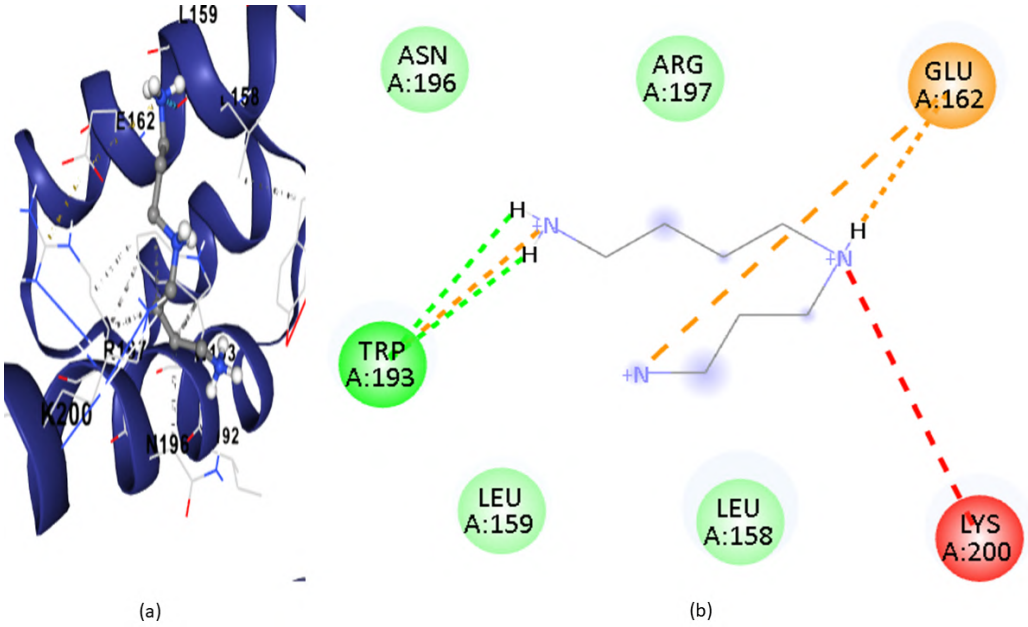

FIGURE 4.61: Analysis of dock complexes of spermidine with PDX-1

Figure 4.61 shows the interaction of spermidine with PDX-1. It shows there are two conventional hydrogen bonds and four van der waals interactions.

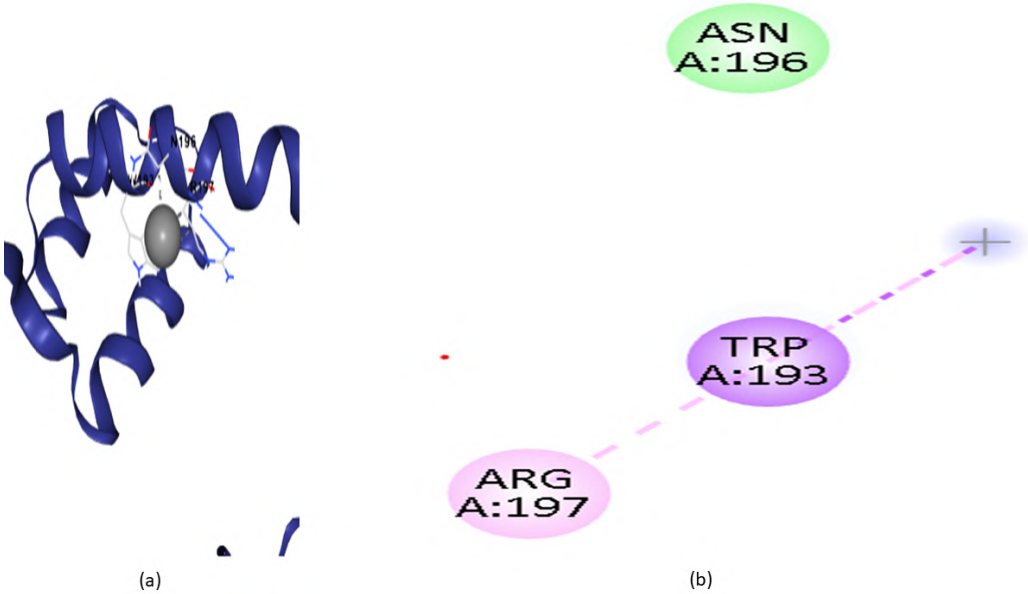

FIGURE 4.62: Analysis of dock complexes of aspartic acid with PDX-1

Figure 4.62 shows the interaction of aspartic acid with PDX-1. It shows there is one alkyl bond and one van der waals interaction.

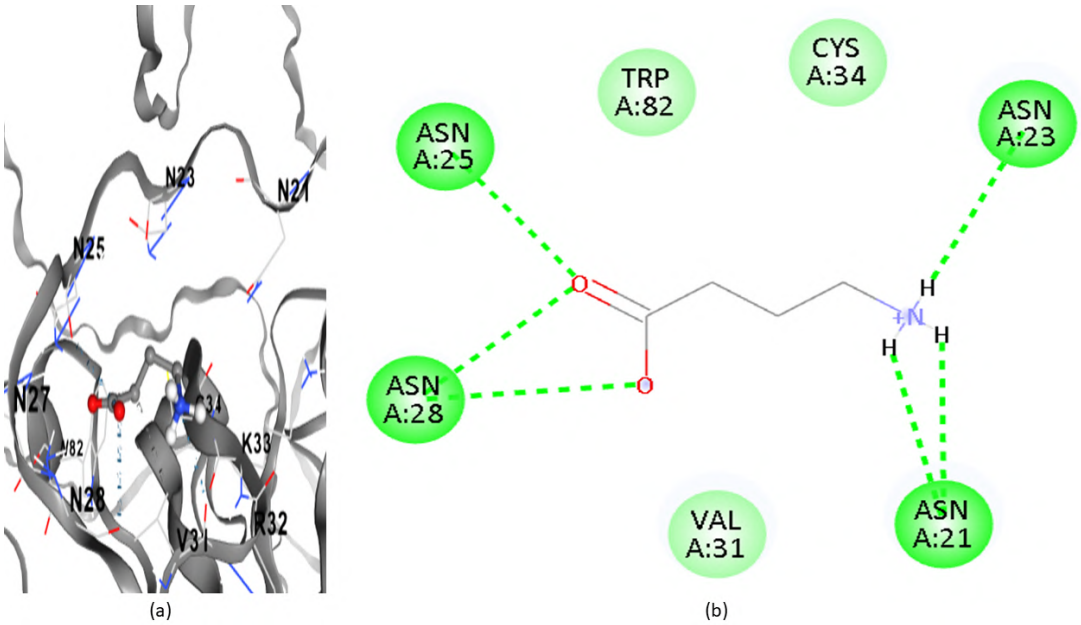

FIGURE 4.63: Analysis of dock complexes of GABA with IRS-2

Figure 4.63 shows the interaction of GABA with IRS-2. It shows there are six conventional hydrogen bonds and three van der waals interactions.

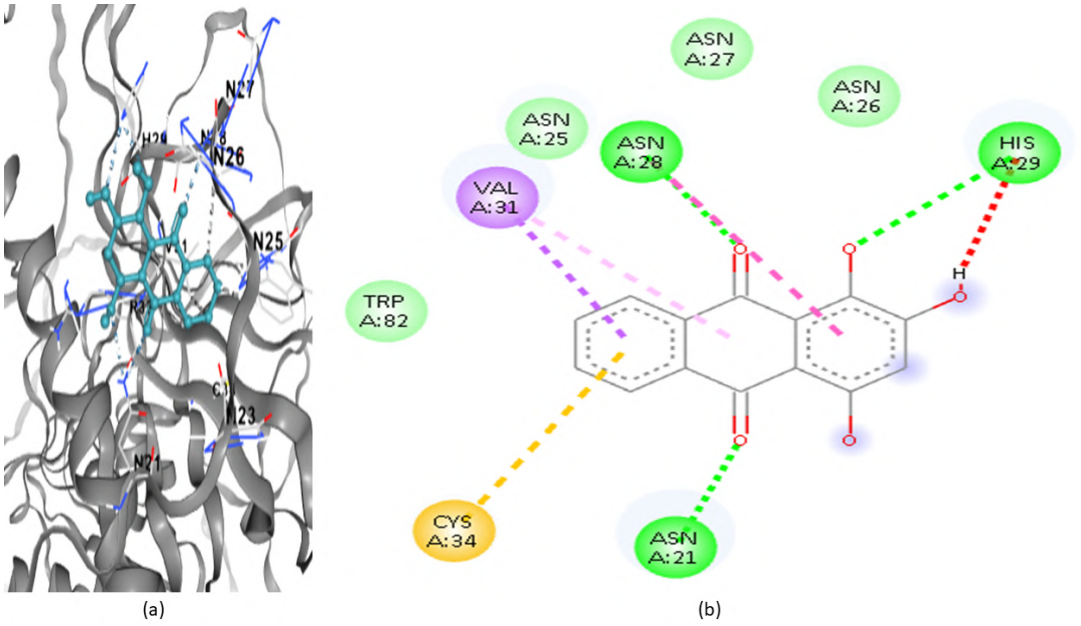

FIGURE 4.64: Analysis of dock complexes of purpurin with IRS-2

Figure 4.64 shows the interaction of purpurin with IRS-2. It shows there are three conventional hydrogen bonds and four van der waals interactions.

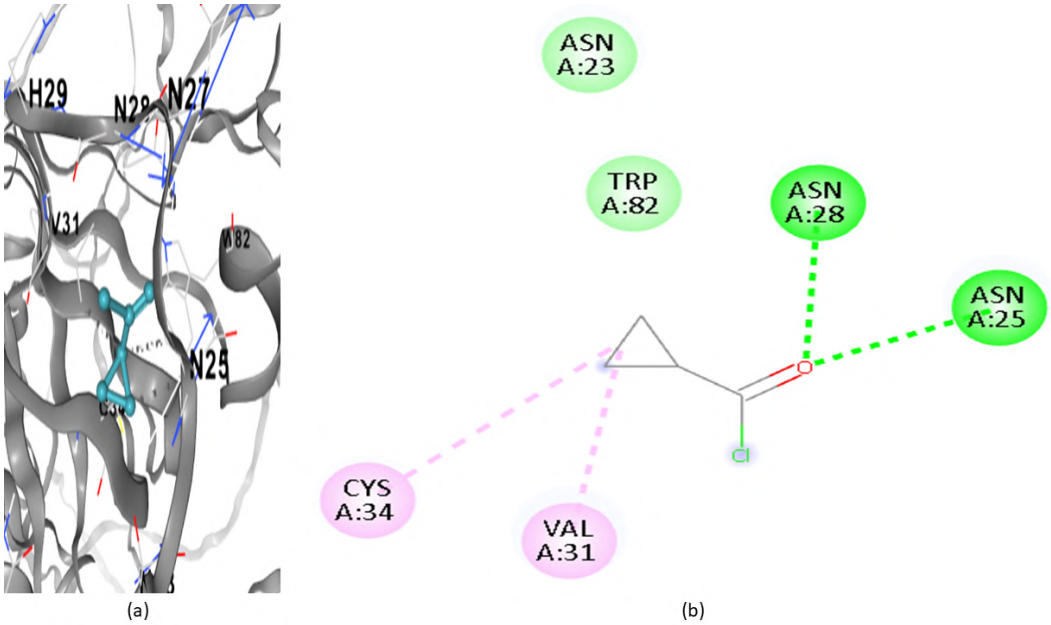

FIGURE 4.65: Analysis of dock complexes of cyclopropanecarbonyl chloride with IRS-2

Figure 4.65 shows the interaction of cyclopropanecarbonyl chloride with IRS-2. It displays two alkyl bonds, two van der Waals contacts, and two typical hydrogen bonds.

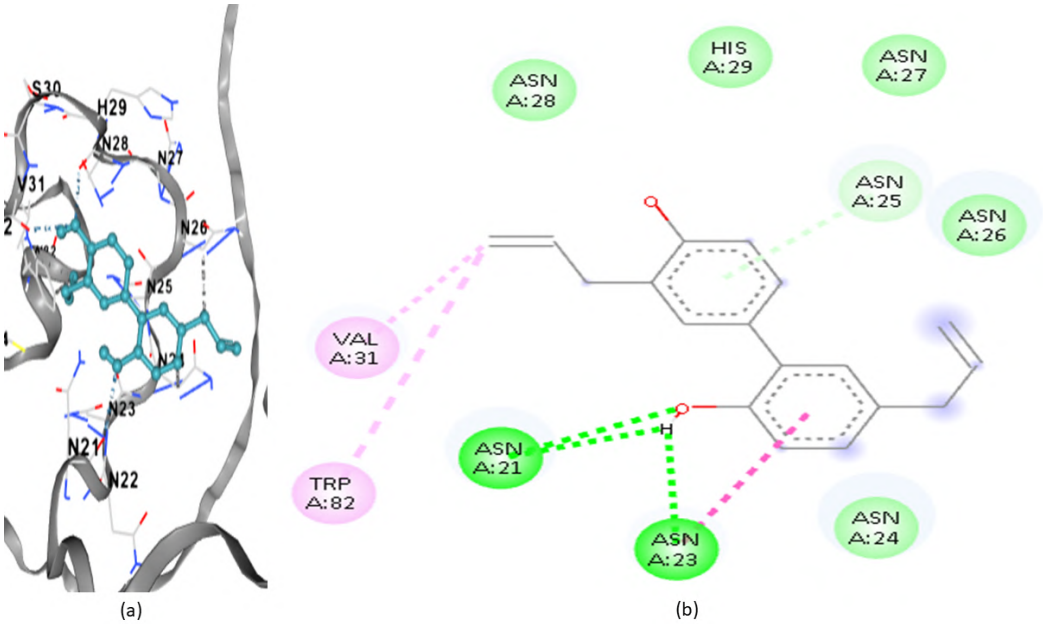

FIGURE 4.66: Analysis of dock complexes of honokiol with IRS-2

Figure 4.66 shows the interaction of honokiol with IRS-2. It shows there are two alkyl bonds accompanied with three conventional hydrogen bonds, one donor hydrogen bond and five van der waals interactions.

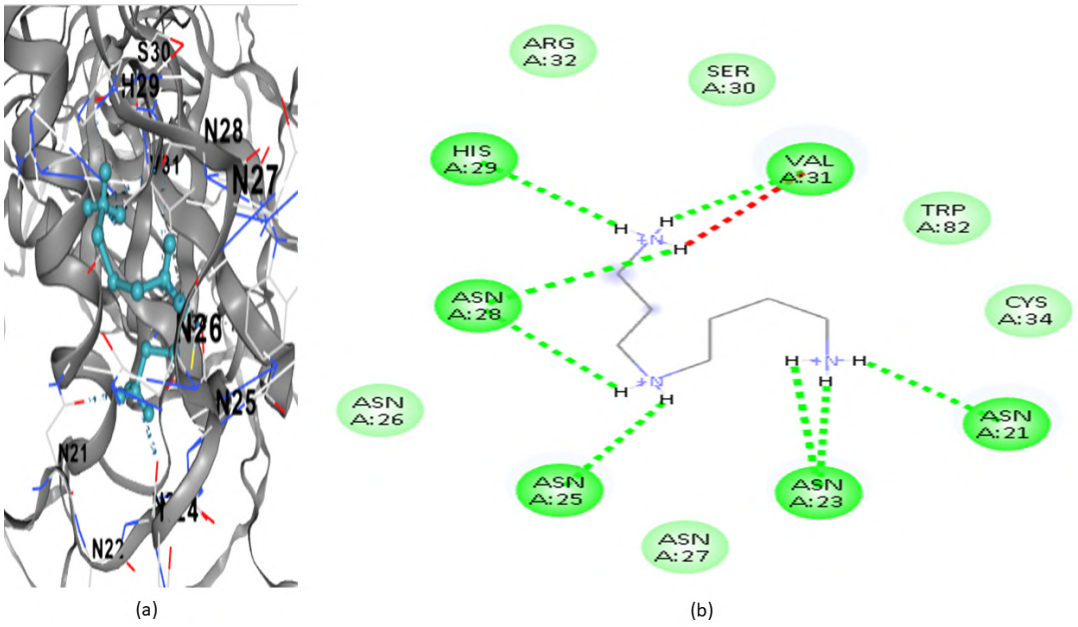

FIGURE 4.67: Analysis of dock complexes of spermidine with IRS-2

Figure 4.67 shows the interaction of spermidine with IRS-2. It shows there are eight conventional hydrogen bonds and six van der waals interactions.

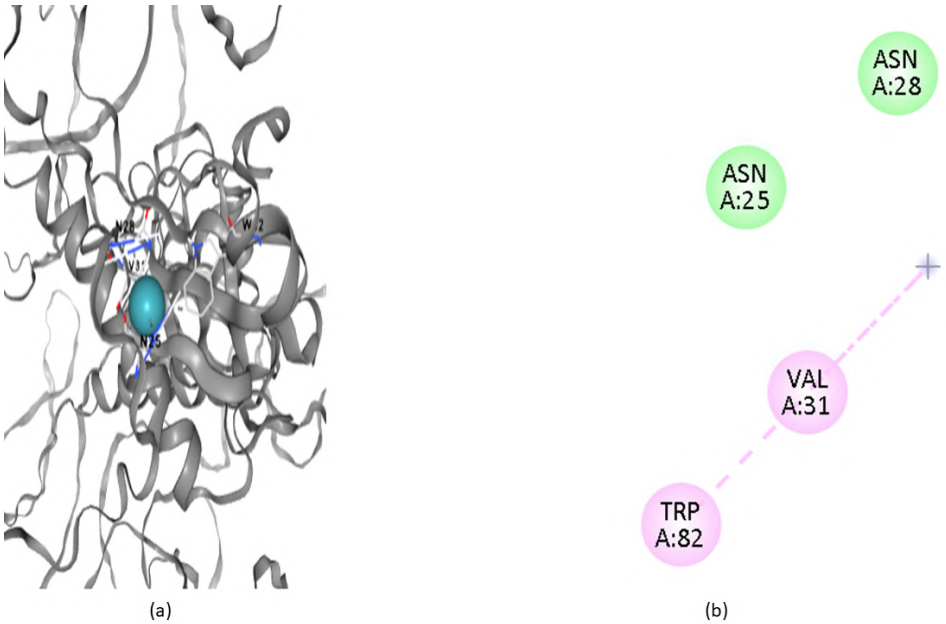

FIGURE 4.68: Analysis of dock complexes of aspartic acid with IRS-2

Figure 4.68 shows the interaction of aspartic acid with IRS-2. It shows there are 02 alkyl bonds and 02 van der waals interactions.

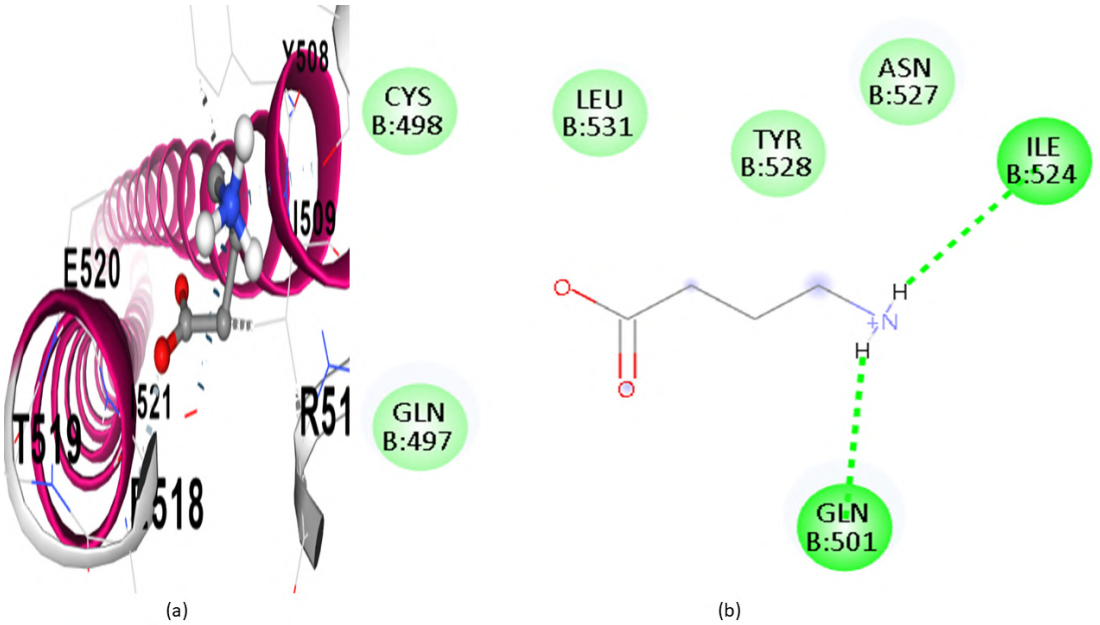

FIGURE 4.69: Analysis of dock complexes of GABA with PI3K-α

Figure 4.69 shows the interaction of GABA with PI3K-α. It shows there are 02 conventional hydrogen bonds along with 05 van der waals contacts.

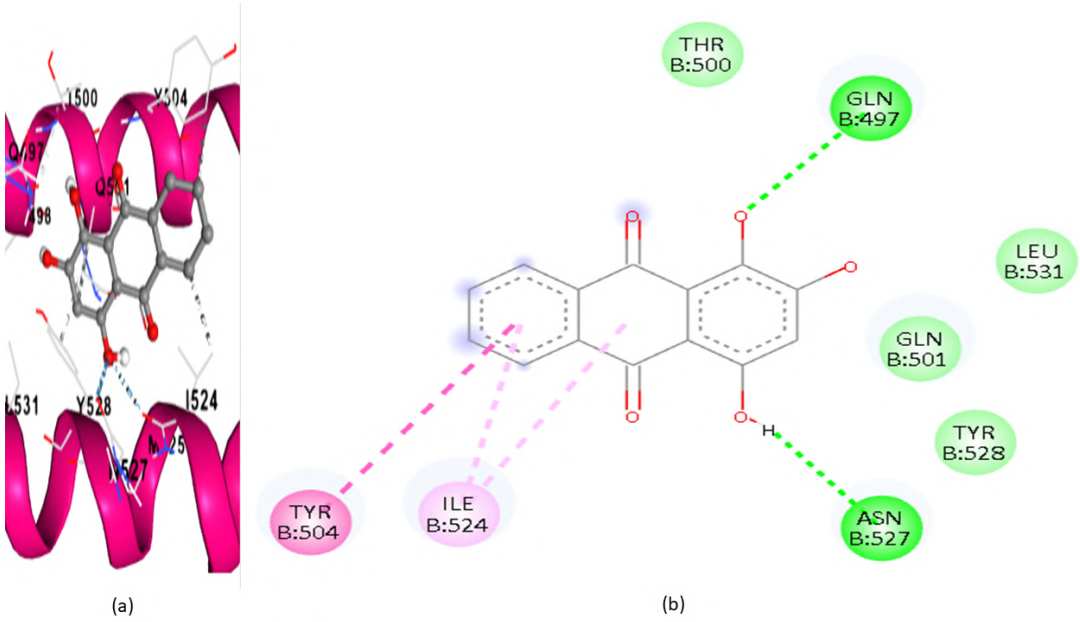

FIGURE 4.70: Analysis of dock complexes of purpurin with PI3K-α

Figure 4.70 shows the interaction of purpurin with PI3K-α. It demonstrates there is 01 alkyl bond along with 02 conventional hydrogen bonds and are 04 van der waals interactions.

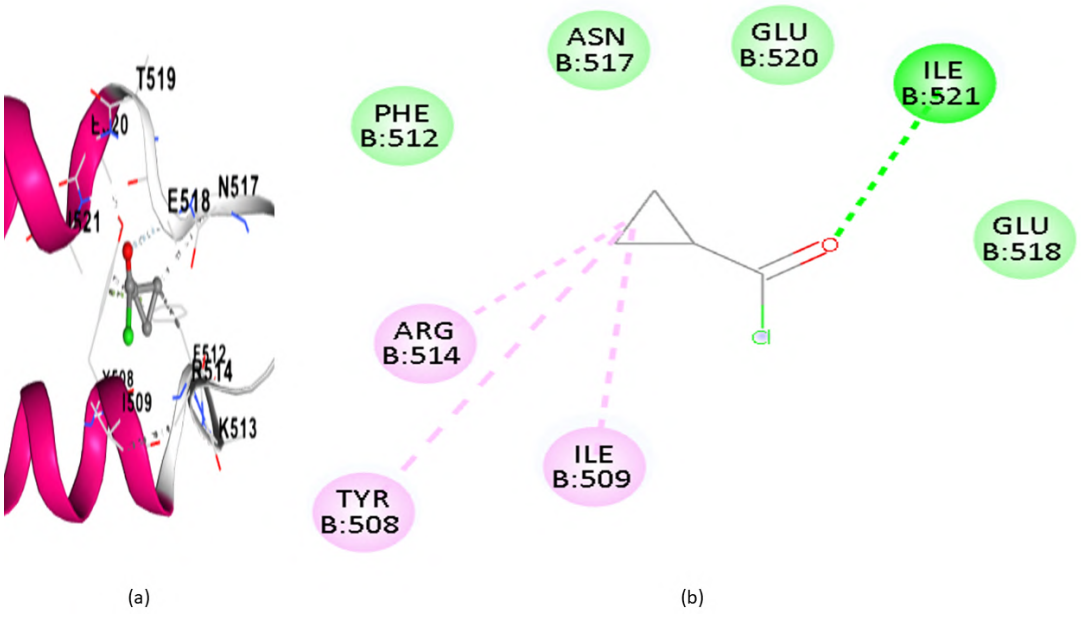

FIGURE 4.71: Analysis of dock complexes of cyclopropanecarbonyl chloride with PI3K-α

Figure 4.71 shows the interaction of cyclopropanecarbonyl chloride with PI3K-α. It shows there are three alkyl bonds, one conventional hydrogen bond and four van der waals connections.

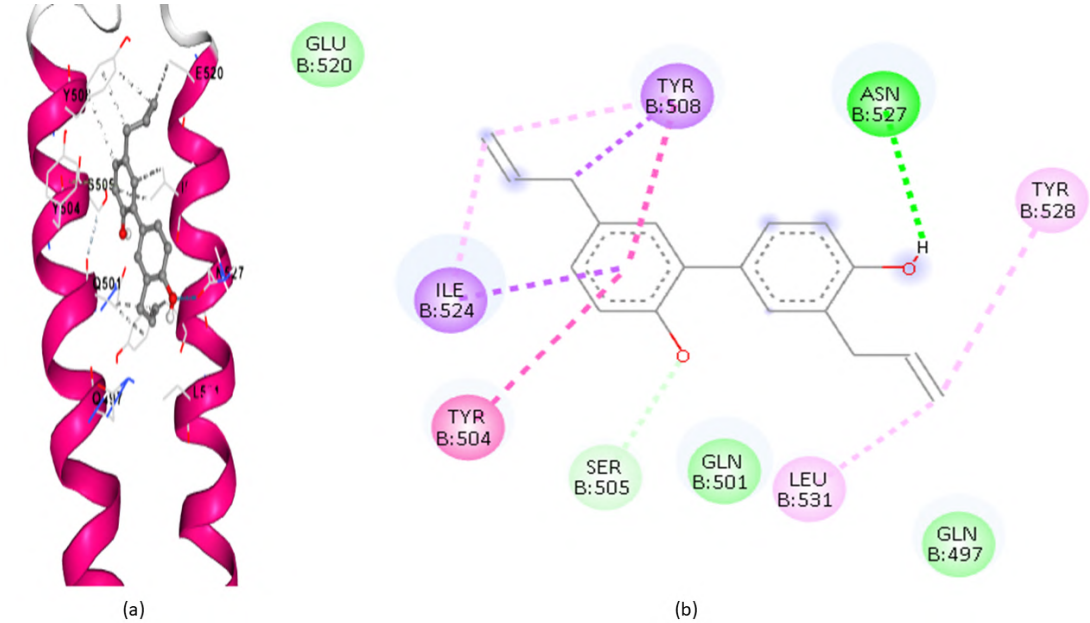

FIGURE 4.72: Analysis of dock complexes of honokiol with PI3K-α

Figure 4.72 shows the interaction of honokiol with PI3K-α. It shows there are 02 alkyl bonds, one carbon hydrogen bond, one conventional hydrogen bond and three van der waals interactions.

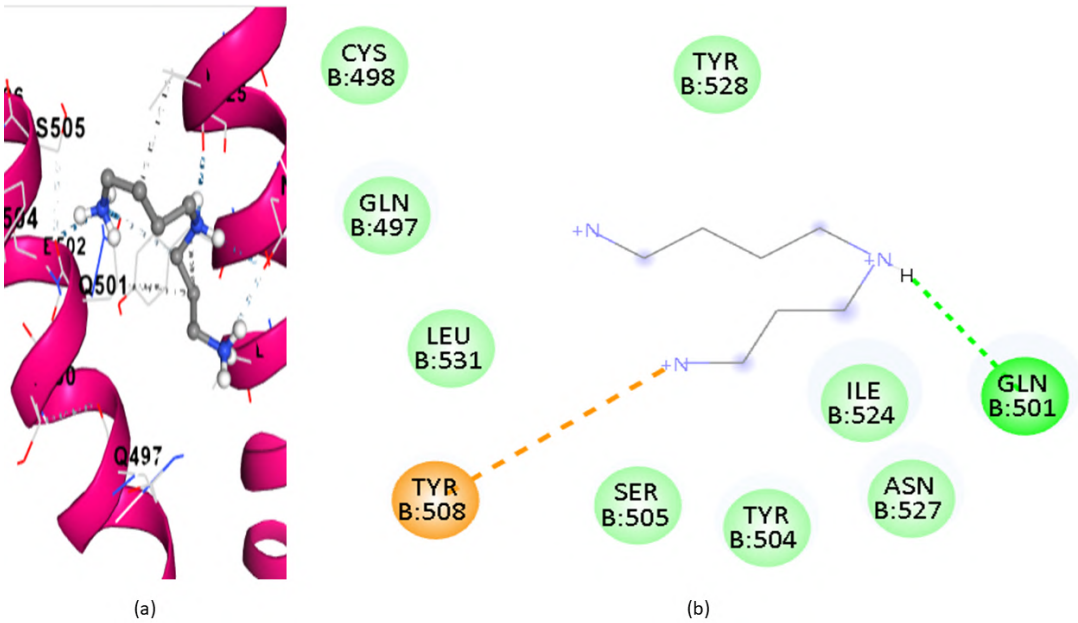

FIGURE 4.73: Analysis of dock complexes of spermidine with PI3K-α

Figure 4.73 shows the interaction of spermidine with PI3K-α. It shows there is one conventional hydrogen bond and eight van der waals interactions.

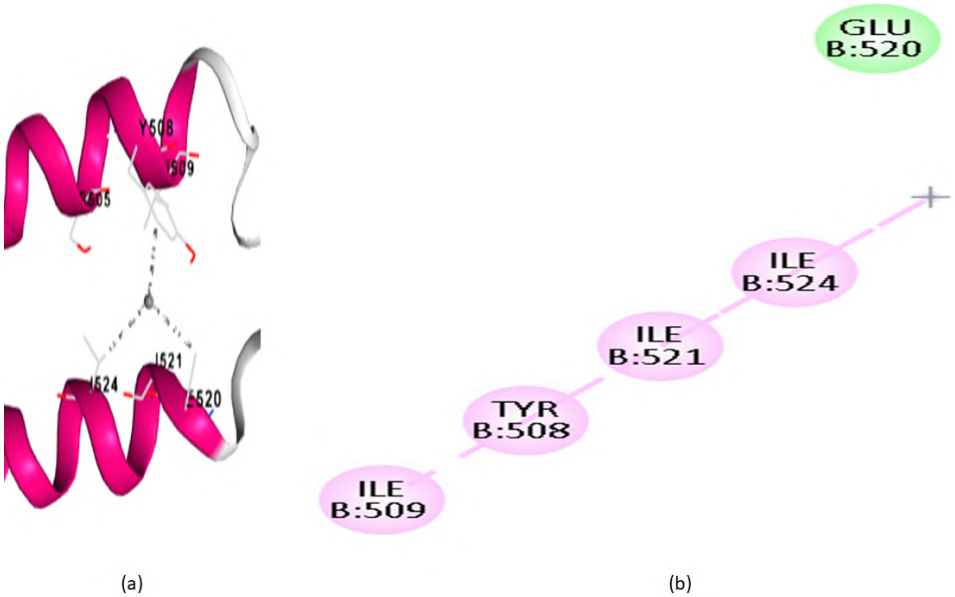

FIGURE 4.74: Analysis of dock complexes of aspartic acid with PI3K-α

Figure 4.74 shows the interaction of aspartic acid with PI3K-α. It shows there are four alkyl bonds and one van der waals interaction.

4.4.8 Lead Compound Identification

The ligands' pharmacokinetic and physicochemical properties determine their fate as either drug or non-drug compounds. Lipinski's rule is the first filter and pharmacokinetics is the second filter for this identification. All ligands were seen obeying the lipinski rule of five so they all got selected for docking. The next knockout stage is pharmacokinetic screening and docking score.

In this screening, purpurin from super-fraction NF1 was selected as lead compound because it showed the best ADMET values concerning high water solubility, good intestinal absorption, and minimal toxicity. Docking score of purpurin is also good against all receptors and highest i.e. -9.5 against Akt2 receptor, followed by -8.4 against PPAR-γ. Additionally, purpurin has a significant quantity of residues having van der waals interactions, alkyl bonds and hydrogen bonds, so purpurin was selected as the lead compound.

4.4.9 Reference Anti-diabetic Drug Identification

Metformin is a commonly used medication for diabetes. It functions by raising insulin sensitivity and decreasing hepatic glucose synthesis. It activates AMP-activated protein kinase, which inhibits gluconeogenic enzymes, decreasing glucose production in the liver.

Additionally, it enhances glucose uptake in muscle and fat tissues by promoting GLUT4 translocation to the cell membrane. It may also reduce intestinal glucose absorption and alter gut microbiota, contributing to its glucose-lowering effect. Metformin is effective in lowering blood glucose levels without significant hypoglycemia, though it can cause gastrointestinal side effects and, rarely, lactic acidosis [141].

4.4.9.1 Metformin and Lead Compound Comparison

Metformin's effective mechanism of action and favorable safety profile make it an ideal reference drug for comparative studies, providing a solid foundation for evaluating new potential therapeutic agents such as purpurin in the context of IRS protein sensitivity and glucose metabolism.

4.4.9.2 Metformin Structure Prediction

First of all metformin structure was downloaded in SDF format from PubChem. Then its energy was minimized by using chem3D pro to get the refined structure. The chemical formula of metformin is C4H11N5 and its refined structure is given in figure 4.75.

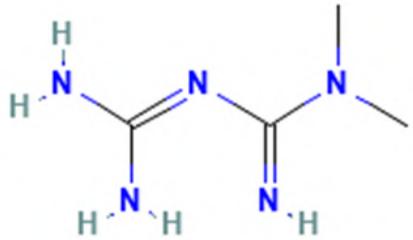

FIGURE 4.75: Structure of metformin

4.4.9.3 Lipinski Rule Comparison

The metformin and purpurin were compared to observe their response to the lipinski rule and to evaluate their pharmacokinetic properties, to assess their bioavailability, safety, efficacy, and drug-likeness. The comparison is given in table 4.17.

TABLE 4.17: The lipinski rule of five comparison

Ligands	**Log P value**	**Molecular weight**	**H-bond donor**	**H-bond acceptor**	**Rotatable bonds**
Metformin	-1.24	129.167	3	1	0
Purpurin	1.57	256	3	5	0

Table 4.17 shows that both compounds are following lipinski rule.

4.4.9.4 ADMET Properties Comparison

The ADMET qualities were used to evaluate the drug's and the lead chemical's absorption, distribution, metabolism, excretion, and toxicity to identify a better drug candidate.

i. The Absorption Properties Comparison

A comparison between metformin and purpurin for checking absorbance models is given in table 4.18.

TABLE 4.18: Absorption properties comparison

	Absorption Properties						
Ligand Name	**Water solubility**	**$CaCO_2$ Permeability**	**Intestinal absorption (human)**	**Skin permeability**	**P - glycoprotein substrate**	**P - glycoprotein I inhibitor**	**P - glycoprotein II inhibitor**
Metformin	-2.707	-0.339	59.401	-2.735	Yes	No	No
Purpurin	-2.901	-0.198	68.97	-2.736	Yes	No	No

Table 4.18 shows that both metformin and purpurin show comparable absorption properties except for intestinal absorption, which is low for metformin.

ii. Distribution Properties Comparison

The comparison between the distribution properties of metformin and purpurin is given in table 4.19.

TABLE 4.19: Distribution properties comparison

	Distribution Properties			
Ligand Name	**VDss (human)**	**Fraction unbound (human) Fu**	**BBB permeability log BB**	**CNS permeability log PS**
Metformin	-0.232	0.811	-0.946	-4.238
Purpurin	0.627	0.237	-0.769	-2.371

The above table 4.19 shows the comparative distribution properties of metformin and purpurin. Both metformin and purpurin share comparable distribution properties except VDSS, which is too low for metformin.

iii. Metabolism Properties Comparison

The comparison between the metabolism properties of metformin and purpurin is given in table 4.20.

TABLE 4.20: Metabolic properties comparison

Ligand Name	**Metabolism Properties**						
	CYP2D6 substrate	**CYP3A4 substrate**	**CYP1A2 inhibitor**	**CYP2C19 inhibitor**	**CYP2C9 inhibitor**	**CYP2D6 inhibitor**	**CYP3A4 inhibitor**
Metformin	No	No	No	No	No	No	No
Purpurin	No	No	No	No	No	No	No

Table 4.20 shows that both metformin and purpurin share similar metabolism profiles.

iv. Excretion Properties Comparison

The comparison between the excretion properties of metformin and purpurin is given in table 4.21.

TABLE 4.21: Excretion properties comparison

Ligand Name	**Excretion Properties**	
	Total Clearance	**Renal OCT2 substrate**
Metformin	0.1	No
Purpurin	0.018	No

Table 4.21 shows that both metformin and purpurin have similar excretion profile.

v. Toxicity Properties Comparison

TABLE 4.22: Toxicity properties comparison

Ligand Name	Toxicity Properties									
	AMES toxicity	**Max tolerated dose (human)**	**hERG I inhibitor**	**hERG II inhibitor**	**Oral rat acute toxicity (LD50)**	**Oral rat chronic toxicity (LOAEL)**	**Hepato toxicity**	**Skin sensitization**	***T. pyriformis* toxicity**	**Minnow toxicity**
Metformin	Yes	0.902	No	No	2.453	2.158	No	Yes	0.25	3.972
Purpurin	No	0.372	No	No	2.261	2.649	No	No	0.433	2.2

Table 4.22 shows that both metformin and purpurin have comparable toxicity profiles except for AMES toxicity and skin sensitization which is shown by the standard drug metformin.

4.4.9.5 Comparison of Docking Score

The standard drug for diabetes metformin and lead phytocompound purpurin were docked against target proteins and binding values were obtained. The docking score comparison between metformin and purpurin is displayed in table 4.23.

TABLE 4.23: Docking comparison of metformin and riboflavin

S. No	Ligands	Target Proteins				
		Akt2	**IRS-2**	**PDX1**	**PI3K-α**	**PPAR-γ**
1.	Metformin	-5.5	-4.5	-3.7	-3.9	-5.1
2.	Purpurin	-9.5	-7	-6.4	-6.4	-8.4

As can be shown in table 4.23, the vina scores of the lead compound purpurin are significantly greater than those of the standard drug metformin. The docking scores of metformin against target proteins Akt2, IRS-2, PDX1, PI3K-α and PPAR-γ are -5.5, -4.5, -3.7, -3.9 and -5.1, respectively, while for purpurin these scores are -9.5, -7, -6.4, -6.4 and -8.4, respectively. These results show that the lead compound purpurin with highest docking score i.e., -9.5 has more binding efficiency than the standard drug metformin with docking score -5.5.

4.4.9.6 Docking Analysis Comparison

Discovery studio evaluated the docking results depending upon the number of interactions between ligand and protein. The following figure shows the docking analysis of standard drug metformin with highest docking score -5.5 against target protein Akt2.

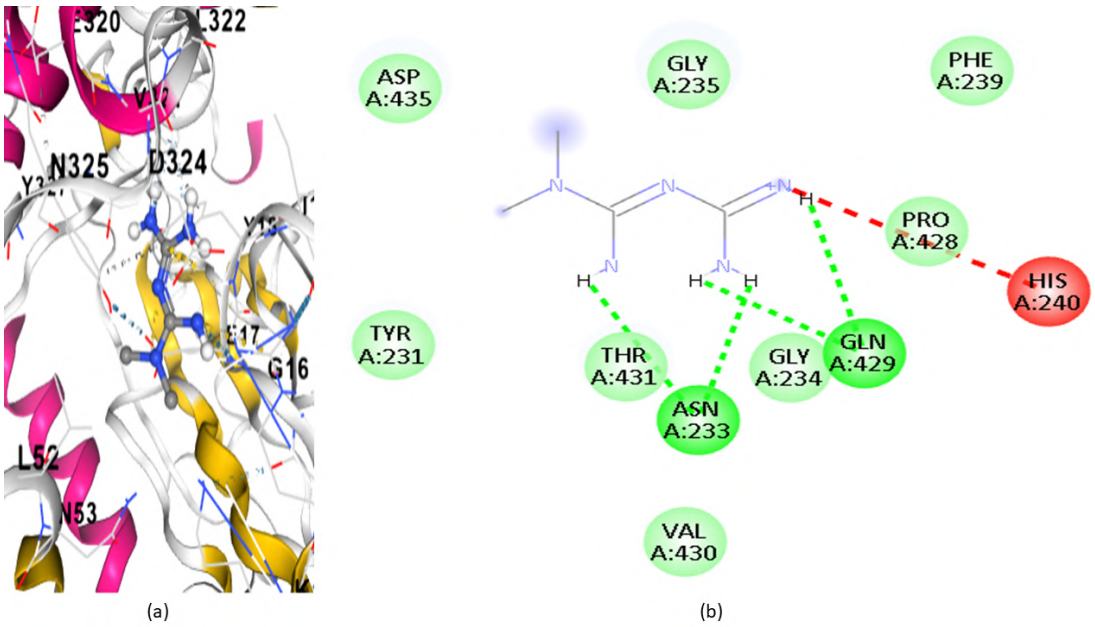

FIGURE 4.76: Docking interaction of metformin with target protein Akt2

Figure 4.76 shows the interaction of metformin with the target protein Akt2. It shows there are four conventional hydrogen bonds, eight van der waals and one unfavorable interaction. Whereas in the case of purpurin interacting with Akt2, figure 4.52 above, it shows two alkyl bonds, one conventional hydrogen bond, three

pi-bonds, one pi-anion, and five van der waals interactions. The data demonstrate that both purpurin and metformin share a robust interaction profile, but the presence of unfavorable interaction in metformin might reduce its overall stability.

Overall, the comparison of metformin and purpurin shows that both share comparable lipinski rules and ADMET analysis. But the docking scores and receptor-ligand interaction profile of the lead compound purpurin are better than those of the standard drug metformin. It shows that purpurin from super-fraction NF1 can act as a promising anti-diabetic therapeutic candidate in the future.

Chapter 5

Discussion

The results obtained from the current study on the fractionation of *Azadirachta indica* leaf extract by column chromatography and its antioxidant and antidiabetic properties are well supported by the existing literature, which confirms the therapeutic use of *Azadirachta indica* [142]. The current study's results on the antioxidant properties of the active fractions are consistent with the existing literature, which has demonstrated that *A. indica* leaf extracts have potent antioxidant properties, even more so than the standard antioxidant ascorbic acid. Additionally, it has been demonstrated that these extracts can decrease lipid peroxidation and enhance the levels of antioxidant enzymes in tissues damaged by diabetes, thus confirming the protective function of the extract [143].

The antidiabetic property of *A. indica* has been extensively documented, proving its efficacy in reducing blood glucose levels in different animal models induced by alloxan or streptozotocin. It has been established that the aqueous extract of *A. indica* leaves can effectively lower blood glucose levels and correct lipid profiles, which is an essential component of diabetes management because the simultaneous treatment of hyperglycemia and dyslipidemia is a key factor in diabetes management [144]. It is pertinent to note that the comparative study between young leaf extract and mature leaf extract has revealed that the young leaf extract may possess better antidiabetic and anti-inflammatory properties, which could be attributed to the differences in their chemical constituents [145]. This emphasizes

the importance of the fractionation method because the different fractions used in this study represent different chemical compositions.

In addition, the importance of these results from a clinical perspective should not be underestimated. Animal trials involving standardized aqueous extracts of *A. indica* leaves and twigs have shown marked benefits in the regulation of blood sugar and vascular functions, even when taken in conjunction with conventional medications such as metformin [146].

This gives a very important translational background to the benefits in in vitro study. The mechanisms of action of the hypoglycemic properties of *A. indica* are complex and involve increased sensitivity to insulin, improved pancreatic β-cell function, and decreased oxidative stress. Some studies even propose the possibility of antiserotonin action in the regulation of blood sugar [147].

Though the existing literature has tended to concentrate on crude extracts or individual compounds such as azadirachtin, but this research covers the very important area of fractionation. This progress enables the determination of which chemical fractions are most responsible for the recorded antioxidant and antidiabetic properties, rather than simply studying general extracts. By examining the activity within the fractions of the leaf extract, this research offers important information for future medical applications, potentially leading to the development of standardized herbal medicine or the isolation of important bioactive compounds. In general, the existing literature is very supportive of the traditional and scientific justification for research into the medicinal properties of *A. indica*, making these results important in the area of natural products research.

Like one of the compound present in *A. indica* "Purpurin" showed unusual response against diabetes during insilico studies. While comparing it with standard antidiabetic drug "Metformin" purpurin is structurally and chemically different substances that fall in different chemical group, their comparison in the current study is scientifically reasonable based on functional pharmacological analysis, as opposed to structural similarity. Metformin is a well-established biguanide antidiabetic agent that is used as a gold standard reference drug in the determination of

antihyperglycemic activity because it has clinically validated efficacy in the promotion of glucose homeostasis mainly by the activation of AMPK, inhibition of hepatic gluconeogenesis and peripheral insulin sensitivity. Purpurin, conversely, is an anthraquinone phytochemical, purpurin, produced by plants that has been reported to have antioxidant and anti-inflammatory activity and can potentially inhibit carbohydrate-metabolizing enzymes, which may indirectly help regulate glycemic control by regulating oxidative stress and metabolic dysregulation. The comparison rationale is the assessment of the fact that purpurin can attain the similar net pharmacological effect in terms of glucose management, even though they are mediated by different molecular and biochemical mechanisms. This method is highly tolerated in phytopharmacological and drug discovery studies, where natural products are tested against standard drug molecules to find possible lead molecules. Thus, the comparison is done on the basis of the principle of pharmacodynamics convergence where chemically unrelated compounds can have a similar effect of therapy through different pathways, and thereby offers a rational basis on which initial consideration of the purpurin as an antidiabetic agent can be made against a clinically established reference standard.

Chapter 6

Conclusion and Future Prospects

In summary, this research emphasizes the great potential of *Azadirachta indica* leaf extract as an antioxidant and antidiabetic agent, especially through fractionation. The findings indicate that the NF1 fraction possesses a strong ability to combat oxidative stress and regulate glucose levels, thus justifying the use of neem in traditional medicine. Moreover, insilico analysis shows the purpurin compound present in NF1 has the potential to bind with target proteins and act as a potential future anti-diabetic agent. Nevertheless, more research is required to validate these observations in vivo and in clinical practice, especially through the use of diabetes special pancreatic cell lines i.e., INS cell lines. Future research should focus on identifying more aspects of the active compounds behind these activities, examining their interactions with other medications, and their uses in functional foods. Generally, *Azadirachta indica* presents a great natural remedy for the treatment of diabetes and other related ailments, as part of efforts to improve public health.

Bibliography

[1] S. Agrawal, D. B. Popli, K. Sircar, and A. Chowdhry, "A review of the anticancer activity of Azadirachta indica (Neem) in oral cancer," *Journal of Oral Biology and Craniofacial Research*, vol. 10, no. 2, pp. 206–209, 2020.

[2] G. Bereda, "Brief overview of diabetes mellitus," *Diabetes Manag*, vol. 1, pp. 21–27, 2021.

[3] A. Katsarou *et al.*, "Type 1 diabetes mellitus," *Nature Reviews Disease Primers*, vol. 3, no. 1, pp. 1–17, 2017.

[4] C. Bommer *et al.*, "Global economic burden of diabetes in adults: projections from 2015 to 2030," *Diabetes Care*, vol. 41, no. 5, pp. 963–970, 2018.

[5] C. Solis-Herrera, C. Triplitt, C. Reasner, R. A. DeFronzo, and E. Cersosimo, "Classification of diabetes mellitus," in *Endotext [Internet]*. MDText.com, Inc., 2018.

[6] P. M. Titchenell, Q. Chu, B. R. Monks, and M. J. Birnbaum, "Hepatic insulin signalling is dispensable for suppression of glucose output by insulin in vivo," *Nature Communications*, vol. 6, no. 1, p. 7078, 2015.

[7] L. Sylow, V. L. Tokarz, E. A. Richter, and A. Klip, "The many actions of insulin in skeletal muscle, the paramount tissue determining glycemia," *Cell Metabolism*, vol. 33, no. 4, pp. 758–780, 2021.

[8] H. Kwon and J. E. Pessin, "Insulin-mediated PI3K and AKT signaling," in *The Liver: Biology And Pathobiology*, 2020, pp. 485–495.

[9] X. C. Dong, "FOXO transcription factors in non-alcoholic fatty liver disease," *Liver Research*, vol. 1, no. 3, pp. 168–173, 2017.

[10] T. Haak, H. Hanaire, R. Ajjan, N. Hermanns, J.-P. Riveline, and G. Rayman, "Flash glucose-sensing technology as a replacement for blood glucose monitoring for the management of insulin-treated type 2 diabetes: a multicenter, open-label randomized controlled trial," *Diabetes Therapy*, vol. 8, no. 1, pp. 55–73, 2017.

[11] M. Nakamura, N. Satoh, S. Horita, and M. Nangaku, "Insulin-induced mTOR signaling and gluconeogenesis in renal proximal tubules: A mini-review of current evidence and therapeutic potential," *Frontiers in Pharmacology*, vol. 13, p. 1015204, 2022.

[12] Z. Yuan *et al.*, "PPARγ and Wnt signaling in adipogenic and osteogenic differentiation of mesenchymal stem cells," *Current Stem Cell Research & Therapy*, vol. 11, no. 3, pp. 216–225, 2016.

[13] R. A. DeFronzo *et al.*, "Type 2 diabetes mellitus," *Nature Reviews Disease Primers*, vol. 1, no. 1, pp. 1–22, 2015.

[14] C. Titus, M. T. Hoque, and R. Bendayan, "PPAR agonists for the treatment of neuroinflammatory diseases," *Trends in Pharmacological Sciences*, vol. 45, no. 1, pp. 9–23, 2024.

[15] K. Mohammedi *et al.*, "Microvascular and macrovascular disease and risk for major peripheral arterial disease in patients with type 2 diabetes," *Diabetes Care*, vol. 39, no. 10, pp. 1796–1803, 2016.

[16] G. Roman and A. P. Stoian, "Cardiovascular risk/disease in type 2 diabetes mellitus," in *Type 2 Diabetes-From Pathophysiology to Cyber Systems*. IntechOpen, 2021.

[17] K. Cai, Y. P. Liu, and D. Wang, "Prevalence of diabetic retinopathy in patients with newly diagnosed type 2 diabetes: A systematic review and meta-analysis," *Diabetes/Metabolism Research and Reviews*, vol. 39, no. 1, p. e3586, 2023.

[18] R. Galiero *et al.*, "Peripheral neuropathy in diabetes mellitus: pathogenetic mechanisms and diagnostic options," *International Journal of Molecular Sciences*, vol. 24, no. 4, p. 3554, 2023.

[19] B. Wu, Z. Niu, and F. Hu, "Study on risk factors of peripheral neuropathy in type 2 diabetes mellitus and establishment of prediction model," *Diabetes & Metabolism Journal*, vol. 45, no. 4, pp. 526–538, 2021.

[20] G. L. Bakris *et al.*, "Effect of finerenone on chronic kidney disease outcomes in type 2 diabetes," *New England Journal of Medicine*, vol. 383, no. 23, pp. 2219–2229, 2020.

[21] K. I. Galaviz, K. V. Narayan, F. Lobelo, and M. B. Weber, "Lifestyle and the prevention of type 2 diabetes: a status report," *American Journal of Lifestyle Medicine*, vol. 12, no. 1, pp. 4–20, 2018.

[22] B. Tomlinson, N. G. Patil, M. Fok, P. Chan, and C. W. K. Lam, "The role of sulfonylureas in the treatment of type 2 diabetes," *Expert Opinion on Pharmacotherapy*, vol. 23, no. 3, pp. 387–403, 2022.

[23] M. A. Davidson, D. R. Mattison, L. Azoulay, and D. Krewski, "Thiazolidinedione drugs in the treatment of type 2 diabetes mellitus: past, present and future," *Critical Reviews in Toxicology*, vol. 48, no. 1, pp. 52–108, 2018.

[24] B. Xu, S. Li, B. Kang, and J. Zhou, "The current role of sodium-glucose cotransporter 2 inhibitors in type 2 diabetes mellitus management," *Cardiovascular Diabetology*, vol. 21, no. 1, p. 83, 2022.

[25] A. M. Dirir, M. Daou, A. F. Yousef, and L. F. Yousef, "A review of alpha-glucosidase inhibitors from plants as potential candidates for the treatment of type-2 diabetes," *Phytochemistry Reviews*, vol. 21, no. 4, pp. 1049–1079, 2022.

[26] C. S. Marathe, C. K. Rayner, T. Wu, K. L. Jones, and M. Horowitz, "Gastrointestinal disorders in diabetes," in *Endotext [Internet]*. MDText.com, Inc., 2024.

[27] A. Aharaz, A. Pottegard, D. P. Henriksen, J. Hallas, H. Beck-Nielsen, and A. T. Lassen, "Risk of lactic acidosis in type 2 diabetes patients using metformin: a case control study," *PloS One*, vol. 13, no. 5, p. e0196122, 2018.

[28] B. Johnson-Rabbett and E. R. Seaquist, "Hypoglycemia in diabetes: the dark side of diabetes treatment. A patient-centered review," *Journal of Diabetes*, vol. 11, no. 9, pp. 711–718, 2019.

[29] C. M. Apovian, J. Okemah, and P. M. O'Neil, "Body weight considerations in the management of type 2 diabetes," *Advances in Therapy*, vol. 36, no. 1, pp. 44–58, 2019.

[30] T. Bardin and P. Richette, "Impact of comorbidities on gout and hyperuricaemia: an update on prevalence and treatment options," *BMC Medicine*, vol. 15, no. 1, p. 123, 2017.

[31] P. Kaur, R. S. K. Sachan, A. Karnwal, and I. Devgon, "A review on clinical manifestation and treatment regimens of UTI in diabetic patients," *Iranian Journal of Medical Microbiology*, vol. 16, no. 2, pp. 98–115, 2022.

[32] N. Tran, B. Pham, and L. Le, "Bioactive compounds in anti-diabetic plants: From herbal medicine to modern drug discovery," *Biology*, vol. 9, no. 9, p. 252, 2020.

[33] M. Przeor, "Some common medicinal plants with antidiabetic activity, known and available in Europe (A Mini-Review)," *Pharmaceuticals*, vol. 15, no. 1, p. 65, 2022.

[34] M. I. Yatoo, A. Saxena, A. Gopalakrishnan, M. Alagawany, and K. Dhama, "Promising antidiabetic drugs, medicinal plants and herbs: An update," *International Journal of Pharmacology*, vol. 13, no. 7, pp. 732–745, 2017.

[35] S. S. Ahmed and M. O. Rahman, "From Flora to Pharmaceuticals: 100 new additions to angiosperms of Gafargaon subdistrict in Bangladesh and unraveling antidiabetic drug candidates targeting DPP4 through in silico approach," *PloS One*, vol. 19, no. 3, p. e0301348, 2024.

[36] S. L. Teoh and S. Das, "Phytochemicals and their effective role in the treatment of diabetes mellitus: a short review," *Phytochemistry Reviews*, vol. 17, no. 5, pp. 1111–1128, 2018.

[37] P. Ansari *et al.*, "Plant-based diets and phytochemicals in the management of diabetes mellitus and prevention of its complications: A review," *Nutrients*, vol. 16, no. 21, p. 3709, 2024.

[38] H. Ardalani, F. H. Amiri, A. Hadipanah, and K. T. Kongstad, "Potential antidiabetic phytochemicals in plant roots: a review of in vivo studies," *Journal of Diabetes & Metabolic Disorders*, vol. 20, no. 2, pp. 1837–1854, 2021.

[39] M. Akdad, R. A. convoys, F. Khallouki, Y. Bakri, and M. Eddouks, "Antidiabetic phytocompounds acting as glucose transport stimulators," *Endocrine, Metabolic & Immune Disorders-Drug Targets*, vol. 23, no. 2, pp. 147–168, 2023.

[40] Y. Xu, G. Tang, C. Zhang, N. Wang, and Y. Feng, "Gallic acid and diabetes mellitus: Its association with oxidative stress," *Molecules*, vol. 26, no. 23, p. 7115, 2021.

[41] S. Liu *et al.*, "The potential of astragalus polysaccharide for treating diabetes and its action mechanism," *Frontiers in Pharmacology*, vol. 15, p. 1339406, 2024.

[42] S. Kottireddy and S. Koora, "Lupeol exerts its antidiabetic activity through insulin receptor and glucose transporter-4 in gracilis muscle in high fat and sucrose-induced diabetic rats," *Drug Invention Today*, vol. 11, no. 9, 2019.

[43] R. Guzman-Avila *et al.*, "Ursolic acid derivatives as potential antidiabetic agents: In vitro, in vivo, and in silico studies," *Drug Development Research*, vol. 79, no. 2, pp. 70–80, 2018.

[44] H.-W. Yang, K. Fernando, J.-Y. Oh, X. Li, Y.-J. Jeon, and B. Ryu, "Anti-obesity and anti-diabetic effects of Ishige okamurae," *Marine Drugs*, vol. 17, no. 4, p. 202, 2019.

[45] P. Kalhotra, V. C. Chittepu, G. Osorio-Revilla, and T. Gallardo-Velazquez, "Discovery of galangin as a potential DPP-4 inhibitor that improves insulin-stimulated skeletal muscle glucose uptake: a combinational therapy for diabetes," *International Journal of Molecular Sciences*, vol. 20, no. 5, p. 1228, 2019.

[46] S. Saleem, G. Muhammad, M. A. Hussain, and S. N. A. Bukhari, "A comprehensive review of phytochemical profile, bioactives for pharmaceuticals, and pharmacological attributes of Azadirachta indica," *Phytotherapy Research*, vol. 32, no. 7, pp. 1241–1272, 2018.

[47] I. Seriana, M. Akmal, D. Darusman, S. Wahyuni, K. Khairan, and S. Sugito, "Phytochemicals characterizations of neem (Azadirachta indica A. Juss) leaves ethanolic extract: an important medicinal plant as male contraceptive candidate," *Rasayan Journal of Chemistry*, vol. 14, no. 1, pp. 343–350, 2021.

[48] G. Benelli *et al.*, "Neem (Azadirachta indica): towards the ideal insecticide?" *Natural Product Research*, vol. 31, no. 4, pp. 369–386, 2017.

[49] S. Maji and S. Modak, "Neem: Treasure of natural phytochemicals," *Chemical Science Review and Letters*, vol. 10, no. 39, pp. 396–401, 2021.

[50] M. R. Wylie and D. S. Merrell, "The antimicrobial potential of the neem tree Azadirachta indica," *Frontiers in Pharmacology*, vol. 13, p. 891535, 2022.

[51] S. Nagini, M. Palrasu, and A. Bishayee, "Limonoids from neem (Azadirachta indica A. Juss.) are potential anticancer drug candidates," *Medicinal Research Reviews*, vol. 44, no. 2, pp. 457–496, 2024.

[52] R. K. Pathak, D.-Y. Kim, B. Lim, and J.-M. Kim, "Investigating multitarget antiviral compounds by screening of phytochemicals from neem (Azadirachta indica) against PRRSV: a vetinformatics approach," *Frontiers in Veterinary Science*, vol. 9, p. 854528, 2022.

[53] M. Iman, M. Taheri, and Z. Bahari, "The anti-cancer properties of neem (Azadirachta indica) through its antioxidant activity in the liver: its pharmaceutics and toxic dosage forms. A literature review," *Journal of Complementary and Integrative Medicine*, vol. 19, no. 2, pp. 203–211, 2022.

[54] S. Kumar, U. K. Vandana, D. Agrwal, and J. Hansa, "Analgesic, anti-inflammatory and anti-pyretic effects of Azadirachta indica (Neem) leaf extract in albino rats," *International Journal of Science and Research*, vol. 4, no. 8, pp. 713–721, 2015.

[55] M. Ali, M. Hassan, S. A. Ansari, H. M. Alkahtani, L. S. Al-Rasheed, and S. A. Ansari, "Quercetin and kaempferol as multi-targeting antidiabetic agents against mouse model of chemically induced type 2 diabetes," *Pharmaceuticals*, vol. 17, no. 6, p. 757, 2024.

[56] Y. Yan, X. Zhou, K. Guo, F. Zhou, and H. Yang, "Use of chlorogenic acid against diabetes mellitus and its complications," *Journal of Immunology Research*, vol. 2020, no. 1, p. 9680508, 2020.

[57] L. Wang *et al.*, "Trends in prevalence of diabetes and control of risk factors in diabetes among US adults, 1999-2018," *JAMA*, vol. 326, no. 8, pp. 704–716, 2021.

[58] R. Goyal and I. Jialal, "Diabetes mellitus type 2," *StatPearls [Internet]*, 2018.

[59] H. D. McIntyre *et al.*, "Gestational diabetes mellitus," *Nature Reviews Disease Primers*, vol. 5, no. 1, p. 47, 2019.

[60] M. N. Nakrani, R. H. Wineland, and F. Anjum, "Physiology, glucose metabolism," *StatPearls [Internet]*, 2020.

[61] O. Kwon, "Glucose metabolism," in *Stroke Revisited: Diabetes in Stroke*. Springer, 2021, pp. 3–13.

[62] A. Tups, J. Benzler, D. Sergi, S. R. Ladyman, and L. M. Williams, "Central regulation of glucose homeostasis," *Comprehensive Physiology*, vol. 7, no. 2, pp. 741–764, 2017.

[63] N. Nirmalan and M. Nirmalan, "Hormonal control of metabolism: regulation of plasma glucose," *Anaesthesia & Intensive Care Medicine*, vol. 21, no. 11, pp. 578–583, 2020.

[64] A. R. Saltiel, "Insulin signaling in health and disease," *The Journal of Clinical Investigation*, vol. 131, no. 1, 2021.

[65] K. Ramasubbu and V. D. Rajeswari, "Impairment of insulin signaling pathway PI3K/Akt/mTOR and insulin resistance induced AGEs on diabetes mellitus and neurodegenerative diseases: a perspective review," *Molecular and Cellular Biochemistry*, vol. 478, no. 6, pp. 1307–1324, 2023.

[66] M. Sasaki *et al.*, "Dual regulation of gluconeogenesis by insulin and glucose in the proximal tubules of the kidney," *Diabetes*, vol. 66, no. 9, pp. 2339–2350, 2017.

[67] S. J. Humphrey, S. B. Azimifar, and M. Mann, "High-throughput phosphoproteomics reveals in vivo insulin signaling dynamics," *Nature Biotechnology*, vol. 33, no. 9, pp. 990–995, 2015.

[68] R. A. Haeusler, T. E. McGraw, and D. Accili, "Biochemical and cellular properties of insulin receptor signalling," *Nature Reviews Molecular Cell Biology*, vol. 19, no. 1, pp. 31–44, 2018.

[69] T. Thoudam *et al.*, "PDK4 augments ER–mitochondria contact to dampen skeletal muscle insulin signaling during obesity," *Diabetes*, vol. 68, no. 3, pp. 571–586, 2019.

[70] N. Jaiswal *et al.*, "The role of skeletal muscle Akt in the regulation of muscle mass and glucose homeostasis," *Molecular Metabolism*, vol. 28, pp. 1–13, 2019.

[71] A. Rabiee, M. Kruger, J. Ardenkjaer-Larsen, C. R. Kahn, and B. Emanuelli, "Distinct signalling properties of insulin receptor substrate (IRS)-1 and IRS-2 in mediating insulin/IGF-1 action," *Cellular Signalling*, vol. 47, pp. 1–15, 2018.

[72] A. Besse-Patin *et al.*, "PGC1A regulates the IRS1:IRS2 ratio during fasting to influence hepatic metabolism downstream of insulin," *Proceedings of the National Academy of Sciences*, vol. 116, no. 10, pp. 4285–4290, 2019.

[73] T. M. Batista, N. Haider, and C. R. Kahn, "Defining the underlying defect in insulin action in type 2 diabetes," *Diabetologia*, vol. 64, no. 5, pp. 994–1006, 2021.

[74] M.-J. Choi *et al.*, "Anti-inflammatory mechanism of galangin in lipopolysaccharide-stimulated microglia: Critical role of PPAR-γ signaling pathway," *Biochemical Pharmacology*, vol. 144, pp. 120–131, 2017.

[75] V. Sharma and V. Patial, "Peroxisome proliferator-activated receptor gamma and its natural agonists in the treatment of kidney diseases," *Frontiers in Pharmacology*, vol. 13, 2022.

[76] S. Wang, E. J. Dougherty, and R. L. Danner, "PPARγ signaling and emerging opportunities for improved therapeutics," *Pharmacological Research*, vol. 111, pp. 76–85, 2016.

[77] N. Bougarne *et al.*, "Molecular actions of PPARα in lipid metabolism and inflammation," *Endocrine Reviews*, vol. 39, no. 5, pp. 760–802, 2018.

[78] U. Galicia-Garcia *et al.*, "Pathophysiology of type 2 diabetes mellitus," *International Journal of Molecular Sciences*, vol. 21, no. 17, p. 6275, 2020.

[79] Y. Tong, S. Xu, L. Huang, and C. Chen, "Obesity and insulin resistance: Pathophysiology and treatment," *Drug Discovery Today*, vol. 27, no. 3, pp. 822–830, 2022.

[80] J. A. Janssen, "Hyperinsulinemia and its pivotal role in aging, obesity, type 2 diabetes, cardiovascular disease and cancer," *International Journal of Molecular Sciences*, vol. 22, no. 15, p. 7797, 2021.

[81] S. E. O'Sullivan, "An update on PPAR activation by cannabinoids," *British Journal of Pharmacology*, vol. 173, no. 12, pp. 1899–1910, 2016.

[82] A. S. Williams, L. Kang, and D. H. Wasserman, "The extracellular matrix and insulin resistance," *Trends in Endocrinology & Metabolism*, vol. 26, no. 7, pp. 357–366, 2015.

[83] J. Pei, B. Wang, and D. Wang, "Current studies on molecular mechanisms of insulin resistance," *Journal of Diabetes Research*, vol. 2022, p. 1863429, 2022.

[84] K. Rehman, M. S. H. Akash, A. Liaqat, S. Kamal, M. I. Qadir, and A. Rasul, "Role of interleukin-6 in development of insulin resistance and type 2 diabetes mellitus," *Critical Reviews in Eukaryotic Gene Expression*, vol. 27, no. 3, 2017.

[85] A. Jennings *et al.*, "Associations between branched chain amino acid intake and biomarkers of adiposity and cardiometabolic health independent of genetic factors: a twin study," *International Journal of Cardiology*, vol. 223, pp. 992–998, 2016.

[86] K. L. Flores-Viveros *et al.*, "Contribution of genetic, biochemical and environmental factors on insulin resistance and obesity in Mexican young adults," *Obesity Research & Clinical Practice*, vol. 13, no. 6, pp. 533–540, 2019.

[87] R. Mathew, M. P. Bhadra, and U. Bhadra, "Insulin/insulin-like growth factor-1 signalling (IIS) based regulation of lifespan across species," *Biogerontology*, vol. 18, no. 1, pp. 35–53, 2017.

[88] M. Matboli *et al.*, "Identification of novel insulin resistance related ceRNA network in T2DM and its potential editing by CRISPR/Cas9," *International Journal of Molecular Sciences*, vol. 22, no. 15, p. 8129, 2021.

[89] S. Thiab *et al.*, "Human-induced pluripotent stem cells (iPSCs) for disease modeling and insulin target cell regeneration in the treatment of insulin resistance: A review," *Cells*, vol. 14, no. 15, p. 1188, 2025.

[90] V. Bellou, L. Belbasis, I. Tzoulaki, and E. Evangelou, "Risk factors for type 2 diabetes mellitus: an exposure-wide umbrella review of meta-analyses," *PloS One*, vol. 13, no. 3, p. e0194127, 2018.

[91] M. Alasqah *et al.*, "Periodontal parameters in prediabetes, type 2 diabetes mellitus, and non-diabetic patients," *Brazilian Oral Research*, vol. 32, p. e81, 2018.

[92] L. Casanova, F. Hughes, and P. Preshaw, "Diabetes and periodontal disease," *BDJ Team*, vol. 1, p. 15007, 2015.

[93] R. Vigersky and M. Shrivastav, "Role of continuous glucose monitoring for type 2 in diabetes management and research," *Journal of Diabetes and its Complications*, vol. 31, no. 1, pp. 280–287, 2017.

[94] B. Silver *et al.*, "EADSG guidelines: insulin therapy in diabetes," *Diabetes Therapy*, vol. 9, no. 2, pp. 449–492, 2018.

[95] C. J. Nolan, N. B. Ruderman, S. E. Kahn, O. Pedersen, and M. Prentki, "Insulin resistance as a physiological defense against metabolic stress: implications for the management of subsets of type 2 diabetes," *Diabetes*, vol. 64, no. 3, pp. 673–686, 2015.

[96] A. Cahn, R. Miccoli, A. Dardano, and S. D. Prato, "New forms of insulin and insulin therapies for the treatment of type 2 diabetes," *The Lancet Diabetes & Endocrinology*, vol. 3, no. 8, pp. 638–652, 2015.

[97] R. Mathu, A. Abarnadevika, and G. Ariharasivakumar, "A study of biguanides in the care of type II diabetes mellitus," *J Pharm Sci Drug Discov*, vol. 1, no. 1, pp. 1–9, 2021.

[98] S. Volcansek *et al.*, "Amylin: From mode of action to future clinical potential in diabetes and obesity," *Diabetes Therapy*, pp. 1–21, 2025.

[99] R. M. DiSogra and J. Meece, "Auditory and vestibular side effects of FDA-approved drugs for diabetes," in *Seminars in Hearing*, vol. 40, no. 4. Thieme Medical Publishers, 2019, pp. 315–326.

[100] G. Sudhakaran *et al.*, "Anti-inflammatory role demonstrated both in vitro and in vivo models using nonsteroidal tetranortriterpenoid, Nimbin (N1) and its analogs (N2 and N3) that alleviate the domestication of alternative medicine," *Cell Biology International*, vol. 46, no. 5, pp. 771–791, 2022.

[101] G. Suresh, G. Gopalakrishnan, and S. Masilamani, "Neem for plant pathogenic fungal control: The outlook in the new millennium," in *Neem: Today and in the new millennium*, 2004, pp. 183–207.

[102] M. J. Latif *et al.*, "Therapeutic potential of Azadirachta indica (neem) and their active phytoconstituents against diseases prevention," *J Chem Chem Sci*, vol. 10, no. 3, pp. 98–110, 2020.

[103] E. Alum, "Phytochemicals in malaria treatment: Mechanisms of action and clinical efficacy," *KIU J. Health Sci*, vol. 4, no. 2, pp. 71–84, 2024.

[104] S. M. Patel, K. C. N. V. xand P. Bhattacharyya, G. Sethi, and A. Bishayee, "Potential of neem (Azadirachta indica L.) for prevention and treatment of oncologic diseases," in *Seminars in Cancer Biology*, vol. 40. Elsevier, 2016, pp. 100–115.

[105] M. S. Nagano and C. Batalini, "Phytochemical screening, antioxidant activity and potential toxicity of Azadirachta indica A. Juss (neem) leaves," *Revista Colombiana de Ciencias Quimico-Farmaceuticas*, vol. 50, no. 1, pp. 29–47, 2021.

[106] M. A. Moga *et al.*, "An overview on the anticancer activity of Azadirachta indica (Neem) in gynecological cancers," *International Journal of Molecular Sciences*, vol. 19, no. 12, p. 3898, 2018.

[107] A. Ullah *et al.*, "Phytoconstituents with cardioprotective properties: A pharmacological overview on their efficacy against myocardial infarction," *Phytotherapy Research*, vol. 38, no. 9, pp. 4467–4501, 2024.

[108] T. Emran, M. N. Uddin, A. Rahman, Z. Uddin, and M. Islam, "Phytochemical, antimicrobial, cytotoxic, analgesic and anti-inflammatory properties of

Azadirachta indica: A therapeutic study," *J Bioanal Biomed S*, vol. 12, no. 2, 2015.

[109] D. D. Sahoo and D. Sharma, "Neem: A good immune booster and blood purifier," *And Its Benefits*, vol. 5, p. 123, 2022.

[110] A. K. Swaroop *et al.*, "Plant derived immunomodulators; a critical review," *Advanced Pharmaceutical Bulletin*, vol. 12, no. 4, p. 712, 2021.

[111] N. Crisp, *Turning the World Upside Down Again: Global health in a time of pandemics, climate change and political turmoil*. CRC Press, 2022.

[112] T. Marevesa, E. Mavengano, and P. N. Nkamta, "Home remedies as a medical development in the context of the Covid-19 pandemic in Zimbabwe: a cultural memory paradigm," *Gender and Behaviour*, vol. 19, no. 1, pp. 17 371–17 383, 2021.

[113] F. Jamshidi-Kia, Z. Lorigooini, and H. Amini-Khoei, "Medicinal plants: Past history and future perspective," *Journal of Herbmed Pharmacology*, vol. 7, no. 1, pp. 1–7, 2018.

[114] A. N. Alamgir, "Herbal drugs: their collection, preservation, and preparation; evaluation, quality control, and standardization of herbal drugs," in *Therapeutic Use of Medicinal Plants and Their Extracts: Volume 1: Pharmacognosy*. Cham: Springer International Publishing, 2017, pp. 453–495.

[115] D. Lee, D. H. Lee, S. Choi, J. S. Lee, D. S. Jang, and K. S. Kang, "Identification and isolation of active compounds from astragalus membranaceus that improve insulin secretion by regulating pancreatic β-cell metabolism," *Biomolecules*, vol. 9, no. 10, p. 618, October 2019.

[116] M. Zych and A. Pyka Pajak, "Tlc in the analysis of plant material," *Processes*, vol. 13, no. 11, p. 3497, October 2025.

[117] X. M. Luan, Q. H. Sun, Y. Yang, R. Rong, and X. Wang, "Improvement of polarity-based solvent system for countercurrent chromatography

in the guidance of solvent selectivity: n-hexane/ethyl acetate/alcohol solvents/water as an example," *Journal of Chromatography A*, vol. 1736, p. 465389, November 2024.

[118] T. Kowalska and M. Sajewicz, "Thin-layer chromatography (tlc) in the screening of botanicals–its versatile potential and selected applications," *Molecules*, vol. 27, no. 19, p. 6607, October 2022.

[119] D. Mayasari, Y. B. Murti, S. U. Pratiwi, and S. Sudarsono, "Antibacterial activity and tlc-densitometric analysis of secondary metabolites in the leaves of the traditional herb, melastoma malabathricum l." *Borneo Journal of Pharmacy*, vol. 5, no. 4, pp. 334–344, November 2022.

[120] L. Y. Ning, A. A. Azmi, D. F. Syamsumir, W. I. Ismail, and M. Maulidiani, "Phytochemical screening, tlc profile and 1h nmr analysis of passiflora foetida extracts," *Universiti Malaysia Terengganu Journal of Undergraduate Research*, vol. 5, no. 2, pp. 65–74, April 2023.

[121] T. Kowalska and M. Sajewicz, "Thin-layer chromatography (tlc) in the screening of botanicals–its versatile potential and selected applications," *Molecules*, vol. 27, no. 19, p. 6607, October 2022.

[122] P. K. Zarzycki, "Staining and derivatization techniques for visualization in planar chromatography," in *Instrumental thin-layer chromatography*. Elsevier, January 2023, pp. 213–257.

[123] R. Pungle, S. H. Nile, N. Makwana, R. Singh, R. P. Singh, and A. S. Kharat, "Green synthesis of silver nanoparticles using the tridax procumbens plant extract and screening of its antimicrobial and anticancer activities," *Oxidative Medicine and Cellular Longevity*, vol. 2022, no. 1, p. 9671594, 2022.

[124] S. A. Jafri, Z. M. Khalid, M. R. Khan, S. Ashraf, N. Ahmad, A. M. Karami, E. Rafique, M. Ouladsmane, N. M. Al Suliman, and S. Aslam, "Evaluation of some essential traditional medicinal plants for their potential free scavenging and antioxidant properties," *Journal of King Saud University-Science*, vol. 35, no. 3, p. 102562, April 2023.

[125] G. J. Molole, A. Gure, and N. Abdissa, "Determination of total phenolic content and antioxidant activity of commiphora mollis (oliv.) engl. resin," *BMC Chemistry*, vol. 16, no. 1, p. 48, June 2022.

[126] S. A. Jaber, "In vitro alpha-amylase and alpha-glucosidase inhibitory activity and in vivo antidiabetic activity of quercus coccifera (oak tree) leaves extracts," *Saudi Journal of Biological Sciences*, vol. 30, no. 7, p. 103688, July 2023.

[127] Y. Elouafy, A. El Yadini, S. Mortada, M. Hnini, H. Harhar, A. Khalid, N. A. Abdalla, A. Bouyahya, K. W. Goh, L. C. Ming, and M. E. Faouzi, "Antioxidant, antimicrobial, and α-glucosidase inhibitory activities of saponin extracts from walnut (juglans regia l.) leaves," *Asian Pacific Journal of Tropical Biomedicine*, vol. 13, no. 2, pp. 60–69, February 2023.

[128] B. Chibuye, I. Sen Singh, L. Chimuka, and K. K. Maseka, "Phytochemical and lcms/ms screening, total phenolic and flavonoid content and antioxidant activity of the leaves of diospyros batokana (ebenaceae)," *Scientific Reports / Research Article (Pending Full Journal Name)*, 2023.

[129] M. Fatima, A. Amin, M. Alharbi, S. Ishtiaq, W. Sajjad, F. Ahmad, S. Ahmad, F. Hanif, M. Faheem, and A. A. Khalil, "Quorum quenchers from reynoutria japonica in the battle against methicillin-resistant staphylococcus aureus (mrsa)," *Molecules*, vol. 28, no. 6, p. 2635, March 2023.

[130] J. Tibbitts, D. Canter, R. Graff, A. Smith, and L. A. Khawli, "Key factors influencing adme properties of therapeutic proteins: A need for adme characterization in drug discovery and development," in *MAbs*, vol. 8, no. 2. Taylor & Francis, 2016, pp. 229–245.

[131] H. Van De Waterbeemd, D. A. Smith, K. Beaumont, and D. K. Walker, "Property-based design: optimization of drug absorption and pharmacokinetics," *Journal of Medicinal Chemistry*, vol. 44, no. 9, pp. 1313–1333, 2001.

[132] E. Sjögren, H. Thorn, and C. Tannergren, "In silico modeling of gastrointestinal drug absorption: predictive performance of three physiologically

based absorption models," *Molecular Pharmaceutics*, vol. 13, no. 6, pp. 1763–1778, 2016.

[133] T. T. V. Tran, H. Tayara, and K. T. Chong, "Recent studies of artificial intelligence on in silico drug distribution prediction," *International Journal of Molecular Sciences*, vol. 24, no. 3, p. 1815, 2023.

[134] S. R. Kazmi, R. Jun, M.-S. Yu, C. Jung, and D. Na, "In silico approaches and tools for the prediction of drug metabolism and fate: A review," *Computers in Biology and Medicine*, vol. 106, pp. 54–64, 2019.

[135] G. Luo *et al.*, "In silico prediction of biliary excretion of drugs in rats based on physicochemical properties," *Drug Metabolism and Disposition*, vol. 38, no. 3, pp. 422–430, 2010.

[136] A. Roncaglioni, A. A. Toropov, A. P. Toropova, and E. Benfenati, "In silico methods to predict drug toxicity," *Current Opinion in Pharmacology*, vol. 13, no. 5, pp. 802–806, 2013.

[137] M. D. Segall and C. Barber, "Addressing toxicity risk when designing and selecting compounds in early drug discovery," *Drug Discovery Today*, vol. 19, no. 5, pp. 688–693, 2014.

[138] S. Vijayakumar, P. Manogar, S. Prabhu, M. Pugazhenthi, and P. Praseetha, "A pharmacoinformatic approach on cannabinoid receptor 2 (cb2) and different small molecules: Homology modelling, molecular docking, md simulations, drug designing and adme analysis," *Computational Biology and Chemistry*, vol. 78, pp. 95–107, 2019.

[139] S. Durdagi, M. G. Papadopoulos, D. P. Papahatjis, and T. Mavromoustakos, "Combined 3d qsar and molecular docking studies to reveal novel cannabinoid ligands with optimum binding activity," *Bioorganic & Medicinal Chemistry Letters*, vol. 17, no. 24, pp. 6754–6763, 2007.

[140] U. Baroroh, M. Biotek, Z. S. Muscifa, W. Destiarani, F. G. Rohmatullah, and M. Yusuf, "Molecular interaction analysis and visualization of protein-ligand docking using biovia discovery studio visualizer," *Indonesian Journal of Computational Biology (IJCB)*, vol. 2, no. 1, pp. 22–30, 2023.

[141] C. J. Bailey, "Metformin: Therapeutic profile in the treatment of type 2 diabetes," *Diabetes, Obesity and Metabolism*, vol. 26, pp. 3–19, Aug 2024.

[142] U. Rekha, M. Anita, S. Bhuminathan, and K. Sadhana, "Known data on the therapeutic use of azadiracta indica (neem) for type 2 diabetes mellitus," *Bioinformation*, vol. 18, no. 2, p. 82, February 2022.

[143] M. Almaqtari, F. Thamer, A. Abduljabbar, A. AlGaadbi, A. Alfaatesh, and H. Al-Maydama, "Evaluation of antioxidant and antibacterial activities of leaf and seeds extracts of neem (azadirachta indica) using different extraction," *Sana'a University Journal of Applied Sciences and Technology*, vol. 2, no. 6, pp. 520–526, December 2024.

[144] R. Baskar, G. Bharathkumar, K. Kumar, R. Shakila, M. Rajammal, S. Selvapriya, and T. Devi, "Standardization of madhumukthi kudineer chooranum using pharmacognostic, physicochemical and hptlc studies," *Pharmacognosy Research*, vol. 16, no. 3, July 2024.

[145] S. Patil, P. Shirahatti, and R. Ramu, "Azadirachta indica a. juss (neem) against diabetes mellitus: A critical review on its phytochemistry, pharmacology, and toxicology," *Journal of Pharmacy and Pharmacology*, vol. 74, no. 5, pp. 681–710, May 2022.

[146] S. A. Abdel-Aziz and A. M. Baghdadi, "The impact of moringa oleifera and azadirachta indica (neem) leaves ethanolic extract on streptozotocin induced diabetes rats," *Journal of Home Economics*, vol. 40, no. 2, pp. 97–124, June 2024.

[147] R. Ganorkar, S. Khan, and K. Chandramohan, "Antidiabetic and other 25 potential features of azadirachta indica a. juss.(neem)," in *Antidiabetic Medicinal Plants and Herbal Treatments*, July 2023, p. 379.